

A system for monitoring and attributing shifts in vegetation activity

Doctoral Thesis

Edward Muhoko

A system for monitoring and attributing shifts in vegetation activity

Doctoral Thesis

submitted in partial fulfillment of the
requirements for a Doctorate in Natural Sciences (Dr. rer. nat.) of the Bayreuth
Graduate School of Mathematical and Natural Sciences (BayNAT) of the
University of Bayreuth, Germany

presented by **Edward Mukoya Muhoko**

born in Rundu, Namibia

Bayreuth, July 2024

”If you can’t fly then run, if you can’t run then walk, if you can’t walk then crawl, but whatever you do you have to keep moving forward.”

- Martin Luther King Jr

This doctoral thesis was prepared at the department of Plant Ecology at the University of Bayreuth from 04/2020 until 07/2024 and was supervised by Prof. Dr. Steven Higgins.

This is a full reprint of the thesis submitted to obtain the academic degree of Doctor of Natural Sciences (Dr. rer. nat.) and approved by the Bayreuth Graduate School of Mathematical and Natural Sciences (BayNAT) of the University of Bayreuth.

Form of the dissertation: Monograph

Date of submission: 03.07.2024

Admission by the executive board: 10.07.2024

Date of defence: 03.06.2025

Acting director: Prof. Dr. Jürgen Köhler

Doctoral committee:

Prof. Dr. Steven Higgins (reviewer)

JProf. Dr. Lisa Hülsmann (reviewer)

Prof. Dr. Cyrus Samimi (chair)

Prof. Dr. Manuel Steinbauer

Contents

Summary	1
Zusammenfassung	3
1 General Introduction	6
1.1 Motivation: Why do we need a system for monitoring and attributing changes in terrestrial vegetation?	6
1.2 Overview on vegetation phenology, biomes and attribution	11
1.3 Vegetation Phenology, Functional Biomes and Attribution - state of the art	14
1.3.1 Changes in Vegetation phenology	14
1.3.2 Changes in Functional Biomes	16
1.3.3 Attribution	17
1.3.4 Study area	22
1.4 Objectives and elements of this thesis	24
2 Patterns of vegetation phenological change in the ecosystems of southern Africa	27
2.1 Summary	27
2.2 Introduction	28
2.3 Materials and Methods	31
2.3.1 Extracting multi-dimensional phenological metrics	31
2.3.2 Clustering pixels into phenomes to detect change	33
2.4 Results	36
2.4.1 Changes in vegetation phenology	36
2.4.2 Phenological change by phenome	42
2.5 Discussion	49
2.6 Supplementary Information	53
3 Assessing changes in the Functional Biomes of southern Africa	60
3.1 Summary	60
3.2 Introduction	61
3.3 Materials and Methods	65
3.3.1 Functional Biomes classification scheme	65
3.3.2 Functional Biomes change analysis	69
3.4 Results	70
3.4.1 Functional Biomes of southern Africa	70
3.4.2 Observed trends in biome shifts	75

3.5	Discussion	80
3.5.1	Management implications	83
3.6	Supplementary Information	85
4	Detecting and attributing changes in vegetation activity to climatic forcing	89
4.1	Summary	89
4.2	Introduction	90
4.3	Materials and Methods	93
4.3.1	Data and site selection	93
4.3.2	The TTR model excluding environmental forcing data	94
4.3.3	The TTR model with environmental forcing data	97
4.3.4	The TTR as a state-space model	99
4.3.5	Extracting anomalies and estimating trends	100
4.4	Results	103
4.4.1	Detected trends in vegetation activity	103
4.4.2	Attribution of shifts in vegetation activity	103
4.5	Discussion	109
4.6	Supplementary Information	113
5	General Discussion	128
5.1	Overview	128
5.2	Dynamics of vegetation phenology	128
5.2.1	Potential mechanisms that underlie the detected phenological patterns	128
5.2.2	Ecological implications of phenological changes	129
5.2.3	Potential future research directions on vegetation phenology	130
5.3	Changes in the Functional Biomes of southern Africa	131
5.3.1	Potential mechanisms that underlie the detected shifts in Functional Biomes	131
5.3.2	Ecological implications of shifts in Functional Biomes	131
5.3.3	Potential future research directions	132
5.4	Beyond detection to attribution	134
5.4.1	Potential mechanisms that underlie the attributed shifts in vegetation activity	134
5.4.2	Ecological implications	135
5.4.3	Potential future research directions	135
5.5	Conclusions	137
	References	139

Contribution Statement	163
Publication list	164
Acknowledgements	165
(Eidesstattliche) Versicherungen und Erklärungen	166

Summary

Vegetation is the biological foundation of terrestrial ecosystems. Plants provide important ecosystem services such as absorbing anthropogenic CO₂ emissions annually, thereby mitigating global warming substantially. Despite the importance of vegetation to the biosphere, ongoing climate change and elevated CO₂ emissions are impacting the functioning and structure of these ecosystems. Such impacts are evident in shifts in vegetation phenology and shifts in biome distribution. Climate change and elevated CO₂ are also anticipated to remain the major drivers of changes in vegetation activity in the next decades, which might have important atmospheric and ecological consequences.

However, assessing changes in vegetation activity and attributing such changes to drivers such as elevated CO₂ and climate change is one of the main challenges in vegetation Ecology. The challenge stems from the fact that the change detection and attribution processes are complex and multifaceted. This therefore limits our understanding of how terrestrial vegetation is responding to changes in environmental drivers, which is important for guiding management efforts in response to current and future changes in vegetation activity.

The goal of this thesis is to develop a system that is useful for detecting and attributing changes in vegetation activity to changes in environmental drivers. To achieve this, I focus on changes in vegetation phenology (Chapter 2) and changes in the Functional Biomes (FB) (Chapter 3) of southern Africa, a region widely regarded as a climate change hotspot, yet vegetation dynamics in this region remain poorly understood. Chapter 4 moves beyond detection to attribution of ecosystem changes to climatic factors. I focus on 100 study sites that are distributed across the major ecosystems of the world to allow for regional conclusions of global ecosystem response to climatic forcing.

We assessed patterns of vegetation phenological change in southern Africa between 2000-2019. The phenological change was assessed within regions with similar phenological properties (phenomes) to account for spatial heterogeneity across ecosystems. We assessed changes in the Functional Biomes of southern Africa by quantifying changes in vegetation units with shared productivity and phenology. Globally, we used solar-induced chlorophyll fluorescence (SIF) and Enhanced Vegetation Index (EVI) data, and an ecophysiological plant growth model to detect and attribute changes in vegetation activity to trends in climatic data at 100 study sites.

The growing season was shortened in 4 phenological regions, primarily driven by earlier initiation of the senescence phase metrics. In contrast, the growing season was extended in 3 phenological regions, mostly driven by delayed initiation of the senescence phase metrics. Our study revealed that phenological metrics have

changed by at least 1 standard deviation in each of the 21 metrics used to study phenological activity, indicating that ecologically relevant changes in the functioning of ecosystems of southern Africa are ongoing. Our FB analyses showed that 3% to 15% of pixels shifted in FB state from 2000-2021 in southern Africa. The most dominant FB transitions shifted to higher productive and non-seasonal states or to solely high productive but moisture-limited states. SIF analyses dominantly showed switches from decreased photosynthetic activity to increased photosynthetic activity, while EVI dominantly showed switches from greening to browning patterns. Attribution analyses showed that vegetation in cooler and moister regions was sensitive to changes in temperature while ecosystems in warmer and drier regions was sensitive to changes in moisture. Our analyses further showed weak CO₂ fertilization effects on the detected change in both datasets, thereby highlighting the dominant role of moisture and temperature constraints on changes in vegetation activity.

The phenological change revealed here provides clear evidence of climate change impacts on the vegetation of southern Africa. This study provides a baseline for developing early warning systems to strengthen the capacity for adaptation and mitigation of climate change in the region.

Current knowledge of biome dynamics is based on model predictions that suggest that elevated CO₂ and climate change will cause an increase in woody biomass coupled with longer growing seasons. Our FB approach provides compelling evidence that such anticipated biome trajectories are already ongoing, with consequences to biodiversity and carbon sequestration. Our study highlights the importance of understanding biome trajectories for evidence-based decisions in conservation initiatives.

The attribution analyses confirm growing evidence that suggests that CO₂ effects on vegetation activity may not be as pronounced as previously thought. The contrasting forcing effects of moisture and temperature detected in different latitudes suggest that regionally focused management strategies will be relevant to promote appropriate response measures. Future studies could consider regional attribution analyses due to differences in forcing effects between biomes. In conclusion, this thesis shows a strong climate change signal on vegetation activity between 2000-2021. The change detection and attribution approaches we applied opens new avenues for detecting and attributing change in ecosystems, allowing for informed planning on adaptation and mitigation responses to changes in terrestrial vegetation.

Zusammenfassung

Die Vegetation ist die biologische Grundlage der terrestrischen Ökosysteme. Pflanzen erbringen wichtige Ökosystemleistungen, wie z. B. die jährliche Absorption von anthropogenen CO₂-Emissionen, wodurch die globale Erwärmung erheblich gemildert wird. Trotz der Bedeutung der Vegetation für die Biosphäre beeinträchtigen der fortschreitende Klimawandel und die erhöhten CO₂-Emissionen die Funktionsweise und Struktur dieser Ökosysteme. Diese Auswirkungen zeigen sich in Verschiebungen in der Phänologie der Vegetation und in der Verteilung der Biome. Es wird erwartet, dass der Klimawandel und die erhöhten CO₂-Emissionen auch in den nächsten Jahrzehnten die Haupttriebkkräfte für Veränderungen der Vegetationsaktivität sein werden, was bedeutende atmosphärische und ökologische Folgen haben könnte.

Die Bewertung von Veränderungen in der Vegetationsaktivität und die Zuordnung dieser Veränderungen zu Triebkräften wie erhöhtem CO₂ und Klimawandel ist jedoch eine der größten Herausforderungen in der Vegetationsökologie. Die Herausforderung ergibt sich aus der Tatsache, dass die Prozesse zur Erkennung und Zuordnung von Veränderungen komplex und vielschichtig sind. Dies schränkt unser Verständnis dafür ein, wie die terrestrische Vegetation auf Veränderungen der Umweltfaktoren reagiert, was für die Steuerung der Bewirtschaftungsmaßnahmen als Reaktion auf aktuelle und zukünftige Veränderungen der Vegetationsaktivität wichtig ist.

Ziel dieser Arbeit ist es, ein System zu entwickeln, mit dem sich Veränderungen der Vegetationsaktivität erkennen und auf Veränderungen der Umweltfaktoren zurückführen lassen. Um dies zu erreichen, konzentriere ich mich auf Veränderungen in der Phänologie der Vegetation (Kapitel 2) und auf Veränderungen in den funktionalen Biomen (FB) (Kapitel 3) des südlichen Afrikas, einer Region, die weithin als ein Hotspot des Klimawandels angesehen wird, deren Vegetationsdynamik jedoch nach wie vor kaum verstanden wird. In Kapitel 4 geht es nicht nur um den Nachweis, sondern auch um die Zuordnung von Ökosystemveränderungen zu klimatischen Faktoren. Ich konzentriere mich auf 100 Untersuchungsstandorte, die über die wichtigsten Ökosysteme der Welt verteilt sind, um regionale Rückschlüsse auf die Reaktion der globalen Ökosysteme auf klimatische Einflüsse zu ermöglichen.

Wir haben die Muster der phänologischen Veränderungen der Vegetation im südlichen Afrika zwischen 2000 und 2019 untersucht. Die phänologischen Veränderungen wurden innerhalb von Regionen mit ähnlichen phänologischen Eigenschaften (Phänomenen) bewertet, um die räumliche Heterogenität der Ökosysteme zu berücksichtigen. Wir bewerteten die Veränderungen in den funktionalen Biomen des südlichen Afrikas, indem wir die Veränderungen in Vegetationseinheiten mit gemeinsamer Produktivität und Phänologie quantifizierten. Weltweit wurden Daten zur so-

larinduzierten Chlorophyllfluoreszenz (SIF) und zum Enhanced Vegetation Index (EVI) sowie ein ökophysiologisches Pflanzenwachstumsmodell verwendet, um Veränderungen in der Vegetationsaktivität zu erkennen und sie den Trends in den Klimadaten an 100 Untersuchungsstandorten zuzuordnen.

Die Vegetationsperiode wurde in vier phänologischen Regionen verkürzt, was in erster Linie auf einen früheren Beginn der Seneszenzphase zurückzuführen ist. Im Gegensatz dazu verlängerte sich die Vegetationsperiode in 3 phänologischen Regionen, was vor allem auf einen verzögerten Beginn der Seneszenzphase zurückzuführen ist. Unsere Studie ergab, dass sich die phänologischen Metriken um mindestens eine Standardabweichung in jeder der 21 zur Untersuchung der phänologischen Aktivität verwendeten Metriken verändert haben, was darauf hindeutet, dass ökologisch relevante Veränderungen in der Funktionsweise der Ökosysteme des südlichen Afrikas im Gange sind. Unsere FB-Analysen zeigten, dass sich der FB-Zustand von 3% bis 15% der Pixel im südlichen Afrika zwischen 2000 und 2021 veränderte. Die vorherrschenden FB-Übergänge führten zu höher produktiven und nicht saisonalen Zuständen oder zu ausschließlich hoch produktiven, aber feuchtigkeitsbegrenzten Zuständen. SIF-Analysen ergaben überwiegend einen Wechsel von verminderter photosynthetischer Aktivität zu erhöhter photosynthetischer Aktivität, während EVI überwiegend einen Wechsel von Vergrünungs- zu Verbräunungsmustern zeigte. Attributionsanalysen zeigten, dass die Vegetation in kühleren und feuchteren Regionen empfindlich auf Temperaturveränderungen reagierte, während Ökosysteme in wärmeren und trockeneren Regionen empfindlich auf Veränderungen der Feuchtigkeit reagierten. Unsere Analysen ergaben außerdem schwache Auswirkungen der CO₂-Düngung auf die festgestellten Veränderungen in beiden Datensätzen, was die dominierende Rolle von Feuchtigkeits- und Temperaturbeschränkungen bei Veränderungen der Vegetationsaktivität unterstreicht.

Die hier festgestellten phänologischen Veränderungen sind ein klarer Beweis für die Auswirkungen des Klimawandels auf die Vegetation im südlichen Afrika. Diese Studie liefert eine Grundlage für die Entwicklung von Frühwarnsystemen zur Stärkung der Kapazitäten für die Anpassung an den Klimawandel und dessen Eindämmung in der Region.

Das derzeitige Wissen über die Dynamik der Biome basiert auf Modellvorhersagen, die darauf hindeuten, dass ein erhöhter CO₂-Gehalt und der Klimawandel eine Zunahme der holzigen Biomasse in Verbindung mit längeren Wachstumsperioden verursachen werden. Unser FB-Ansatz liefert überzeugende Beweise dafür, dass die erwarteten Entwicklungen in den Biomen bereits im Gange sind, mit entsprechenden Folgen für die biologische Vielfalt und die Kohlenstoffbindung. Unsere Studie unterstreicht, wie wichtig das Verständnis von Biotopverläufen für evidenzbasierte Entscheidungen bei Naturschutzinitiativen ist.

Die Zuordnungsanalysen bestätigen die zunehmenden Hinweise darauf, dass

die Auswirkungen von CO₂ auf die Vegetationsaktivität möglicherweise nicht so ausgeprägt sind wie bisher angenommen. Die in verschiedenen Breitengraden festgestellten gegensätzlichen Auswirkungen von Feuchtigkeit und Temperatur lassen darauf schließen, dass regional ausgerichtete Bewirtschaftungsstrategien für die Förderung geeigneter Reaktionsmaßnahmen von Bedeutung sind. Künftige Studien könnten regionale Attributionsanalysen in Betracht ziehen, die auf die Unterschiede in den Antriebswirkungen zwischen den Biomen zurückzuführen sind. Zusammenfassend lässt sich sagen, dass diese Arbeit ein starkes Signal des Klimawandels auf die Vegetationsaktivität im Zeitraum 2000-2021 zeigt. Die von uns angewandten Ansätze zur Erkennung und Zuordnung von Veränderungen eröffnen neue Wege für die Erkennung und Zuordnung von Veränderungen in Ökosystemen und ermöglichen eine fundierte Planung von Anpassungs- und Abschwächungsmaßnahmen in Bezug auf Veränderungen der Landvegetation.

Chapter 1

1 General Introduction

1.1 Motivation: Why do we need a system for monitoring and attributing changes in terrestrial vegetation?

Vegetation is the biological foundation of terrestrial ecosystems, constituting 82% of the Earth's terrestrial biomass (Bar-On et al., 2018). Vegetation absorbs about 30% of anthropogenic CO₂ emissions annually (Terrer et al., 2021), thereby mitigating global warming substantially. Plants further support biodiversity by providing habitats and food to other organisms across trophic levels (Bascompte and Jordano, 2007; Scherber et al., 2010). Despite the importance of vegetation to the biosphere, environmental drivers such as land use change, elevated CO₂ concentrations and climate change are impacting changes in the functioning and structure of these ecosystems (Settele et al., 2014; Parmesan et al., 2022). For example, such impacts are evident in shifts in vegetation phenological activity (Buitenwerf et al., 2015; Piao et al., 2015; Menzel et al., 2020) and shifts in biome distribution (Higgins et al., 2016). These drivers are further anticipated to remain the major factors of ecosystem change in the foreseeable future (IPBES, 2019; IPCC, 2019). Therefore, a thorough understanding of changes in vegetation activity and the underlying drivers of such change is urgently needed as it has consequent implications for ecosystem functioning, ecosystem services provision and overall global sustainability.

An important part of Ecology is, and has always been, about detecting and attributing changes in terrestrial ecosystems (Parmesan et al., 2013). Yet ecologists face challenges in detecting ecosystem change and attributing such change to environmental drivers. Detection involve demonstrating that a system has statistically undergone change without offering a specific reason of the observed change (Parmesan et al., 2013; Cramer et al., 2014). However, this is difficult to achieve because challenges such as randomness within ecosystems, observation errors in the data and biases associated with short time series may interact to dilute the detection process (Parmesan et al., 2013; Higgins et al., 2023a).

Attribution involves quantifying and determining the relative contribution of environmental drivers to the detected ecosystem change (Parmesan et al., 2013; Cramer et al., 2014). However, most studies fall short in attribution. They either speculate that the observed system change is related to environmental drivers or do not attempt to attribute the detected change at all (Hansen et al., 2016; Van de Pol et al., 2017). This may be because vegetation response to the driving factors is non-linear and this is further compounded by correlations between drivers (Parmesan

et al., 2013, 2022; Higgins et al., 2023a). Such challenges have led to a limited number of robust detection and attribution studies, thereby hindering adaptation and mitigation efforts (Parmesan et al., 2013, 2022).

Measurements of changes in terrestrial vegetation involve assessing changes in vegetation phenology and changes in biomes (Mucina, 2019; Piao et al., 2019). Assessing changes in the magnitude and timing of phenological activity (for instance, shifts in the timing of flowering and greening events) provide early warning signals of vegetation responses to changing climatic conditions. Analyses of changes in vegetation classified by similarities in their functional attributes (i.e. Functional Biomes (FB)), can also reveal climate-driven impacts on ecosystem functioning. For example, changes in moisture-limited biomes may suggest altered precipitation patterns (Higgins et al., 2016). Therefore, assessing changes in vegetation phenology and changes in biomes is important for improving our understanding of how terrestrial vegetation respond to drivers such as elevated CO₂, climate change and land use change (Piao et al., 2019; Conradi et al., 2020; Parmesan et al., 2022).

Satellite remote sensing provide time-series data that enable monitoring of shifts in vegetation phenological activity and biomes. For example, studies have used remote sensing data to analyse changes in vegetation phenology (Zhang et al., 2006; Jeong et al., 2011; Jones et al., 2011; Zhu et al., 2012; Gill et al., 2015; Buitenwerf et al., 2015; Liu et al., 2016; Wang et al., 2016) and changes in vegetation classified as biomes (Higgins et al., 2016; Seddon et al., 2016; Zhu et al., 2016; Song et al., 2018). These studies have detected widespread changes in vegetation activity. However, these studies contain land use change effects that can mask climate change impacts on vegetation activity or may act in synergy (Sirami et al., 2017), making it difficult to accurately attribute each driver to the detected change. Most studies have primarily focused on northern latitudes or globally, leading to recent criticisms of geographic bias towards northern latitudes (Feeley et al., 2017). This suggests that ignoring southern latitudes may overlook the diversity of species response to climatic change. For example, ongoing climate change is anticipated to trigger species migrations globally, but species in southern latitudes will struggle to keep pace with climate change compared to species in northern latitudes (Feeley et al., 2015; Perez et al., 2016). One of the regions in the southern latitudes is southern Africa, which has been described as a climate change hotspot (Niang et al., 2014; Trisos et al., 2022), and is projected to be severely impacted by future climate change (Engelbrecht and Engelbrecht, 2016; Hoegh-Guldberg et al., 2018; Trisos et al., 2022).

The challenges highlighted in the previous paragraphs mean that we still lack a robust detection and attribution system. A robust detection and attribution system should overcome problems associated with inherent randomness in natural ecosystems, biases with short time series, observation errors, geographic biases,

the non-linear response of ecosystems to climatic forcing, the confounding land use change effects on vegetation change and co-limitation by climatic drivers. Such an integrated system serve as a foundation for effective adaptation and mitigation planning in response to current and future ecosystem change. This system has been advocated for (Pettorelli et al., 2014; Feeley et al., 2017), but to my knowledge it is yet to be developed. It is for this reason I synthesised and expanded on established approaches (Buitenwerf et al., 2015; Higgins et al., 2016, 2023a), to develop an integrated system for detecting and attributing changes in terrestrial vegetation to climatic factors.

I did this by studying changes in vegetation phenology, changes in Functional Biomes (hereafter FB) and attribution of changes in vegetation activity to climatic drivers. These were explored in 3 separate studies constituting the three main components of this thesis. Essentially, the first two studies are change detection approaches and focuses on the protected areas of southern Africa. The third study goes beyond detection to attribution of change by focusing on 100 study sites spanning the major ecosystems globally. I chose the protected areas of southern Africa for the two detection approaches because our knowledge on changes in terrestrial vegetation in this region remains relatively limited, yet changes in these ecosystems can potentially have significant ecological and atmospheric consequences (Buitenwerf et al., 2015). I chose the global 100 study sites because they allow us to draw regional conclusions of global ecosystem response to climatic forcing, thereby addressing recent criticism of geographic bias in detection and attribution studies (Feeley et al., 2017).

To better understand how terrestrial ecosystems are responding to changes in climatic factors and thereby formulate appropriate management responses, my thesis addresses the following research questions **(i)** What are the patterns and magnitude of vegetation phenological change in the ecosystems of southern Africa? **(ii)** What are the Functional Biomes of southern Africa and how have they changed over time? **(iii)** How do global trends in climatic factors influence vegetation activity over time, and what is the relative importance of the climatic factors in explaining changes in vegetation activity?

In line with the research questions of the thesis, I give a brief introduction to the concepts of vegetation phenology, Functional Biomes and attribution in the next section. I then present a concise literature review of studies that have assessed changes in vegetation phenology, changes in Functional Biomes and attribution of ecosystem change. I further point out knowledge gaps in these studies and then introduce the aims of the study in more detail. Moreover, I will introduce the study area and present the underlying objectives of this thesis. Box 1 describes the key concepts and terms used in this thesis.

Box 1: Definitions and descriptions of key concepts used in this thesis.

Climate Change: Refers to the multi-decadal average change in Earth's local, regional or global climatic patterns. This includes changes in temperature and precipitation over long periods (NASA, 2024).

Adaptation: The process of change by which ecosystems become better suited to cope with new environmental conditions driven by a disturbance such as climate change or land use change.

Mitigation: Mitigation refers to efforts aimed at reducing elevated greenhouse gas emissions and increasing carbon sinks. Such actions are aimed at combating the impact of climate change on terrestrial ecosystems (UNFCCC, 2024).

Remote Sensing: Remote Sensing is the scientific process of detecting and monitoring the physical characteristics of the Earth by measuring reflected or emitted energy at a distance. This technology uses sensors mounted on platforms such as satellites and aircraft to collect data from Earth (USGS, 2024).

Normalised Difference Vegetation Index (NDVI): NDVI is a normalised ratio between near-infrared light and red light commonly used to quantify vegetation greenness (Didan, 2015).

Enhanced Vegetation Index (EVI): EVI is a normalised ratio between near-infrared light, red light and the blue light used to quantify vegetation greenness. EVI decouples atmospheric and soil contamination from the vegetation signal (Didan, 2015).

Solar-Induced Fluorescence (SIF): SIF is a light signal emitted by excited chlorophyll molecules during photosynthesis light reactions. SIF is a proxy in studying the physiology of photosynthesis and the SIF signal can be measured by remote sensing platforms (Frankenberg et al., 2011; Porcar-Castell et al., 2014).

Terrestrial ecosystems: Terrestrial ecosystems are a community of biotic and abiotic factors based on land and their interaction with each other in space and time (NG, 2024).

Carbon dioxide (CO₂): CO₂ is a greenhouse gas responsible trapping the Earth System's energy exchange and thus contributes to global warming.

Land use change: Refers to changes on Earth's land cover driven by human activities.

Protected areas: Protected areas are geographic boundaries designated to conserve biodiversity while remaining free of land use effects (UNEP-WCMC and IUCN, 2021).

Vegetation phenology: Vegetation phenology is the study of the timing and duration of recurring annual life-cycle events in plants triggered by seasonal and environmental changes (Lieth, 1974).

Phenomes: Vegetation zones with similar phenological signatures (Buitenwerf et al., 2015).

Biomes: Biomes are large-scale vegetation zones characterized by similar functional and structural attributes (Higgins et al., 2016; Moncrieff et al., 2016).

Functional Biomes (FB): Functional Biomes classifies biomes as units with shared productivity and phenology based on metrics monitored by remote sensing satellites (Higgins et al., 2016).

Detection: Detection refers to a process of demonstrating that a system has statistically undergone change without offering a specific reason of the observed change (Parmesan et al., 2013).

Attribution: Attribution is the process of quantifying and determining the relative contribution of climatic drivers to the observed biological change (Parmesan et al., 2013).

State-space model: State-space model is a mathematical and statistical framework used to study the behaviour of dynamic systems over time. It usually consists of a state equation which describes how an underlying process in the system influences state variables, and an observation equation which links the observed data to the underlying process in the system.

Process-based models: Process-based models explicitly incorporate the underlying ecological processes that drive species distribution. In these models, parameters have a clear ecological interpretation and are predefined. This allows for a mechanistic understanding of how species interact with their environment (Dormann et al., 2012).

Thornley Transport Resistance (TTR) model: This is a process-based model which describes how abiotic factors influence plant growth, carbon and nitrogen assimilation. The TTR model conceptually describes a plant's physiological niche (Thornley, 1998; Higgins et al., 2012).

1.2 Overview on vegetation phenology, biomes and attribution

Vegetation phenology refers to the timing and duration of repetitive annual life-cycle events in plants triggered by seasonal and environmental changes (Lieth, 1974). The annual life-cycle events include the timing of the onset of the growing season, timing of senescence and duration of the growing season, and how these events relate to climatic and non-climatic factors. Plant phenology regulates water, carbon and energy feedbacks between terrestrial ecosystems and the atmosphere. In particular, the timing and length of a plant's growing season influence energy budgets and CO₂ exchanges (Peñuelas and Filella, 2009). Therefore, phenological cycles provide information on ecosystem functioning.

Vegetation phenology can be measured using field assessments and citizen science knowledge (Wolfe et al., 2005; Dickinson et al., 2012; Ge et al., 2015; Hufkens et al., 2019). Advances in satellite remote sensing have ensured that large-scale vegetation phenological assessments are now possible (Zhang et al., 2003; Buitenwerf et al., 2015; Piao et al., 2015; Menzel et al., 2020).

Factors like temperature, precipitation, nutrient availability and photoperiod control variations and changes in vegetation phenology (Adole et al., 2019; Piao et al., 2019). Globally, studies have shown that temperature and photoperiod are the dominant drivers of vegetation phenology in mid and high latitudes (Jolly et al., 2005; Piao et al., 2015), whereas precipitation is the primary driver of vegetation phenology in the tropics (Jolly et al., 2005; Zhang et al., 2006; Verger et al., 2016). These drivers interact with each other to influence the timing of phenological activity (Jolly et al., 2005; Wang et al., 2020a). For example, interactions between photoperiod effects and warmer spring temperatures in the northern hemisphere initiate an earlier start and a delayed end of the growing season, resulting in a longer growing season and increased productivity (Jeong et al., 2011). Thus, long-term observations of vegetation phenological activity is a reliable means of monitoring ecosystem response to changes in climatic factors (Cleland et al., 2007; Piao et al., 2019).

Biomes are large-scale vegetation zones characterized by similar functional and structural attributes (Higgins et al., 2016; Moncrieff et al., 2016). Schimper (1903) coined the modern biome concept, emphasising that plant formations are primarily determined by climatic and edaphic factors. Whittaker (1975) further expanded on Schimper (1903)'s emphasis on the dominant role of climate on plant distribution. However, this climatic determinism is not absolute. This is because evidence suggests that orographic factors and disturbances from fire and herbivores can override climatic factors in shaping biome distribution (Walter, 1973; Bond, 2005). Despite existing differences in biome concepts, the general consensus in Earth science is that biomes are useful constructs for organising our knowledge of ecosystem func-

tioning and how such ecosystems respond to drivers such as climate change and land use change (Higgins et al., 2016; Moncrieff et al., 2016; Conradi et al., 2020).

Dynamic Global Vegetation Models (DGVMs) are commonly used tools to predict biome response to climatic forcing. DGVMs mimic how ecophysiological processes, for example, carbon assimilation, growth, competition and consumption interact over large spatio-temporal scales and how biomes might respond to changes in the climate system (Prentice et al., 2007). Model variables like Leaf Area Index of various Plant Functional Types (PFTs) or their fractional cover are utilised to categorize vegetation into biomes classes (Scheiter et al., 2013, 2020; Martens et al., 2021). The simulated changes in model variables allow the detection of biomes most vulnerable to future climatic forcing.

The phytoclimate concept is another data-driven prediction tool of biome shifts that has garnered recent focus (Conradi et al., 2020; Higgins et al., 2023b; Conradi et al., 2024). Phytoclimates are climatic regions that support a particular combination of plant types. Specifically, the phytoclimate concept uses range modelling of plant species and climate data to identify geographic regions that are most conducive to specific plant growth forms. The plant growth forms are closely related to biomes. In fact, recent studies have suggested that phytoclimates can be used as an alternative for assessing biome shifts (Conradi et al., 2020).

Earth observation satellites provide opportunities to develop monitoring tools that can be used to assess historical shifts in Functional Biomes (FB). The FB concept classifies biomes as units with similar productivity and phenology. FB is by definition pragmatic, it is based on metrics that can be monitored by satellites (Higgins et al., 2016). Like the phytoclimates concept, the FB emerge from the data, thereby offering an objective approach on how the dominant life forms respond to environmental drivers over time. The advantage of the FB approach is that it is based on satellite data records, thereby directly providing empirical evidence of changes in actual biomes, making it a useful monitoring tool.

Attribution involves quantifying the relative contributions of environmental drivers to detected biological changes (Parmesan et al., 2013; Settele et al., 2014; Parmesan et al., 2022). The first step in attribution is demonstrating that change has occurred. The second step then assess the relative influence of drivers on the detected change. Confidence in attribution studies increases when they are supported by multiple lines of evidence, or when a deep understanding of the mechanisms that underlie the detected ecological change is demonstrated (Parmesan et al., 2013). Understanding how environmental drivers influence terrestrial ecosystems is important for advancing ecological research and also serves as a foundation for mitigation and adaptation responses (Parmesan et al., 2013; Feeley et al., 2017; Parmesan et al., 2022).

Various methods are used in attribution studies, which include statistical in-

ferences, experimental manipulation, correlative studies, historical comparisons, model simulations and expert judgment (Parmesan et al., 2013; Settele et al., 2014; Parmesan et al., 2022). Such approaches have identified drivers such as elevated CO₂, climate change, land use change and nitrogen deposition as the underlying drivers of the detected ecosystem change (Zhu et al., 2016; Piao et al., 2020; Higgins et al., 2023a).

The increasing availability of remotely sensed datasets means that large-scale change detection in natural ecosystems is now possible. Scientists have combined remote sensing data and ecophysiological models to detect and attribute changes in terrestrial ecosystems to changes in environmental drivers (Higgins et al., 2023a). Such analyses in natural systems to environmental drivers greatly improve our ability to predict and mitigate consequent changes in ecosystem functioning (Feeley et al., 2017; Higgins et al., 2023a).

1.3 Vegetation Phenology, Functional Biomes and Attribution - state of the art

Environmental drivers such as climate change, elevated CO₂ and land use change are impacting the functioning of terrestrial vegetation, with consequences for global biodiversity (Settele et al., 2014; Parmesan et al., 2022). It is therefore important we detect ongoing change and attribute such change to environmental drivers, thereby enabling informed management responses.

Although our capacity to quantify changes in terrestrial vegetation and attribute the quantified change to environmental drivers is still limited (Parmesan et al., 2022; Higgins et al., 2023a), some insights have accumulated in recent periods. I will present a concise review of studies that have focused on detecting changes in vegetation phenology, changes in Functional Biomes and attribution of ecosystem change.

1.3.1 Changes in Vegetation phenology

A study by Archibald and Scholes (2007) combined NDVI and meteorological data to detect tree and grass green-up dates and determined the drivers for such green-up dates in the Kruger National Park, South Africa. The findings showed that day length was the most important factor for tree green-up, while soil moisture and relative humidity were most important for grass green-up. The study provides insights into the environmental cues for tree and grass green-up in the savanna biome, with implications for understanding the ecological dynamics of savanna ecosystems. This study's sole focus on the green-up phase provides an incomplete picture of the dynamics of vegetation phenology in savanna ecosystems. A complete picture of phenological activity should study dynamics across the entire phenological cycle, including phases such as peak phase (day of highest vegetation activity) and senescence phases (yellowing). The study does not also address whether the timing of the green-up phase has changed. Such an aspect is important under ongoing global change. Another study by Cho et al. (2017) used time series of Leaf Area Index (LAI) to investigate the influence of tree cover on land surface phenology of South Africa. Phenological metrics were extracted from LAI data using a Gaussian model approach and then assessed the impact of rainfall on the metrics. They found that tree cover had a significant influence on the senescence period metrics (t-test, $p < 0.05$), but not on the green-up period metrics. They also found that rainfall influenced the green-up metrics but not the senescence metrics. The study highlights the potential of senescence period metrics to assess spatial variability of fire spread in savanna ecosystems. However, this study does not provide evidence on temporal changes in the extracted metrics or their variability relative to rainfall patterns or tree cover.

A study by Dubovyk et al. (2015) is one of the limited stz that have directly assessed changes in vegetation phenology in southern Africa. Dubovyk et al. (2015) used harmonic regression models and trend analysis to derive phenological metrics from MODIS EVI data between 2000-2013. They found qualitative changes in timing of metrics such as Peak greenness and Overall greenness. The changes in the Overall greenness metric was attributed to land use effects. This study demonstrates how the EVI signal can be confounded by land use effects, as most detected phenological changes were dominantly attributed to land use change than climate change. Another regional study by Ryan et al. (2017) also used MODIS EVI data to study the relationship between the pre-rain phenological phase and climate. They found that in 70% of the region, the green-up phase preceded rain onset by at least 20 days. The findings suggest that vegetation may show resistance to the delay in rain onset predicted under climate change. This study solely focuses on the green-up phase of the phenological cycle, ignoring other equally important phases of the growing season.

Work by Whitecross et al. (2017) assessed the drivers and frequency of early green-up phase across a latitudinal gradient in Zambia and South Africa. They found that early-greening was more prevalent in the northern sites (Zambia) than in southern sites (South Africa), with temperature and precipitation being the primary drivers of green-up dates. The findings suggest that climate change may be impacting the timing of the greening of savanna trees, with consequences for ecosystem function and services provision. Similar to Ryan et al. (2017), the sole focus of this study on changes in the green-up phase means that dynamics across other phenological phases remain relatively unknown.

The study by Adole et al. (2018a) combined MODIS EVI, regression models and existing land cover maps, to estimate trends in Land Surface Phenology (LSP) between 2001-2015 in several regions of Africa. They found that the length of the growing season was extended, driven by delayed end-of-the-season metrics. The study differentiated LSP trends not driven by land cover change from trends driven by land cover change, thereby directly implicating climatic forces. The study highlights the need for future studies to consider how climatic and non-climatic factors influence vegetation phenology in Africa. However, existing land cover maps have been criticized for their subjective approach and poor accuracy (Congalton et al., 2014; Higgins et al., 2016). Therefore, biases may be inherent in this study's detected land cover change.

Overall, a limited number of studies have assessed patterns of phenological change in southern Africa. Upon reviewing such existing studies, our knowledge remains incomplete. Most of these studies have solely focused on the green-up phase of the phenological cycle and completely ignored other equally important phases. Yet, it has been shown that vegetation phenology is a multi-dimensional

phenomenon, a multi-metric approach has therefore been advocated (Buitenwerf et al., 2015). Despite most studies focusing on the green-up phase, only a few studies have directly assessed changes in the green-up phase metrics. This makes it difficult to infer how widespread such changes are and where they are most severe. Most studies have ignored the confounding effects of land use change and climate change on the changes in vegetation phenology, except for Adole et al. (2018). Most studies have also relied on NDVI to assess vegetation phenology. However, NDVI tend to saturate in regions with dense vegetation and is susceptible to soil and atmospheric effects (Didan, 2015). These challenges limit our understanding of how vegetation phenology responds to climate change in the region and its potential to either accelerate or dampen climate change rates by altering energy exchange in the biosphere (Bonan, 2008).

1.3.2 Changes in Functional Biomes

Several studies have used DGVMs (Dynamic Global Vegetation Model) and aDGVMs (adaptive Dynamic Global Vegetation Model) to assess the potential response of biomes to future climatic forcing (Bond et al., 2003; Scheiter and Higgins, 2009; Higgins and Scheiter, 2012; Martens et al., 2021). These studies predict that climate change, elevated CO₂ and changes in fire regimes will cause an increase in woody biomass by the end of the 21st century. Bond et al. (2003) identifies elevated CO₂ as the primary driver of this trend. Higgins and Scheiter (2012) support this notion, indicating that the combined effects of CO₂ fertilization and reduced light competition would contribute to the trend. Although Bond et al. (2003) showed that fire can facilitate the spread of vegetation to humid regions, Scheiter and Higgins (2009) suggest that fire suppression, warming temperatures and elevated CO₂ could lead to tree-dominated biomes with extended growing seasons. Despite consistencies in predictions of increased woody biomass in the region, studies acknowledge large uncertainties in such predictions (Martens et al., 2021). Martens et al. (2021) suggests that it is important to consider such uncertainties, as changes in fire management practices and variations in future climate change scenarios can influence patterns of future biome shifts.

Species distribution models have also been used to predict future biome shifts in southern Africa. Rutherford et al. (1999) used a species distribution model to make spatially explicit predictions of South African biomes in response to future climate change. The findings show significant changes in biome distribution driven by climate change. Higgins et al. (2023b) uses the phytoclimate concept to predict how the vegetation of southern Africa may respond to future climate change by the end of the 21st century. The study uses an ecophysiological model fitted for over 5000 plant species data to predict widespread changes in phytoclimate state. The study also finds differences in the timing of the change within the region, with the

central interior predicted to change earlier compared to the western and southern parts of the region. The differences in the timing of change were primarily driven by contrasting responses of C3 and C4 grasses, trees and succulents to the global circulation models (GCMs) forecasts. While phytoclines provide valuable information on how vegetation might respond to climatic forcing, ecological processes such as species competition, recruitment, dispersal, disturbance (e.g., fire and herbivory) interact over time to ensure that phytoclines are rarely realized as biome formations (Higgins et al., 2023b).

Another commonly used biome map is that of Mucina and Rutherford (2006). Mucina and Rutherford (2006) combine a data-driven approach with expert knowledge to delimit the biomes of southern Africa through a bottom-up approach. They recognized 9 major biomes of southern Africa, each with its own distinct vegetation and climate. This map is useful because it shows vegetation that actually grows in southern Africa. However, the static nature of the map makes it less informative for monitoring biome changes.

A thorough literature search I performed revealed that studies assessing changes in the Functional Biomes of southern Africa do not exist. While a global study exists (Higgins et al., 2016), there is a lack of regionally-focused research in this area. This limits our understanding of changes in Functional Biomes within the region.

Overall, our knowledge is massively skewed toward predictions of future biome changes in southern Africa, while ongoing biome changes have surprisingly been ignored and therefore remain unnoticed. The high variability of climate change, land use changes and ecological processes such as competition and disturbance (herbivory and fire) may interact over time to ensure that predicted biome changes may never be realised (Higgins et al., 2023b). Assessing ongoing changes using the Functional Biomes approach has several advantages. First, it uses Earth observation data to provide empirical evidence of actual biome changes in the region. Second, the data on changes in FB state can be used to validate biophysical models used in current predictions of future biome shifts. Third, the FB data can also be used to inform the development of more robust biome prediction tools. Therefore, the FB approach serves as a useful bridge between observed biome changes and modelled biome changes, thereby improving our ability to understand, validate and predict vegetation dynamics in an era of widespread ecosystem change.

1.3.3 Attribution

Robust detection and attribution studies are limited despite extensive research in Earth science (Higgins et al., 2023a). Parmesan et al. (2013) and Settele et al. (2014) outline criteria studies should satisfy to be regarded as robust (or convincing) in detecting and attributing changes in terrestrial vegetation to changes

in climatic factors: First, the observation windows should be long (i.e. decades), thereby allowing for trends in vegetation activity to be statistically linked to trends in climatic factors; Second, assessing large geographic areas such that it diminishes local confounding factors; Third, a mechanistic link between climatic factors and ecosystem responses is supported by empirical evidence; Fourth, data and model uncertainty are minimized; and Fifth, climate change fingerprints are uniquely implicated as the primary driver of ecosystem change, while at the same time, confounding factors are accounted for or are of limited influence on the detected change. These criteria constitute multiple lines of converging evidence that identify climate change, for example, as the underlying driver of ecosystem change (Parmesan et al., 2013; Settele et al., 2014). However, the complexity of ecosystem response to change and the correlation and co-limitation among drivers means that such criteria are difficult to fulfil. I provide a brief review of studies that have detected and attributed changes in vegetation activity.

A prominent study by Zhu et al. (2016) detected and attributed changes in leaf area to environmental drivers between 1982-2009, globally. The study showed that global leaf area increased up to 50%. The underlying drivers of this greening trend were CO₂ fertilization (about 70%), enriched soil nitrogen (about 9%), climatic shifts (about 8%) and alterations in land cover (about 4%). Furthermore, CO₂ fertilization effects were more pronounced in the tropics while climate change was dominant in northern latitudes. This suggests that the effects of these drivers on vegetation productivity are region-specific. This study implicitly considers the confounding effects of land use change and other drivers by identifying land use effects as one of the drivers. However, the land use change data used in this study is a simulated product (Hurtt et al., 2011). Modelled products, unlike empirical data, may be limited by uncertainties and assumptions.

Smith et al. (2016) characterized the role of global terrestrial CO₂ fertilization effects on global vegetation productivity between 1982-2011. The findings show a significant increase in global NPP driven by elevated CO₂. Yet, comparisons between Ecosystem System Models (ESM) NPP and satellite-derived NPP reveal significant differences with satellite-derived NPP increases less than half of ESM-derived increases within the same study period. This suggests that EMS models may overestimate the effects of elevated CO₂ on global vegetation productivity, thereby highlighting observation errors in the detection and attribution process.

Chen et al. (2019) assesses the drivers of the global greening between 2000-2017 using MODIS LAI data. The results show that one-third of the global vegetated area exhibited greening patterns, with the most prominent greening trends observed in China and India. The study attributed land-use practices such as multiple cropping, irrigation and afforestation as the underlying drivers of the greening pattern. The study suggests that biophysical models need to realistically represent

land-use effects to better understand greening effects and its potential impacts to ecosystem services. Although this study improves our understanding on how human activities are modifying terrestrial vegetation, it provides limited information on ecosystems' natural response to drivers such as climate change. Understanding ecosystems' natural response is important for predicting future vegetation patterns under ongoing change.

A study by Song et al. (2018) quantified global land cover changes between 1982-2016 using satellite data. They further use non-parametric trend analysis and a global probability samples to attribute observed changes to land use change and climate change. The findings show that global tree cover increased by 7%, relative to 1982. The overall net gain in tree cover offset tree cover losses in the tropics which were outweighed by net gains in the extratropics. Most of these changes were attributed to human activities (60%) while climate change contributed 40% of the change. The mapped land cover changes reflect a human-dominated Earth system. Overall, this study disentangles the relative contribution of land use change and climatic factors on the detected pattern. However, it is not clear where and how these drivers were most dominant. For example, of the 40% attributed to climate change, its not clear how much of the greening was attributed temperature and moisture, or the geographic region where either of these drivers were most dominant. The study did not also consider other drivers such as solar radiation and CO₂ fertilization that have been known to influence vegetation activity (Nemani et al., 2003; Zhu et al., 2016).

Another study by Bjorkman et al. (2018) assessed the relationship between temperature, moisture and 7 important functional traits over 3 decades at 117 tundra sites. They found that spatial temperature–trait relationships were generally strong, but soil moisture influenced the strength and direction of these relationships. The study also found that the increase in community height was driven by warming temperatures, while other traits showed changes that were slower compared to the predicted rates of change. This study is one of the most convincing attribution studies because it assesses multiple study sites at large temporal scales with limited confounding effects of land use change on the detected trends. Since it uses ground-based observations, it is unclear how drivers such as CO₂ fertilisation and solar radiation contributed to the detected change.

Reich (2014) assessed the effects of elevated CO₂ fertilization on vegetation activity under varying levels of nitrogen and moisture availability. The findings showed that elevated CO₂ increased plant biomass by 33% when summer rainfall and nitrogen supply were at higher levels but found weak CO₂ fertilization effects on plant biomass when rainfall and nitrogen supply were at lower levels. This suggests that CO₂ fertilization effects are dependent on nitrogen and moisture availability. This also suggests that the role of CO₂ fertilization is not ubiquitous

given the limitations of nitrogen and moisture availability. The short temporal scale of 5 years limits our understanding of the long-term changes and driver dynamics over time.

Winkler et al. (2021) uses global leaf area data and a process-based model to investigate the drivers of changes in the activity of natural vegetation between 1981-2017. They find a dominant signal of climate change on many biomes, with greening in the northern latitudes driven by warming temperatures and moisture constraints driving browning patterns in the southern latitudes. They also find minimal CO₂ fertilization effects, thereby challenging a widely held narrative of the dominance of global-scale CO₂ effects. Overall, the study shows a weakening of greening patterns and strengthening of browning patterns in terrestrial ecosystems. The study suggests that most ecosystem models underestimate the emerging browning patterns. Although this study is informative, it contains the pervasive land use change effects on the detected change.

Higgins et al. (2023a) used NDVI and EVI data, and a plant growth model to detect and attribute changes in terrestrial ecosystems to climatic variables between 1981 to 2019. The findings showed that in most ecosystems, greening trends have transitioned to browning trends, indicating a decrease in vegetation biomass and potentially less carbon assimilation. Such transitions were dominantly driven by warming temperatures in northern latitudes and moisture constraints in the southern latitudes, suggesting geographic coherence in the detected response. CO₂ effects on vegetation activity were found to be surprisingly weak. This study is robust because it addresses most detection and attribution challenges highlighted by Parmesan et al. (2013) and Settele et al. (2014). However, this study relied on vegetation indices to infer carbon assimilation. Vegetation indices provide an implicit picture of carbon assimilation in plants (Frankenberg et al., 2011; Porcar-Castell et al., 2014). Vegetation indices are also not sensitive to changes in LUE, which increases with elevated CO₂ (Ainsworth and Long, 2005). Therefore, vegetation indices are not a direct proxy for GPP. This suggests that additional datasets are required to study trends in carbon assimilation.

Zhao et al. (2011) assessed the effects of climate change on global NPP trends using data records of FPAR, LAI and climate records between 2000-2009. The global MODIS algorithm was used to assess spatially explicit changes in the study period, while the Palmer Drought Severity Index (PDSI) (Palmer, 1965) was used to measure water environmental stress. They found a decrease in global NPP by 0.55 petagrams of carbon driven by large-scale droughts in southern latitudes, counteracting increased NPP in northern latitudes. The findings suggest a weakening terrestrial carbon sink is ongoing. Although the study assessed how climate change may be impacting global NPP trends, it did not directly evaluate CO₂ fertilisation effects on NPP. CO₂ has been regarded as an important driver of changes

in vegetation activity (Zhu et al., 2016). Furthermore, the study does not consider land use change effects on the detected NPP trends.

Overall, although these studies are useful in synthesising our knowledge of how terrestrial vegetation respond to environmental drivers, these studies also highlight challenges associated with detection and attribution of changes in vegetation activity (Parmesan et al., 2013; Settele et al., 2014). Most studies fall short on meeting the fourth and fifth criteria outlined by Parmesan et al. (2013) and Settele et al. (2014). That is, minimizing data and model uncertainty, as well as directly implicating climate change while accounting for other confounding factors have proven difficult. This is particularly true for studies that have not considered the confounding effects of land use change and climatic factors on ecosystem dynamics. This is surprising because about 60% of changes in vegetation are driven by human activity (Song et al., 2018). One would therefore expect most studies to consider land use effects when studying climate change impacts on vegetation activity. My assessment of these studies suggests that the Bjorkman et al. (2018) and Higgins et al. (2023a) approaches appear to be the most convincing attribution studies as they satisfy the above-mentioned criteria. This clearly suggests that high-confidence attribution studies remain limited.

1.3.4 Study area

In this section, I present a description of the two study areas. The first study area is the major protected areas of southern Africa (Figure 1). Protected areas are geographic boundaries designated to conserve biodiversity while remaining free of land use effects (UNEP-WCMC and IUCN, 2021). Such boundaries encompass forest reserves, nature reserves, national parks and game parks. The second study area are the 100 global sites of the major ecosystems of the world (Figure 2). I then briefly describe the methods I applied in this thesis. All analyses were performed in the R programming language (R Core Team, 2021, 2022, 2023).

In the context of this thesis, southern Africa comprises Zimbabwe, Botswana, South Africa, Eswatini, Lesotho and Namibia. Southern Africa is one of the most ecologically heterogeneous regions in Africa, consisting of ecosystems such as the desert, grassland, savanna and Mediterranean ecosystems. The region has a rich floristic diversity and high levels of endemism (Cowling et al., 2004). Furthermore, 18% of international biodiversity hot-spots are found in southern Africa (Davis-Reddy and Vincent, 2017), making it a region of global significance.

Summer begins from December to February, autumn is from March to May, winter is from June to August, and spring is from September to November. The region has a warm climate, with most parts experiencing mean annual temperatures above 17°C (Davis-Reddy and Vincent, 2017). Summer temperatures can exceed 40°C in the deserts of Namibia and Botswana (Davis-Reddy and Vincent, 2017). Temperatures in the region are anticipated to rise by 4°C to 6°C in the next decades, which is more than double rate of global warming (Engelbrecht et al., 2015).

Rainfall patterns vary spatially within the region, driven by ocean currents and prevailing winds (Davis-Reddy and Vincent, 2017). Mean annual rainfall can vary from less than 100 mm in western Namibia to above 1500 mm in eastern Zimbabwe (Davis-Reddy and Vincent, 2017). Most of the rainfall occur in the summer months, with an exception of the Mediterranean ecosystems that receive winter rainfall driven by mid-latitude cyclones (Hobbs et al., 1998). Precipitation patterns are characterised by strong inter-annual and inter-decadal variability (Davis-Reddy and Vincent, 2017).

The 100 global study sites were previously identified by Higgins et al. (2023a). These sites are wilderness landscapes representing the diversity of global terrestrial ecosystems stratified by biome type: savanna, grassland, shrubland, temperate evergreen and temperate deciduous forest, boreal forest, tropical evergreen forest, Mediterranean-type ecosystems and tundra (Figure 2). Higgins et al. (2023a) selected the sites using the following criteria: (1) A selected site should be dominated by homogenous vegetation. Minimal heterogeneity (for instance, peatlands, drainage lines, catenas) was permitted provided that these features were frequently

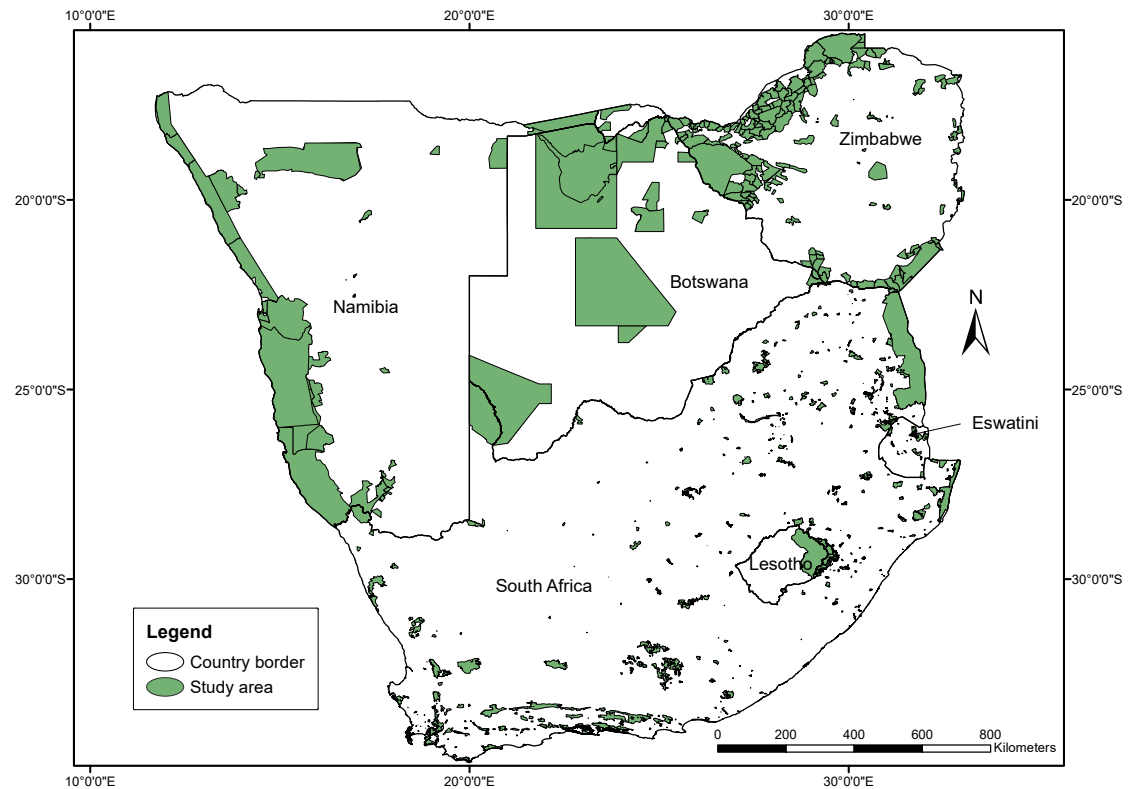


Figure 1: Study area: The major protected areas of southern Africa identified using the UNEP-WCMC and IUCN (2021)'s classification scheme. The study area map is adapted from Higgins et al. (2024).

observed on a site over the study period (2) A site should have no evidence of land use effects (for instance, no evidence of tree harvesting, crop farming, or paved surfaces). Small agricultural or pastoral fields were allowed as long they remained constant in size over time (3) Sites should not contain large water bodies, but small water bodies were permitted if they did not violate criteria (1). (4) Sites should not be adjacent to each other (i.e. neighboring pixels were not considered). To verify that all criteria were fulfilled, Google Earth Pro's Time Tool, which offers high resolution time series Earth observation imagery from 1984, was used (Higgins et al., 2023a).

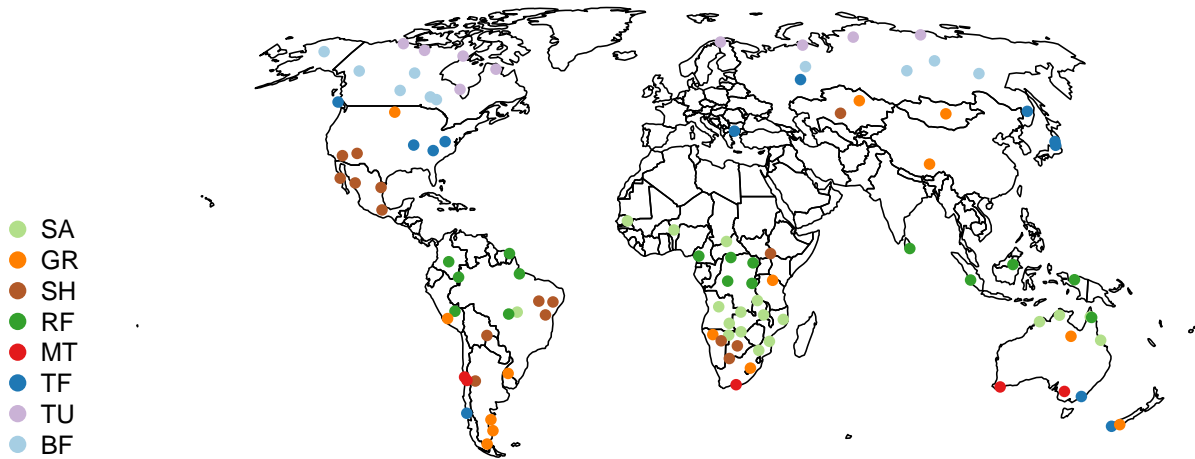


Figure 2: Geographic distribution of the study sites adapted from Higgins et al. (2023a). The 100 sites represent the diversity of terrestrial ecosystems globally. Letters in the map legend indicate the biome type: SA= savanna, GR= grassland, SH= shrubland, RF= tropical evergreen forest, MT= Mediterranean type ecosystems, TF= temperate forest, TU= tundra, BF= boreal forest.

1.4 Objectives and elements of this thesis

The goal of this thesis is to develop a system that is useful for detecting and attributing changes in vegetation activity to changes in climatic factors. To achieve this, I focus on changes in vegetation phenology and changes in Functional Biomes. This is because the two aspects serve as sensitive indicators of ecosystem response to environmental drivers (Parmesan et al., 2022).

This thesis has three main objectives: **(i)** to assess patterns and magnitude of vegetation phenological change in the ecosystems of southern Africa **(ii)** to define and assess changes in the Functional Biomes of southern Africa, and **(iii)** to detect and attribute changes in vegetation activity to changes in climatic factors globally. Investigating these objectives deepens our knowledge of how ecosystems are responding to climatic factors, thereby allow us to identify and monitor areas vulnerable to change. Such knowledge may be used to formulate informed

policy decisions for sustainable management of ecosystems. Furthermore, addressing these objectives might be useful in validating biogeophysical models that are commonly used to predict future change.

This thesis comprises three key elements that focuses on improving our understanding of terrestrial vegetation response to environmental change: Changes vegetation phenology, changes in Functional Biomes, and attribution of changes in vegetation activity. These investigations are presented in three corresponding themes:

Chapter 2: Shifts in vegetation phenology. I assessed changes in vegetation phenology using time series of EVI data. I estimated ecologically interpretable metrics representative of a plant's phenological cycle from the data. I then measured phenological change within phenologically similar zones to account for spatial heterogeneity between ecosystems.

Chapter 3: Shifts in Functional Biomes. I defined Functional Biomes (FB) as vegetation units with similar productivity and phenological properties estimated from time series reanalysis climate data and EVI data. An essential component of this approach is that the FB emerge from the data, it therefore allowed me to objectively investigate their distribution. I then assessed whether time has played a statistically significant role in the changes in FB state.

Chapter 4: Attributing shifts in vegetation activity. While **Chapter 2** and **Chapter 3** focus on detecting changes in terrestrial vegetation, **Chapter 4** delves beyond detection to attributing the detected change in terrestrial vegetation to trends in climatic factors. I investigated whether trends in carbon uptake and biomass assimilation are decreasing or increasing and then assessed the underlying drivers behind these trends. Such effects were displayed geographically to reveal regional differences in vegetation responses to climatic factors.

Overall, this thesis demonstrates that detecting and attributing changes in vegetation activity is important for understanding the trajectory of change ecosystems are on, as well as the underlying drivers of such trajectories. Such knowledge is needed for predicting future change in vegetation activity. Current knowledge on detection and attribution of changes in terrestrial vegetation is dominantly based on studies that do not consider the confounding effects of human activities and climatic factors on vegetation activity. The findings of this thesis will provide novel insights into the dynamics of vegetation activity when minimising such confounding factors. Existing knowledge suggests that CO₂ fertilisation is a dominant driver of changes in vegetation activity. This thesis shows, by revealing the relative importance of drivers of changes in vegetation activity, that temperature and moisture are the dominant drivers of changes in vegetation activity and thereby challenges the notion of the dominance of CO₂ effects. Therefore, this thesis contributes to the mechanistic understanding of changes in terrestrial ecosystems

and their underlying drivers, with implications for policy makers and conservation managers.

Chapter 2

2 Patterns of vegetation phenological change in the ecosystems of southern Africa

2.1 Summary

Plant phenology plays an important role in regulating moisture, carbon and energy feedbacks between the atmosphere and terrestrial ecosystems. In addition, vegetation phenological shifts are a sensitive indicator of climate change. Despite being highly vulnerable to climate change, how southern Africa's vegetation phenology is changing is poorly understood. Using the Enhanced Vegetation Index (EVI) as an indicator of vegetation activity, we applied a systematic change detection analysis to assess patterns of vegetation phenological change in the protected areas of southern Africa between 2000-2019. We focused on protected areas to avoid the potentially confounding factors related to land use change. We used an unsupervised clustering of the 21 phenological metrics to group the study area into 7 regions with similar phenological properties. We found that the growing season was shortened in 4 phenological regions, primarily driven by earlier initiation of the senescence phase metrics. In contrast, the growing season was extended in 3 phenological regions, mostly driven by delayed initiation of the senescence phase metrics. Our study reveals that phenological metrics have changed by at least 1 SD over the 19-year study period, indicating that ecologically relevant changes in the functioning of ecosystems of southern Africa are ongoing. The magnitude and spatial extent of change revealed here provide clear evidence of contrasting vegetation responses to climatic shifts in southern Africa. This study provides a baseline for developing early warning systems to strengthen the capacity for adaptation and mitigation of climate change in the region.

2.2 Introduction

An overwhelming body of evidence suggests that terrestrial ecosystems are responding to changes in climatic factors (Parmesan and Yohe, 2003; Zhu et al., 2016; Bonan and Doney, 2018; Song et al., 2018; Higgins et al., 2023a). Such responses are evident in shifts in species distribution (Parmesan and Yohe, 2003; Chen et al., 2011), shifts in biome distribution (Higgins et al., 2016) and shifts in leaf phenology (Buitenwerf et al., 2015; Piao et al., 2015; Menzel et al., 2020). Changes in vegetation phenology have led to mismatches between trophic levels (Tylianakis et al., 2008; Thackeray et al., 2016; Renner and Zohner, 2018). Such desynchronized phenological cycles may have profound effects on ecosystem functioning and structure. As a sensitive indicator of changes in the climate system, plant phenology plays an important role in regulating moisture, carbon and energy feedbacks between the atmosphere and terrestrial ecosystems. In particular, the timing and length of a plant's growing season influence energy budgets and CO₂ exchanges (Peñuelas and Filella, 2009). Therefore, deepening our knowledge of changes in vegetation phenology, the underlying drivers of such changes and their effects on ecosystem functioning, is useful for understanding and predicting ecosystem dynamics in response to ongoing climate change (Piao et al., 2019).

Recent advances in Earth observation satellites coupled with improved computer-based analyses of spatial data provide opportunities for extensive monitoring of vegetation phenology. Several studies have shown that the start and end of the growing season have changed globally (Zhang et al., 2006; Jones et al., 2011; Buitenwerf et al., 2015), thus illustrating that vegetation is responding to climate change. Similarly, studies conducted in the northern hemisphere have reported an extended growing season primarily due to an earlier green-up initiation phase and delayed senescence phase (Jeong et al., 2011; Zhu et al., 2012; Gill et al., 2015; Liu et al., 2016; Wang et al., 2016). Such studies demonstrate that vegetation phenology is a meaningful fingerprint of changes in vegetation activity and the severity of change.

Although global and northern hemisphere vegetation phenological shifts are well studied (Zhang et al., 2006; Jeong et al., 2011; Jones et al., 2011; Zhu et al., 2012; Gill et al., 2015; Buitenwerf et al., 2015; Liu et al., 2016; Wang et al., 2016), the southern hemisphere, southern Africa in particular, remains understudied with only a few existing regional studies (Dubovyk et al., 2015; Whitecross et al., 2017; Adole et al., 2018b). As such, decadal changes in vegetation phenology in the region and its potential impact on the feedbacks in the biosphere are poorly understood. The region has a pronounced level of climatic seasonality in the Mediterranean, grassland and savanna ecosystems. This suggests that the seasonal pattern of leaf deployment and leaf senescence may be critical adaptation strategies of vegetation to climate. Given its status as highly vulnerable to climate change (Niang

et al., 2014; Davis-Reddy and Vincent, 2017; Trisos et al., 2022), southern Africa is projected to be severely impacted by future climate change (Engelbrecht and Engelbrecht, 2016; Hoegh-Guldberg et al., 2018; Trisos et al., 2022). Furthermore, 18% of international biodiversity hot-spots are found in southern Africa (Davis-Reddy and Vincent, 2017), making it a region of global significance.

Previous regional studies in southern Africa have quantified changes in vegetation phenology using different approaches (Dubovyk et al., 2015; Whitecross et al., 2017; Adole et al., 2018b). Although these studies provide useful insights regarding the dynamics of plant phenology, assessing the severity and nature of these changes has proven difficult. This is because these studies do not provide a clear picture of how widespread the changes are or where in the region the changes are most pronounced. Such an implicit picture of phenological changes limits our ability to identify areas that are at risk of phenological mismatches. Moreover, single-date phenological metrics such as ‘start of season’ and ‘end of season’ have been applied to represent the beginning and end of the growing season, respectively (Adole et al., 2018b). However, vegetation phenology is a multi-dimensional phenomena that is difficult to describe using single-date metrics. A multi-metric approach has therefore been advocated (Buitenwerf et al., 2015). Existing studies do not also consider the confounding effects of land use change on vegetation activity. This is because land use change can override climate change effects on vegetation activity (Sirami et al., 2017). Therefore, ignoring land use effects on changes in vegetation phenology may misinterpret the detected phenological patterns (Piao et al., 2019). This suggests that focusing on geographic regions, such as protected areas, would minimise the confounding effects of land use effects on vegetation phenology and thereby provide a clearer picture of climate-driven phenological changes.

Here we present a regional assessment of changes in vegetation phenology using the Enhanced Vegetation Index (EVI) from Moderate Resolution Imaging Spectroradiometer (MODIS). EVI is a proxy for chlorophyll content in vegetation biomass and is therefore a sensitive indicator of vegetation activity. The importance of vegetation indices such as the EVI and the Normalised Difference Vegetation Index (NDVI) for Earth system science is highlighted by their usage to calculate global Leaf Area Index (LAI), GPP and NPP estimates (Running and Zhao, 2019). Our approach builds on a global study (Buitenwerf et al., 2015) and we improve on this study in two ways. First, we restrict our study area to the protected areas of southern Africa (Figure 3) to eliminate land use effects, which may contaminate the EVI signal and confound our interpretation of the analysis. In this context, we refer to protected areas as geographic regions designated for biodiversity conservation purposes without land use effects as defined by the world database on protected areas (UNEP-WCMC and IUCN, 2021). Such designated areas include forest reserves, nature reserves, game parks and national parks. Second, Buiten-

werf et al. (2015) used 9 km NDVI data to assess global phenological change. We use 1 km EVI data which has advantages over NDVI such as superior sensitivity in dense vegetation and less sensitivity to soil and atmospheric contamination (Didan, 2015). However, the disadvantage of using MODIS is that the MODIS record starts in the year 2000 whereas the Advanced Very High Resolution Radiometer (AVHRR) record used by Buitenwerf et al. (2015) starts in 1981.

2.3 Materials and Methods

2.3.1 Extracting multi-dimensional phenological metrics

The EVI MOD13A2 product was used for this analysis. The MODIS compositing algorithm that generates the MOD13A2 product selects the least biased estimate of the EVI of each pixel within a 16-day period using criteria such as lowest cloud cover, lowest aerosol content, lowest view angle. The resulting EVI product is thereby an atmospherically corrected surface reflectance data set consisting of 16-day image composites with high-quality observations (Didan, 2015). These observations are provided with data quality scores. EVI products dating from 2000 to 2019 (downloaded from <https://lpdaac.usgs.gov/products/mod13a2v006/>) represented the range of our time series.

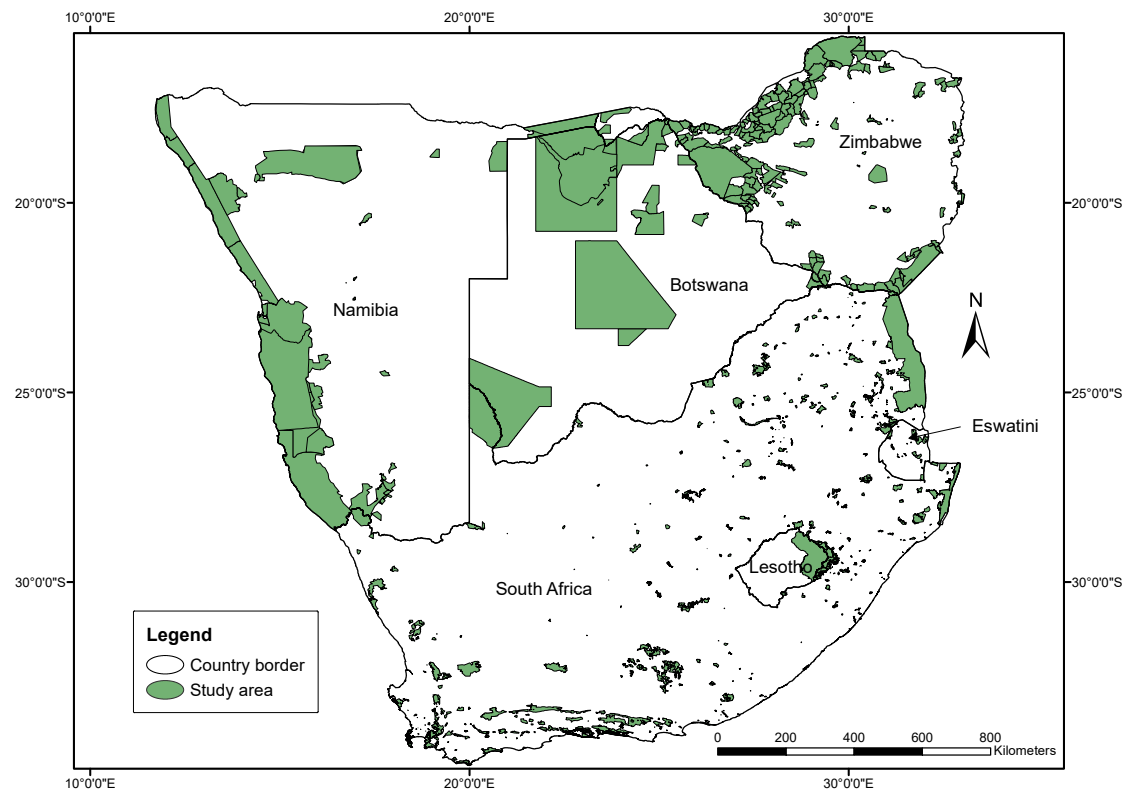


Figure 3: Study area: We exclusively focus on the major protected areas of southern Africa.

We fitted a cubic spline (using R (R Core Team, 2022) command `stats::smooth.spline`) to smooth the EVI time series of each pixel. The smoothed time series was used to estimate 21 phenological metrics (Figure 4). For each pixel, we defined the start

and end of the time series as follows. First, the 19-year mean 'peak day' and 19-year mean 'trough day', which are the mean day of the year of maximum EVI and the mean day of the year of minimum EVI, respectively, were estimated using the fitted spline. This enabled us to define 180-day windows (90 days on both sides) that includes the trough and peak of the annual cycle. Second, we then used the 180-day window to calculate the exact trough day and its associated EVI value for each phenological year (Buitenwerf et al., 2015). The number of days between two successive trough days defines a phenological year.

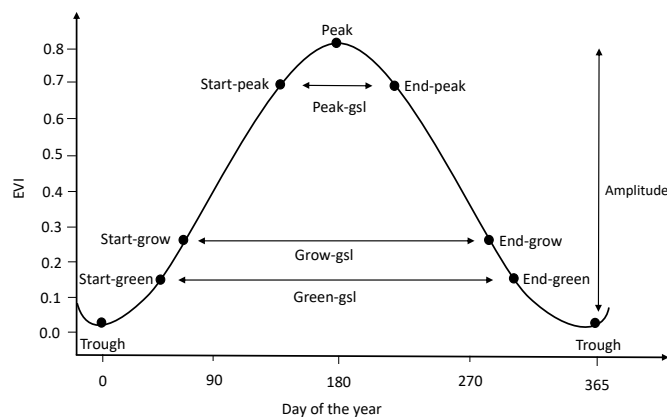


Figure 4: A schematic representation of vegetation phenological activity for an EVI pixel. Labeled points represent 2-dimensional metrics within a phenological year such that each metric consists of an EVI intensity value and a date. The sequence of days (x-axis) is arranged to begin from the start to the end of a phenological year. The EVI integral over a phenological year is calculated as the area under the curve between trough days. gsl: growing season length

We followed an approach outlined by Buitenwerf et al. (2015) to derive metrics representing the start and end of a plant's phenological cycle. These metrics, namely Start-green, Start-grow, and Start-peak represented the start of the growing season, while End-peak, End-grow and End-green represented the end of the growing season (Figure 4). To calculate these metrics, we used the continuous first and second derivatives of the cubic spline function. Specifically, we identified the day of the year at which the sum of the derivatives was at its maximum (Start-green) or minimum (End-peak). The maximum and minimum values of the first derivative were used to estimate Start-grow and End-grow, respectively. We determined Start-peak and End-green by identifying the day of the year at which the difference between the derivatives was at its maximum (Start-peak) or mini-

mum (End-green). Therefore, metrics representing the start of the growing season were calculated by selecting the day of the year at which the maximum of the first derivative is closer to the maximum of the second derivative in the first half of a phenological year. Similarly, metrics representing the end of the growing season were calculated by selecting the day of the year at which the minimum of the first derivative is closer to the minimum of the second derivative in the second half of a phenological year. These procedures produced multi-dimensional start and end of the growing season metrics measured in day of the year and EVI intensity values.

The start of the growing season metrics represent the rate of increase in photosynthetic activity, with Start-green representing the beginning of increase, Start-grow represents the quickest increase and Start-peak represents the end of the increase and beginning of peak photosynthetic activity. That is, the start of the growing season metrics may be construed to refer to date of leaf emergence, quickest rate of leaf expansion and end of leaf expansion (Buitenwerf et al., 2015). The three end of the growing season metrics represent analogous metrics that describe the rate of decrease in photosynthetic activity. The number of days between the Start/End dates define three additional metrics used to denote the growing season length (gsl), namely; Green-gsl, Grow-gsl, and Peak-gsl. The metric EVI integral, which is the area under the EVI curve, was calculated by summing the EVI value on each day of a phenological year. Amplitude was estimated by calculating the difference between the highest EVI value (Peak) and the lowest EVI value (Trough) for each phenological year. These steps produced 21 phenological metrics for 345,718 pixels over a 19-year time series.

2.3.2 Clustering pixels into phenomes to detect change

The phenological characteristics of vegetation in southern Africa vary by ecosystem type. Such phenological variation is primarily driven by multiple factors such as climate, disturbance regimes and species composition. For example, forest, grassland and Mediterranean ecosystems have different phenological signatures mostly driven by climatic factors which also vary geographically (Davis-Reddy and Vincent, 2017). Therefore, the magnitude and nature of change in phenological behaviour also vary by ecosystem type. To effectively assess these changes and facilitate spatial comparability, we clustered pixels with similar phenological signatures into phenological groups (phenomes hereafter) and compared the change of each pixel by phenome. This approach unmask divergent phenological signals of change while ensuring consistency in evaluating the magnitude and nature of such change across phenomes.

Prior to the clustering analysis, we performed several preprocessing steps on the data to ensure its compatibility and scaling. We first calculated the 19-year average for each of the 21 phenological metrics per pixel. The eight time variables

(i.e. circular variables measured in day of the year, for example, Start-green) were first transformed to angles and then cartesian coordinates before calculating the 19-year average per pixel. These steps produced a matrix with 10 (EVI variables) + 3 (growing season length variables measured in days) + 8 (sine of day of the year variables) = 21 columns and 345,718 rows. We further reduced the dimensionality of the data using the R command *stats::prcomp*, by applying a principal component analysis to centred and scaled values (mean of 0 and standard deviation of 1). The first 4 principal components explained 92% of the variation in the data and were thus used in subsequent analysis steps. This resulted in a matrix with 4 columns and 345,718 rows subsequently used for clustering.

Phenomes were determined by performing an unsupervised model-based cluster analysis of the data using the R command *mclust::Mclust* (Scrucca et al., 2016). We first estimated the optimal number of clusters using the Bayesian Information Criterion (BIC) on a random 10% subset of the data (34,572 pixels). This step also identified the best Gaussian mixture model required to fit the data (unconstrained covariances, ellipsoidal, varying volume, shape and orientation model ‘VVV’). The identified Gaussian model was then applied to the full data set to classify the phenological data.

We applied a systematic change detection analysis by calculating the differences in the mean of each metric in the first part of the time series (2000-2009) and the second part of the time series (2011-2019) per pixel. Assessing changes in the means of two periods enabled us to reduce the influence of inter-annual variations from masking long-term trends in vegetation phenology. The mean change per pixel was normalised (mean of 0 and standard deviation of 1) by the variance of change within its assigned phenome. We report the magnitude of change in standard deviations (SD). Changed values in SD indicate the extent to which variations deviate from the mean phenological signal. A summary of the methodological workflow is illustrated in Figure 5.

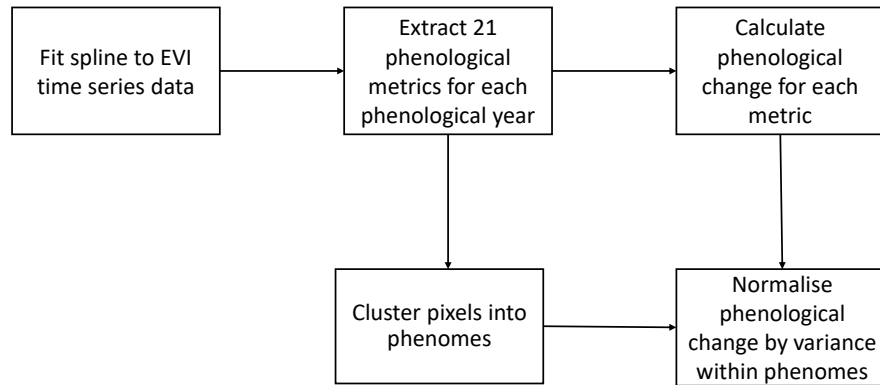


Figure 5: An illustrative workflow indicating the methods applied in this study. These methods were adapted from Buitenwerf et al. (2015).

2.4 Results

2.4.1 Changes in vegetation phenology

We found that for each pixel in our study area, at least one of the 21 examined phenological metrics changed by more than 1 SD (Figure 6). The total change in phenological metrics (Figure 6a) shows that it was primarily driven by changes in vegetation vigour (metrics in EVI units) (Figure 6b) and less driven by changes in the timing of the phenological cycle (metrics in time units) (Figure 6c). The most pronounced changes occurred in Namibia, Botswana, and Zimbabwe, indicating a widespread and homogeneous pattern.

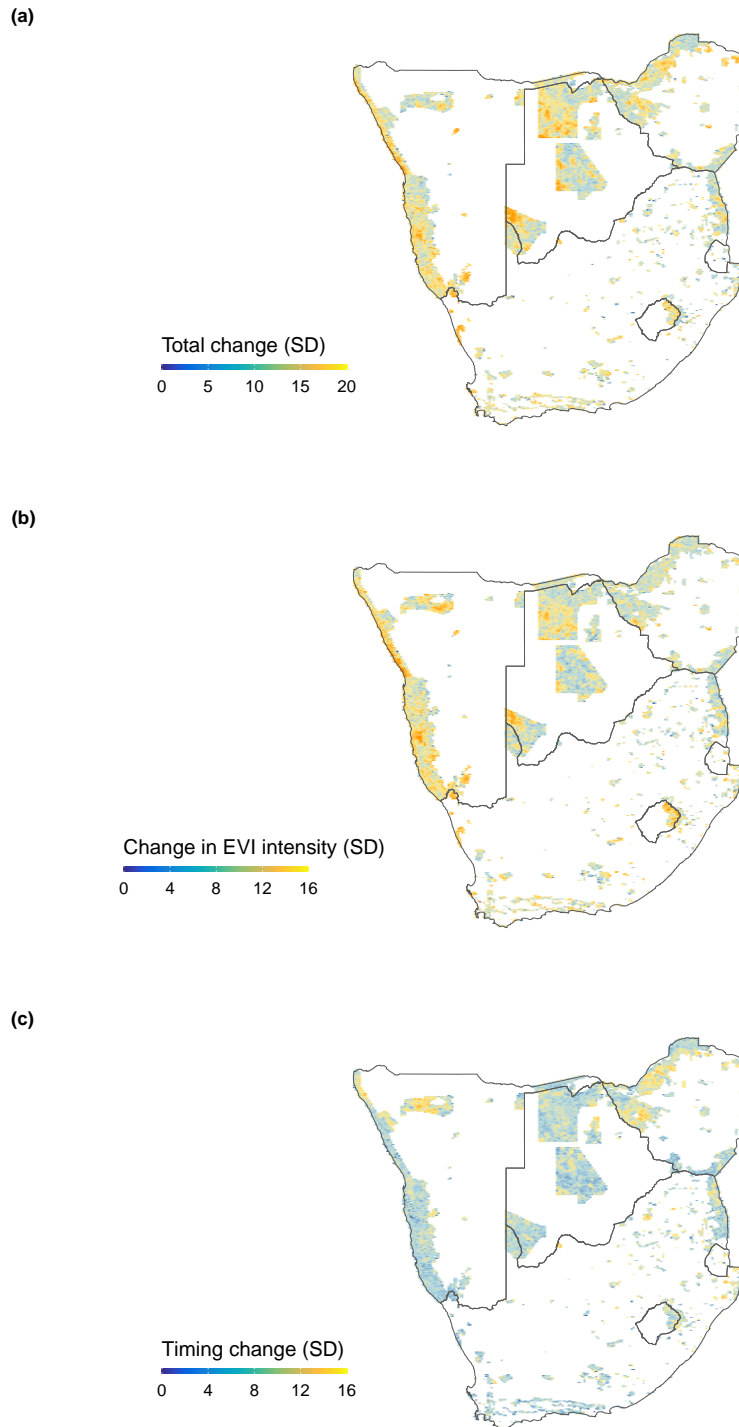


Figure 6: Magnitude of change in vegetation phenology between 2000-2019 expressed in standard deviations (SD). (a), Summed change in 21 phenological metrics. (b), Summed changes in 10 metrics assessing EVI intensity, indicating changes in vegetation vigour. (c), Summed changes in 11 metrics reflecting the timing of the phenological cycle. These metrics were assessed in day of the year (DoY) or days.

Plotting changes in each of the 21 phenological metrics revealed widespread decreases and increases up to 1 SD (Figure 7). For instance, the integral of the annual EVI values decreased in northwest and southwest Namibia, the Drakensberg mountain range bordering South Africa and Lesotho and northern Zimbabwe. Conversely, the integral of the annual EVI values increased in northwestern and southwestern Botswana.

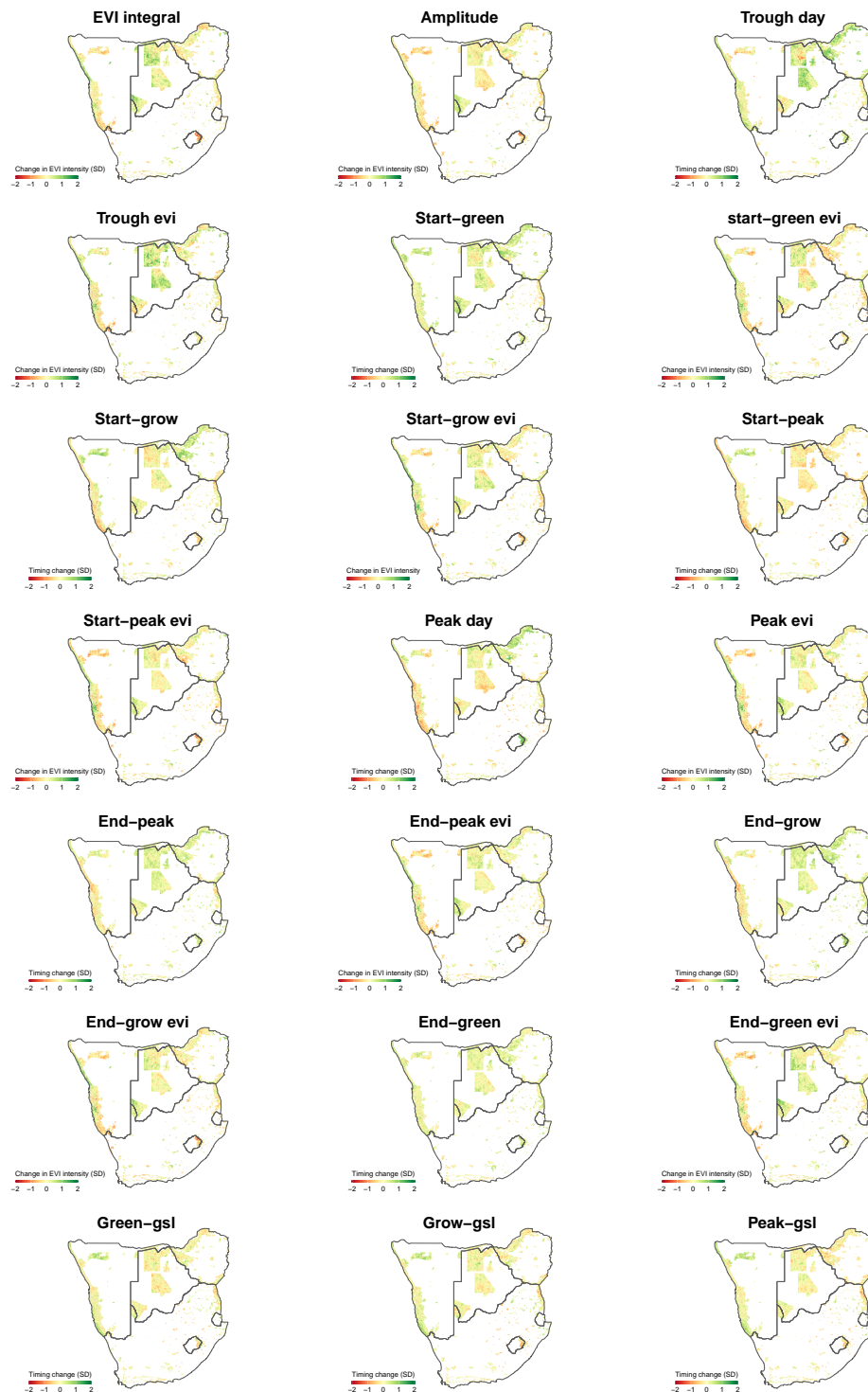


Figure 7: Change in vegetation phenology between 2000-2019 in each of the individual 21 metrics expressed in standard deviations (SD). Some metrics had 2 dimensions (EVI units and time units) while others had 1 dimension (either EVI units or time units). Metrics are defined as in Figure 4.

We also found that the growing season shortened strongly in north-central Botswana, southern Zimbabwe and northeastern South Africa, while it was extended in northern Namibia, northeastern and western South Africa as shown by the Green-gsl, Grow-gsl and Peak-gsl metrics (Figure 7). Changes in the length of the growing season suggest changes in the start and end of the growing season phases in these regions. Most of the changed values were distributed between -1 SD to 1 SD, implying that changes within these range of values was the most common in the study period (Figure 8).

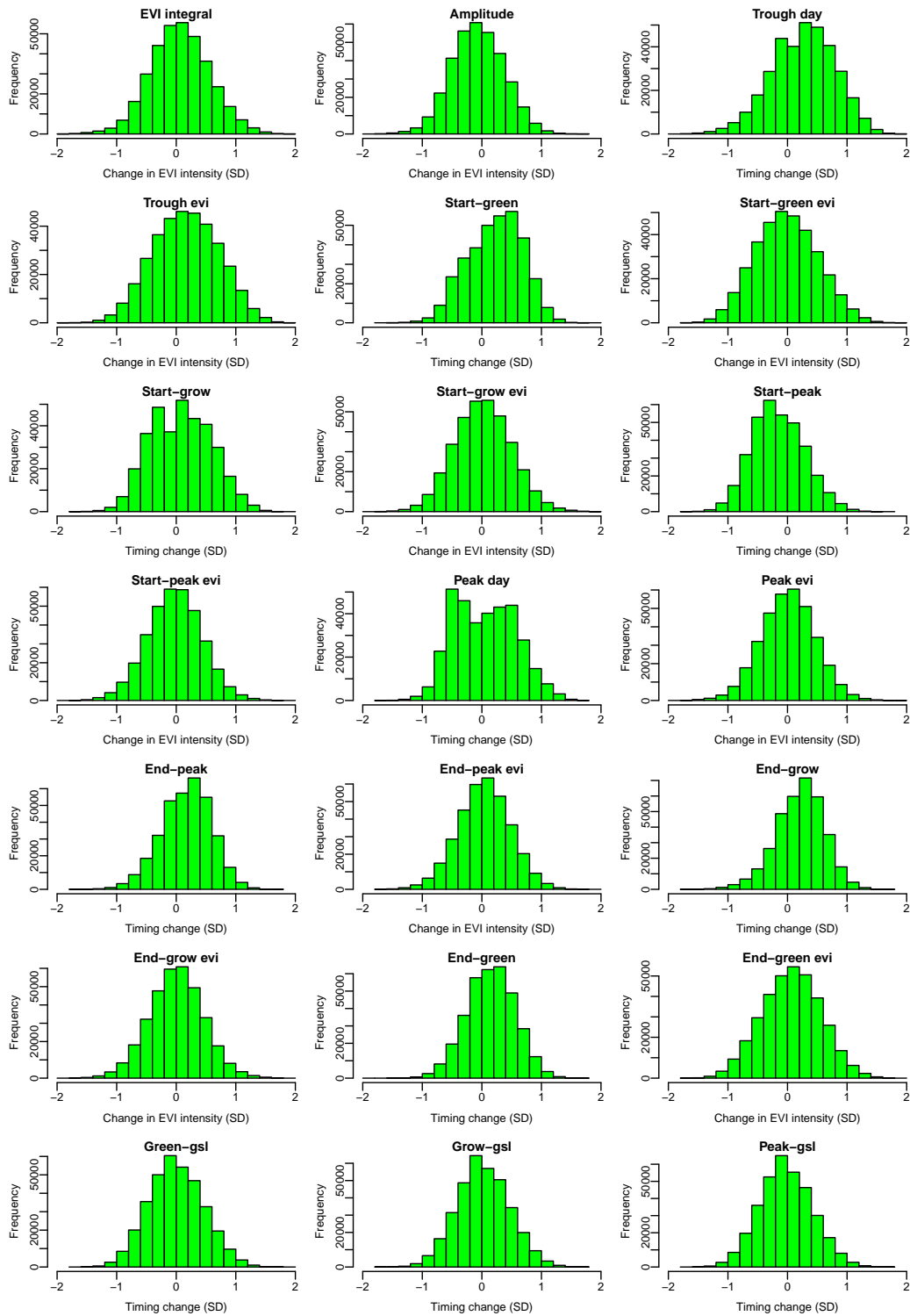


Figure 8: Frequency distribution of changes in vegetation phenological activity between 2000-2019 for each of the 21 metrics, expressed in standard deviations (SD). Some metrics had 2 dimensions (EVI units and time units) while others had 1 dimension (either EVI units or time units). Metrics are defined as in Figure 4.

2.4.2 Phenological change by phenome

A BIC versus cluster number plot revealed that the optimal number of clusters necessary to describe the data was 38. However, we found little variation in BIC values between 7 and 38 clusters (Figure 12). To facilitate interpretation, we therefore used 7 clusters to plot the phenome map (Figure 9). Although our phenome map shows concordance with existing biome maps (Figure 10), it should not be considered a traditional biome map but rather a grouping of EVI and timing metrics. The phenomes were further plotted in a temperature and precipitation space (Figure 13) which is superimposed on Whittaker (1975)'s biome scheme. Our phenomes fall under the 'Temperategrassland/desert', 'Woodland/shrubland' and 'Tropical seasonal forest/savanna' classes along a broad climate range.

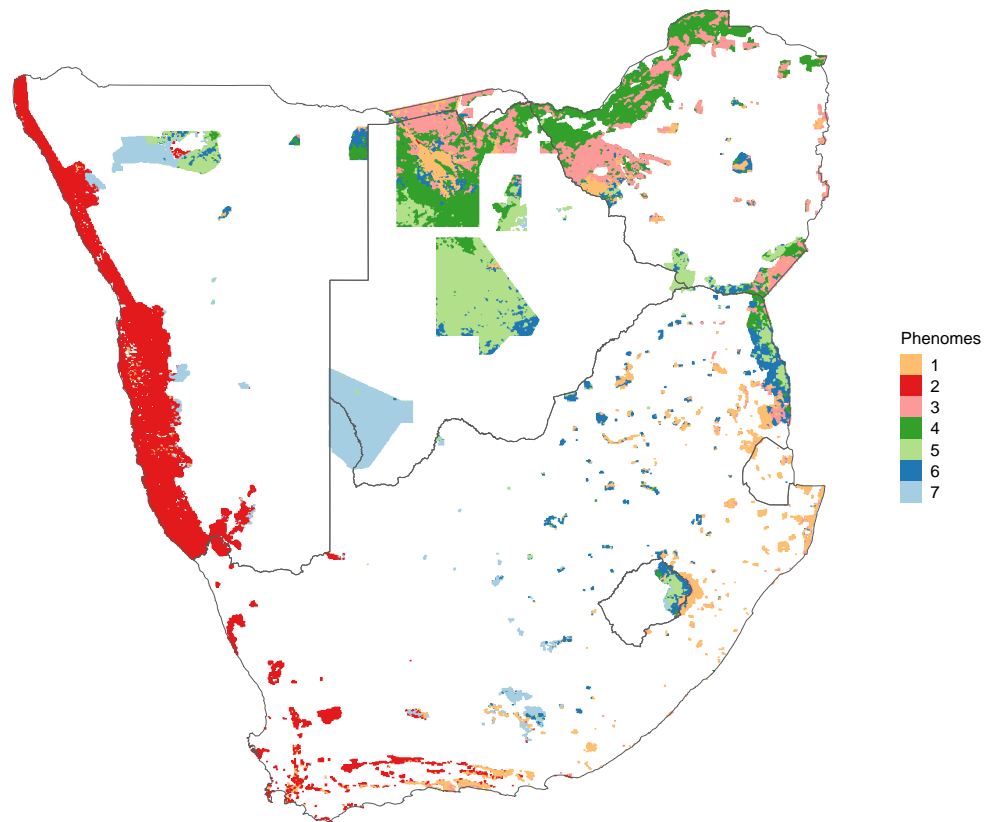


Figure 9: Phenomes of the protected areas of southern Africa. The phenomes were produced by performing an unsupervised clustering of the data. The 7 regions represent zones with similar phenological behaviour. Locations of the protected areas mentioned in the text are labeled with numbers on the map in Figure 14. The geographic coordinates corresponding to each numbered area are detailed in Table VI.

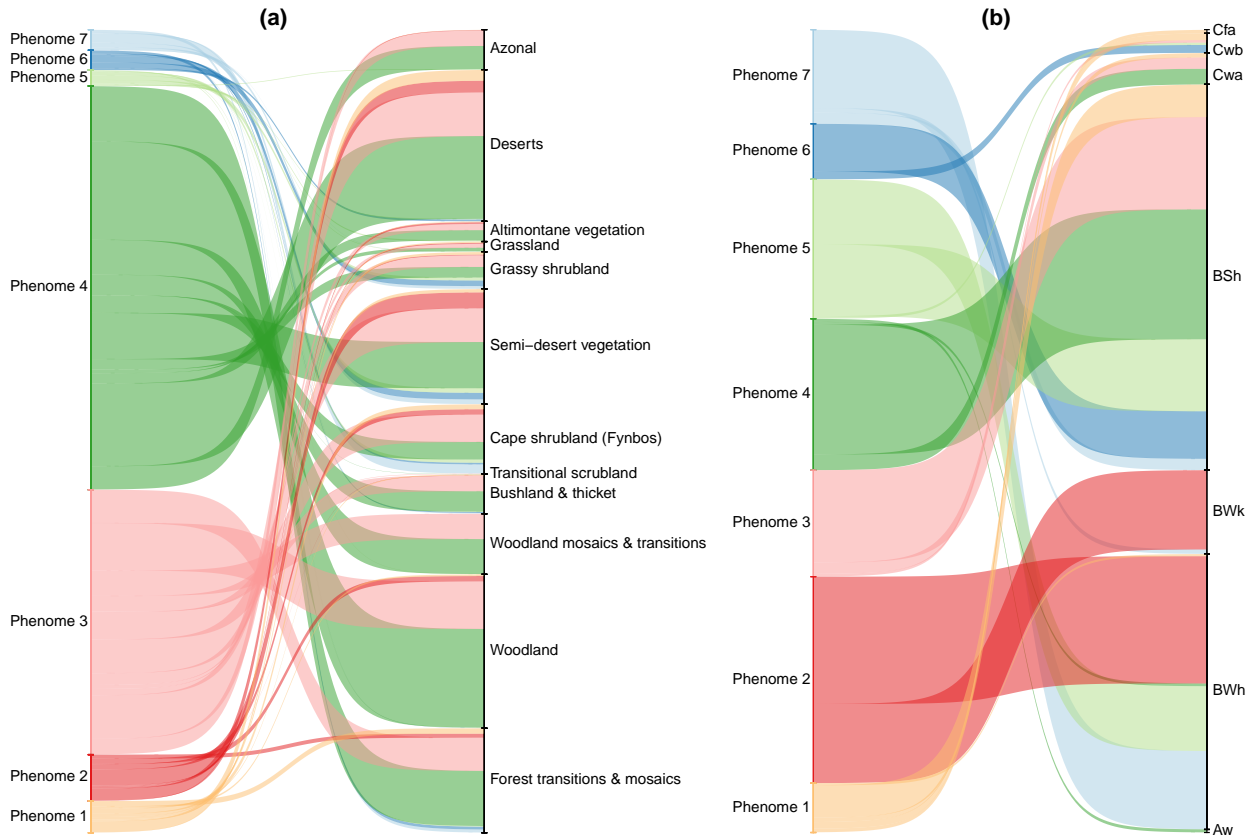


Figure 10: Concordance of our phenomes with (a) White (1983)'s biomes and Beck et al. (2018)'s biomes (b). The biome class names in Beck et al. (2018) are adapted from Peel et al. (2007).

For each phenome shown in Figure 9, we plot the mean phenological signature in the first (2000-2009) and second (2011-2019) parts of the time series in Figure 11. We further plot vectors of change in EVI and time dimensions between the first and second parts of the time series.

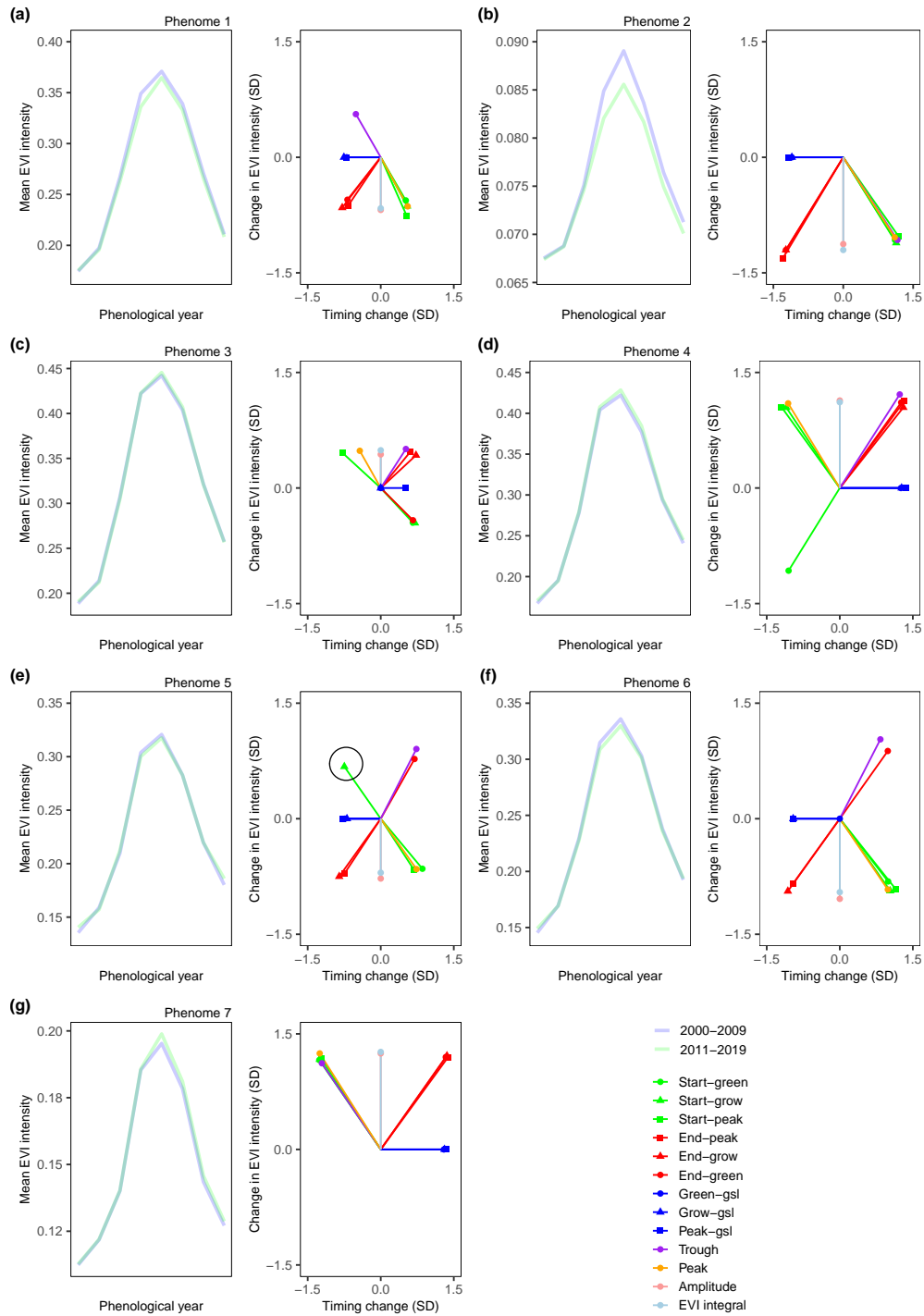


Figure 11: Phenological change by phenome. For each phenome in Figure 9, we plot the mean EVI signal of a phenological year in the first (2000-2009) and second (2011-2019) parts of the time series. We also show vector of change plots for each metric by phenome. The angular vectors represent 2-dimensional metrics (EVI units and time units measured in day of the year) in SD. Vectors parallel to the axes represent 1-dimensional metrics estimated in EVI units or time units (days). The circle under phenome 5 shows change in the metric Start-grow, that is, the timing of the Start-grow metric occurred earlier with an increased EVI value. Metrics are defined as in Figure 4.

Phenome 1 covered a diverse range of Cowling et al. (2004)'s phytogeographical regions. It included elements of the Zambebian region, the Kalahari-Highveld Transition Zone, the Tongaland-Pondoland Region, Afromontane Region and the Cape Region (Figure 15). It spread from the Moremi in northwest Botswana through the Songimvelo in the northeast to the Maloti-Drakensberg in the southeast of South Africa (Figure 14 and Table VI). In this phenome, the dominant trend was an earlier end to the phenological cycle, primarily driven by the earlier end of the growing season metrics. For example, while the Start-green and the Peak day both occurred 2 days later, the End-green occurred 4 days earlier (Table V). The larger shift in the End-green metric ensured that the growing season length (Green-gsl) was shortened by 6 days. Furthermore, the Start-grow, Start-peak, End-grow and End-peak metrics and their associated gsl metrics behaved in a qualitatively similar manner. Consistent with the shortened growing season length, the overall EVI integral decreased, and this trend was enhanced by the lower Green, Grow and Peak EVI metrics, which more than offset the slightly higher trough EVI.

Phenome 2 was primarily distributed in the xeric Karoo-Namib and the Cape regions, spreading southwards from the Skeleton Coast in northwestern Namibia towards the Anysberg in South Africa. Similar to Phenome 1, this phenome was characterized by a shift towards a later start and an earlier end in the phenological cycle. Specifically, the Start-green and Peak day metrics both occurred 1 day later, while the End-green occurred 3 days earlier (Table V). The larger shift in the End-green metric ensured that the growing season length (Green-gsl) was shortened by 4 days. Furthermore, similar qualitative patterns were observed in the metrics Start-grow, Start-peak, End-grow and End-peak, along with their corresponding gsl metrics. Total vegetation activity decreased in this phenome as depicted by declines in the EVI integral and Amplitude metrics, while the Trough day occurred 2 days later with a lower EVI value.

Phenome 3 was mainly distributed in the Zambebian phytogeographical region, spreading from the Bwabwata in northeast Namibia through the Chobe in northern Botswana to the Hwange in northwest Zimbabwe. Further in Zimbabwe, it was distributed in the Charara in the north as well as the Gonarezhou in the south. The dominant trend in this phenome was a later start and later end in the phenological cycle. The Start-green and the End-green metrics both occurred 2 days later, resulting in no change in the Green-gsl metric (Table V). The Start-grow and End-grow metrics also behaved in a qualitatively similar manner. The Peak-gsl was extended by 6 days, primarily driven by an earlier Start-peak metric with 4 days and a later End-peak metric with 2 days. Additionally, the EVI integral and Amplitude increased in this region, consistent with higher Start-peak, Peak, End-peak, End-grow and Trough EVI metrics.

Phenome 4 was mainly distributed in the Zambebian and the Kalahari-Highveld

Transition Zone phytogeographical regions. This phenome stretched from the Moremi in northern Botswana through the Chewore in northern Zimbabwe to the northern parts of Kruger in northeastern South Africa. The phenological cycle in this region was characterized by an earlier start and a later end to the growing season. For instance, the Start-green metric occurred 1 day earlier and the End-green metric occurred 5 days later, resulting in the extension of the Green-gsl metric by 6 days. Furthermore, the Start-grow, Start-peak, End-peak and End-grow metrics and their associated gsl metrics demonstrated similar qualitative behaviours (Table V). These shifts in phenological activity align with observed increases in EVI integral, Amplitude and Trough EVI, providing further evidence of the phenome's dynamics.

Phenome 5 occurred mainly in the Zambebian and the Kalahari-Highveld Transition Zone phytogeographical regions, spreading from eastern Etosha in northern Namibia towards the Kalahari in central Botswana to the eastern parts of Kruger in northeast South Africa and the Tsehlanyane in eastern Lesotho. This phenome showed an overall trend of a later start and an earlier end to the growing season. The Start-grow and End-green metrics which deviated from this trend. Specifically, while the Start-green and Start-peak occurred 3 days later and 1 day later, respectively, the Start-grow occurred 2 days earlier. Similarly, the End-peak occurred 2 days earlier, the End-grow occurred 3 days earlier, and the End-green occurred 1 day later. A later Start-green and a later End-green ensured that the Green-gsl metric was shortened by 2 days. We also observed decreases in EVI integral, Amplitude, and Peak EVI, providing additional evidence of the decline in vegetation productivity in this phenome.

Phenome 6 was primarily distributed in the Zambebian and the Kalahari-Highveld Transition Zone phytogeographical regions, spreading from the Khaudum in northeast Namibia through the Kalahari in central Botswana and extending to the western parts of Kruger in South Africa and the eastern parts of Tsehlanyane in Lesotho. Like Phenome 5, the main trend in the phenological cycle was characterized by a later start and an earlier end to the growing season. The notable exception was the End-green which occurred 2 days later. Furthermore, a later Start-green of 2 days and the later End-green resulted in no change in the Green-gsl metric. However, the Grow-gsl shortened by 12 days, driven by a later shift in the Start-grow by 5 days and an earlier shift in the End-grow by 7 days. The Start-peak and End-peak and their associated gsl metric also behaved similarly. Moreover, the overall EVI integral, Amplitude and Peak EVI decreased in this region, consistent with the overall decline in vegetation productivity.

Phenome 7 was primarily distributed in the Kalahari-Highveld Transition Zone phytogeographical region, extending from western Etosha in northern Namibia through the Kgalagadi in southwestern Botswana to Camdeboo in southern South

Africa. The dominant trend in the phenological cycle was an earlier start and a later end to the growing season. Such phenological activity led to the overall extension of the growing season. In particular, the Start-green occurred 3 days earlier while the End-green occurred 6 days later leading to an extension of the Green-gsl metric by 9 days. The Start-grow, Start-peak, End-grow, End-peak and their corresponding gsl metrics behaved qualitatively similarly. Total vegetation activity increased in this region as shown by increased EVI integral, Amplitude and Peak EVI.

Overall, the phenological patterns detected suggest that the end-of-growing season metrics played a dominant role compared to the start of the growing season metrics.

2.5 Discussion

We assess multi-dimensional changes in the phenological behaviour of vegetation across ecosystems of southern Africa. Our approach has two advantages. First, we focus on natural ecosystems which allows us to minimise land use effects from confounding the detected change. Second, we categorise the study area into regions with similar phenological signatures (phenomes) to account for differences in information content between ecosystems (Buitenwerf et al., 2015). This approach reveals qualitatively different phenological signals that would otherwise be diluted by averaging across pixels and thereby remain unnoticed. We detected substantial changes (at least 1 SD) in each of the 21 metrics used to assess the phenological behaviour of the vegetation of southern Africa. Our findings show that these changes are widespread and qualitatively different. Given that these protected areas do not have land use change effects, we can deduce that the observed changes are primarily driven by climatic forcing.

Our findings support ground-based phenological studies in southern Africa. For example, Masia et al. (2018) reported early leaf drop dates among species grouped in 4 phenological functional groups in northeastern South Africa. This study region in Masia et al. (2018) corresponds to phenomes 1 and 6 in our study. In both phenomes, we found that the end of the growing season metrics (End metrics) occurred earlier in this region. Furthermore, our study also confirms early leaf drop dates observed in *Acacia karroo* species in the Free State province of South Africa (Janecke and Smit, 2011). Their study region falls in phenome 6 in our study. This suggests consistency in phenological patterns between field observations and satellite-based observations.

The findings of this study are also consistent with previous remote sensing-based phenological studies in the region. Our findings agree with the early greening patterns reported by Whitecross et al. (2017) who used MODIS NDVI data to detect early green-up dates along a latitudinal gradient from Zambia to South Africa. Phenome 4 covers portions of their study region and shows an earlier start to the growing season. We detected a decrease in the metric EVI integral in phenome 1 and 6, consistent with Dubovyk et al. (2015), who used MODIS EVI data to attribute the overall decline in vegetation productivity to anthropogenic effects in southern Africa. Therefore, such consistencies with previous studies suggest that our approach is robust in detecting changes in the phenological patterns of the ecosystems of southern Africa.

The extended growing season and increased overall vegetation activity detected in phenomes 3, 4 and 7 suggests an increase in vegetation biomass, which is consistent with increases in vegetation cover reported in these regions (Skowno et al., 2017; Stevens et al., 2017; Venter et al., 2018). In these regions, it has been shown that the start of the growing season metrics are primarily driven by precipitation

and day length (Archibald and Scholes, 2007; Cho et al., 2017; Whitecross et al., 2017). This suggests that early onset of the rainfall season coupled with longer days may trigger plant growth, leading to early initiation of the start of the growing season metrics. Our results also show that the late occurrence of the end of the growing season metrics played a dominant role in these phenomes. The delayed end of the growing season metrics suggest CO₂ effects. Elevated CO₂ enhances carbon uptake and plant growth rates, which also improves water use efficiency. This relieves moisture constraints on plant productivity, resulting in an extended growing season (Peñuelas and Filella, 2009; Higgins and Scheiter, 2012; Martens et al., 2021). However, the CO₂ fertilisation phenomena may be co-limited by moisture, temperature and nutrient constraints (Peñuelas et al., 2017), suggesting that CO₂ effects on plant growth are not ubiquitous and may vary depending on climatic and soil conditions.

The late initiation of the green up metrics detected in phenomes 1, 2, 5 and 6 coincide with evidence in these regions that have reported delayed onset, shortened duration of the rainfall season and frequent dry spells (Kniveton et al., 2009; Davis-Reddy and Vincent, 2017; Trisos et al., 2022)). In these regions, plant growth is strongly related to moisture availability (Higgins et al., 2023a; Wigley et al., 2024). This suggests that soil moisture constraints may hinder the triggering of green up cues of vegetation in these regions. The early initiation of the end of the growing season metrics in these phenomes are consistent with studies that suggest that senescence metrics may be driven by temperature (Cho et al., 2017). Indeed, these phenomes represent regions where temperatures have risen by at least twice the rate of global warming (Engelbrecht et al., 2015), with such warming rates associated with frequent heatwaves (Trisos et al., 2022). This suggests that prolonged and frequent dry spells are further compounded by warming temperatures and higher evapotranspiration rates (Konapala et al., 2020), leading to an earlier end of the growing season. This is because plants may adapt to the changing climatic conditions by closing their stomata or reduce photosynthetic activity to conserve moisture. These phenomes also coincide with regions where disturbances from fire and herbivory have led to losses of woody cover and large trees (Eckhardt et al., 2000; Asner et al., 2009). Disturbances from fire and herbivory can structurally fragment landscapes, thereby exposing the remaining vegetation cover to drought and heat stress.

The increased vegetation activity in phenome 3, 4, and 7, which suggests a greening effect, has implications for biodiversity. Increased biomass in these regions implies that these regions are a carbon sink, and our data might be useful in Net Primary Productivity (NPP) estimates. However, increases in vegetation biomass can also decrease populations of mammal, bird and reptile species that require grassy habitats (Péron and Altwegg, 2015; McCleery et al., 2018). Increased

vegetation cover also promotes invasive species which can alter plant communities and may disrupt ecosystem services (Pejchar and Mooney, 2009). This is true for protected areas as they are susceptible to invasive species compared to non-protected areas (Hiley et al., 2013). Therefore, there may be trade-offs between carbon sequestration and biodiversity loss because of increased vegetation biomass. This study might be useful in guiding management efforts in identifying hotspots of phenological change, where phenological mismatches are likely to be higher (Renner and Zohner, 2018). Management interventions would include removal of invasive species, implementing heterogeneous fire management regimes (Fuhlendorf et al., 2009) and increasing populations of browsers to diversify herbivore functional guilds (Hempson et al., 2015). Such restoration efforts would promote ecosystem resilience.

The decreased vegetation biomass detected in phenomes 1, 2, 5, 6 coincide with regions where warming and drying climates have led to long-term declines in plant and bird biodiversity (Slingsby et al., 2017; McKechnie et al., 2021). This has also led to species migrations (Foden et al., 2007). Where restoration and resilience interventions are not feasible, conservation managers could embrace and facilitate the change. For example, Using field data assessments, conservation managers could identify vulnerable species to drier and warmer climates. Corridors of suitable habitats could then be established to connect current and potential future migrations of vulnerable species. Managers could also promote drought and heat tolerant species (Ouédraogo et al., 2013; Abraham et al., 2019) or increase artificial water sources to safeguard biodiversity.

Remote sensing-based phenological estimates can be influenced by spatial resolution, with phenological metrics extracted at finer scales associated with lower conditional bias (Adole et al., 2018a). We used a coarse 1 km MODIS EVI product if compared to existing alternatives such as the 30 m Landsat series which also has a longer record. It is therefore possible that micro scale changes in phenological activity might go undetected in our analysis. We used the MODIS EVI record because the data has undergone consistent and robust calibration steps (Didan, 2015), which is useful in large scale time series analyses. Our findings are also consistent with both in situ and satellite-based phenological studies as previously highlighted.

There is a lack of ground monitoring phenological networks in Africa compared to other continents (Adole 2016). This limits ground verification of satellite-based phenological estimates. Future studies could incorporate field phenological assessments in satellite-based phenological estimates. For example, citizen science of phenological observations could be incorporated into early warning monitoring systems to validate satellite-based phenological estimates. Restricting our study area to protected areas allows us to exclude land use change as a causal factor,

leaving climate change, nitrogen deposition, CO₂, herbivory and fire, as potential drivers of the detected phenological changes. Future research could use biophysical models to identify and attribute the most important regional drivers that underlie the detected changes. Such analyses will be useful for deepening our knowledge of ecosystem dynamics in the region.

Overall, we reveal widespread changes in the phenological cycle of the vegetation of southern Africa, dominantly driven by the end of the growing season phenological metrics. We detected qualitatively different changes in phenological groups (phenomes). Some phenomes exhibited an extended growing season, suggesting increased vegetation biomass. While other phenomes exhibited a shortened growing season, which suggests reduced vegetation biomass. The magnitude and spatial extent of change revealed here provide clear evidence of contrasting response of vegetation to climate change in the region. The findings of this study may assist conservation managers in identifying hotspots of phenological change, thereby developing monitoring systems to strengthen the capacity for adaptation and mitigation of ongoing ecosystem changes. Future studies could attribute the detected change to environmental drivers, thus improving our understanding of the relative contributions of the forcing factors on changes in vegetation phenology.

2.6 Supplementary Information

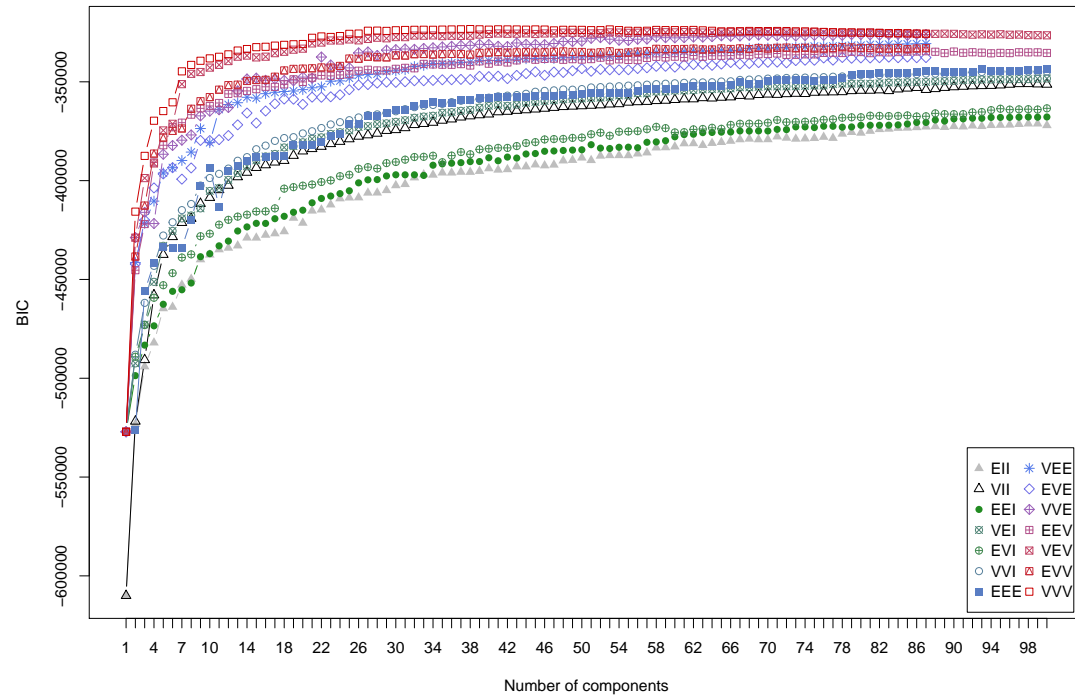


Figure 12: The Bayesian Information Criterion (BIC) was used to determine the optimal number of clusters and the Gaussian mixture model for unsupervised model-based clustering.

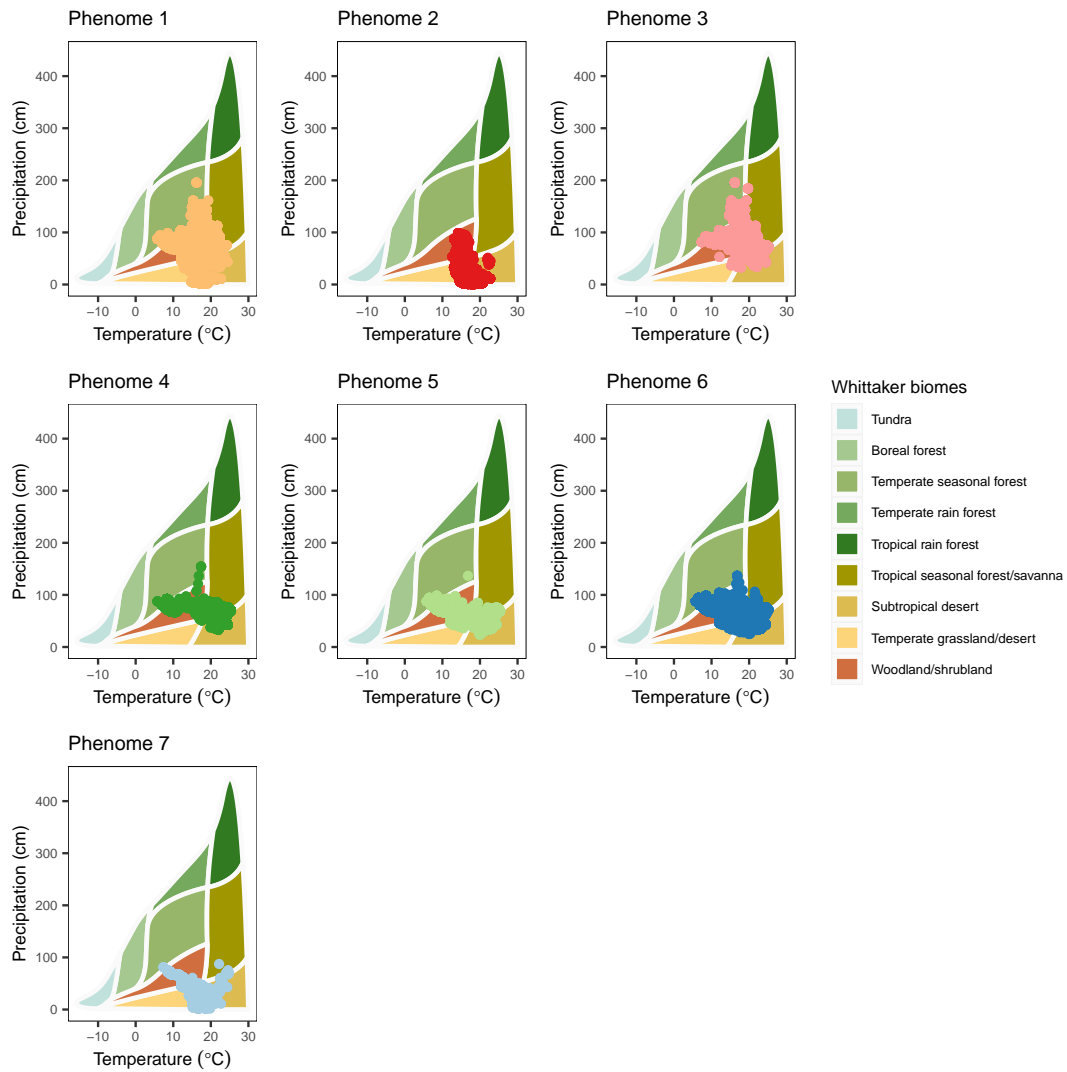


Figure 13: Our phenomes in a climate space. The phenomes were superimposed on Whittaker (1975)'s biome classification scheme and climate space.

TABLE I: A cross-classification between our phenomes vs White (1983)'s biomes.

	Phenome 1	Phenome 2	Phenome 3	Phenome 4	Phenome 5	Phenome 6	Phenome 7
Forest transitions & mosaics	23	17	142	235	3	12	13
Woodland	7	23	203	420	2	1	0
Woodland mosaics & transitions	0	0	108	149	1	0	0
Bushland & thicket	4	1	67	87	2	4	3
Transitional scrubland	0	0	2	1	0	0	0
Cape shrubland (Fynbos)	21	23	117	75	14	7	39
Semi-desert vegetation	14	68	144	197	20	28	20
Grassy shrubland	11	3	50	45	13	24	12
Grassland	5	4	17	15	2	0	1
Altimontane vegetation	3	7	27	44	5	0	0
Deserts	46	50	186	353	3	8	0
Azonal	1	2	66	99	3	0	0

TABLE II: A cross-classification between our phenomes vs Beck et al. (2018)'s biomes. The Beck et al. (2018) biome names are adapted from Peel et al. (2007).

	Phenome 1	Phenome 2	Phenome 3	Phenome 4	Phenome 5	Phenome 6	Phenome 7
Aw	0	0	62	386	5	9	5
BWh	274	16084	0	352	8197	170	9897
BWk	180	10014	0	0	0	0	581
BSh	4112	246	11669	16421	9105	6015	1421
BSk	195	106	7	1	36	226	216
Csb	12	152	0	0	0	0	0
Cwa	554	0	1441	1989	0	40	0
Cwb	841	0	330	108	312	1000	0
Cfa	452	0	37	0	0	13	0
Cfb	339	129	0	0	0	0	0

TABLE III: Average of EVI variables measured over 19 years (2000-2019).

Phenomes	Start-green	Start-grow	Start-peak	Peak	End-peak	End-grow	End-green	Trough	Amplitude	EVI integral
1	0.20	0.26	0.34	0.34	0.27	0.21	0.37	0.17	0.19	13.82
2	0.07	0.07	0.08	0.09	0.08	0.08	0.07	0.07	0.02	3.90
3	0.21	0.31	0.42	0.44	0.41	0.32	0.26	0.19	0.25	15.59
4	0.19	0.28	0.41	0.43	0.38	0.29	0.24	0.17	0.26	13.83
5	0.16	0.21	0.30	0.32	0.28	0.22	0.18	0.14	0.18	10.54
6	0.17	0.23	0.31	0.33	0.30	0.24	0.19	0.15	0.19	11.65
7	0.12	0.14	0.19	0.20	0.18	0.14	0.13	0.11	0.08	7.16

TABLE IV: Average of temporal variables measured over 19 years (2000-2019). The values are presented in day of the year for metrics that represent the start and end of growing season, while values are presented in days for metrics that represent the length of the growing season.

Phenomes	Start-green	Start-grow	Start-peak	Peak	End-peak	End-grow	End-green	Trough	Green-gsl	Grow-gsl	Peak-gsl
1	271	294	237	77	86	124	164	225	252	117	102
2	122	124	132	195	245	264	266	148	217	170	133
3	296	318	163	45	76	117	157	244	224	152	75
4	300	305	109	45	72	109	138	247	193	134	61
5	279	255	116	66	84	118	145	248	191	137	68
6	283	285	165	58	82	120	153	240	216	152	79
7	204	152	99	86	107	138	164	266	179	130	70

TABLE V: Average change in temporal variables in the first (2000-2009) and second (2011-2019) parts of the time series. The values are presented in days.

Phenome	Start green	Start-grow	Start-peak	Peak day	End-peak	End-grow	End-green	Trough	Green-gsl	Grow-gsl	Peak-gsl
1	2	3	2	2	-4	-5	-4	-1	-6	-8	-6
2	1	2	4	1	-6	-3	-3	2	-4	-5	-10
3	2	3	-4	1	2	3	2	2	0	0	6
4	-1	-3	-5	-3	6	6	5	4	6	9	11
5	3	-2	1	2	-2	-3	1	3	-2	-1	-3
6	2	5	7	3	-3	-7	2	1	0	-12	-10
7	-3	-3	-2	-3	10	7	6	-4	9	10	12

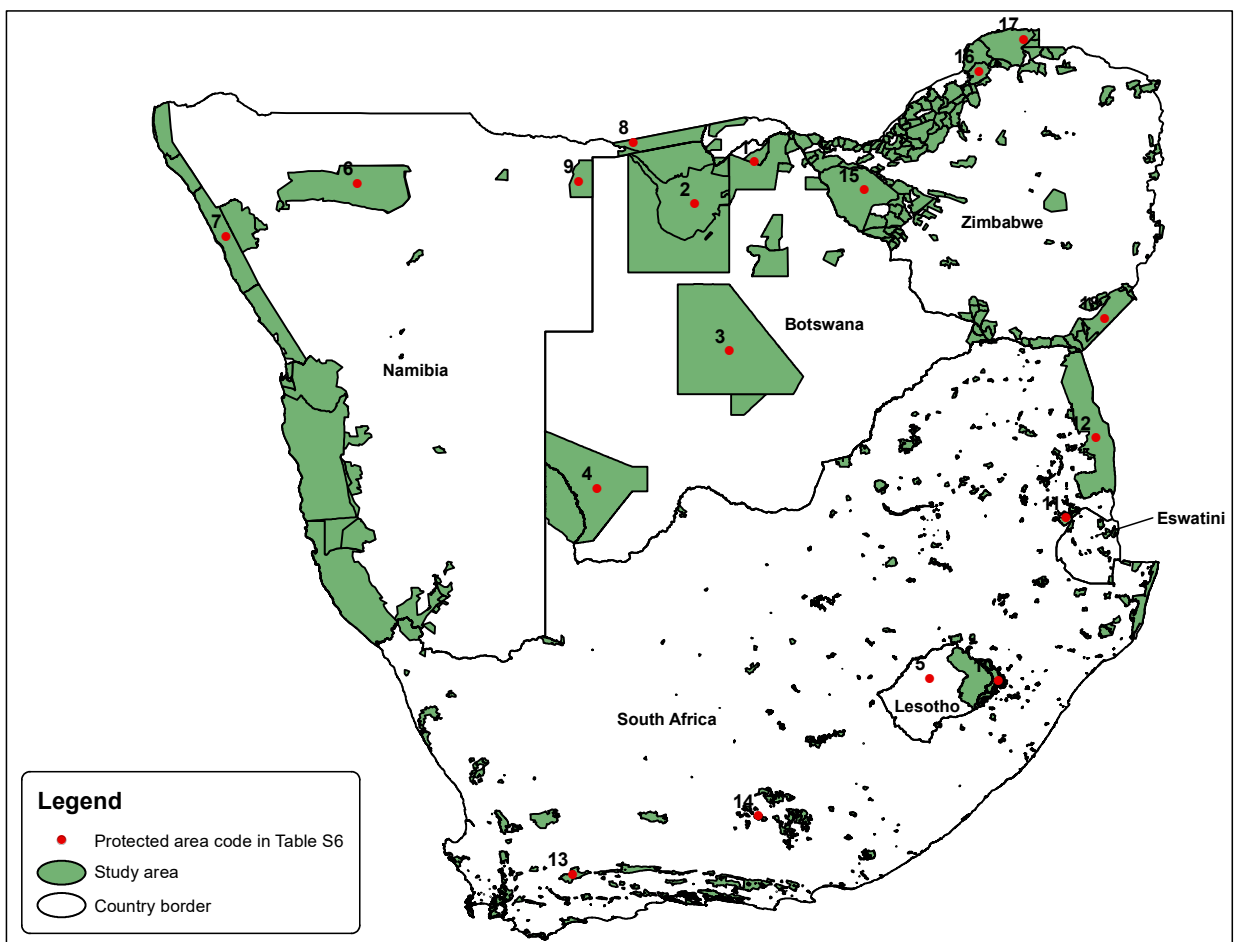


Figure 14: Locations of protected areas discussed in the text, numbered according to the codes in Table (VI).

TABLE VI: Locations of protected areas discussed in the text. The protected area code corresponds to the numbered points in Figure 14.

Protected area name	IUCN classification	Country	Lat	Long	Code
Chobe	National Park	Botswana	-18.421015	24.421832	1
Moremi	Game Reserve	Botswana	-19.310700	23.159593	2
Central Kalahari	Game Reserve	Botswana	-22.409874	23.894009	3
Kgalagadi	National Park	Botswana	-25.313036	21.095487	4
Tsehlanyane	National Park	Lesotho	-29.323878	28.116879	5
Etosha	National Park	Namibia	-18.881923	16.043102	6
Skeleton Coast	National Park	Namibia	-19.987356	13.269609	7
Bwabwata	National Park	Namibia	-18.011045	21.865686	8
Khaudum	National Park	Namibia	-18.837279	20.705816	9
Maloti-Drakensberg	National Park	South Africa	-29.357456	29.567174	10
Songimvelo	Nature Reserve	South Africa	-25.939326	30.996112	11
Kruger	National Park	South Africa	-24.249213	31.622663	12
Anysberg	Nature Reserve	South Africa	-33.463485	20.589365	13
Camdeboo	National Park	South Africa	-32.224315	24.504368	14
Hwange	National Park	Zimbabwe	-19.013810	26.734951	15
Charara	Safari	Zimbabwe	-16.520278	29.161508	16
Chewore	Safari	Zimbabwe	-15.829794	30.102935	17
Gonarezhou	National Park	Zimbabwe	-21.731903	31.814015	18

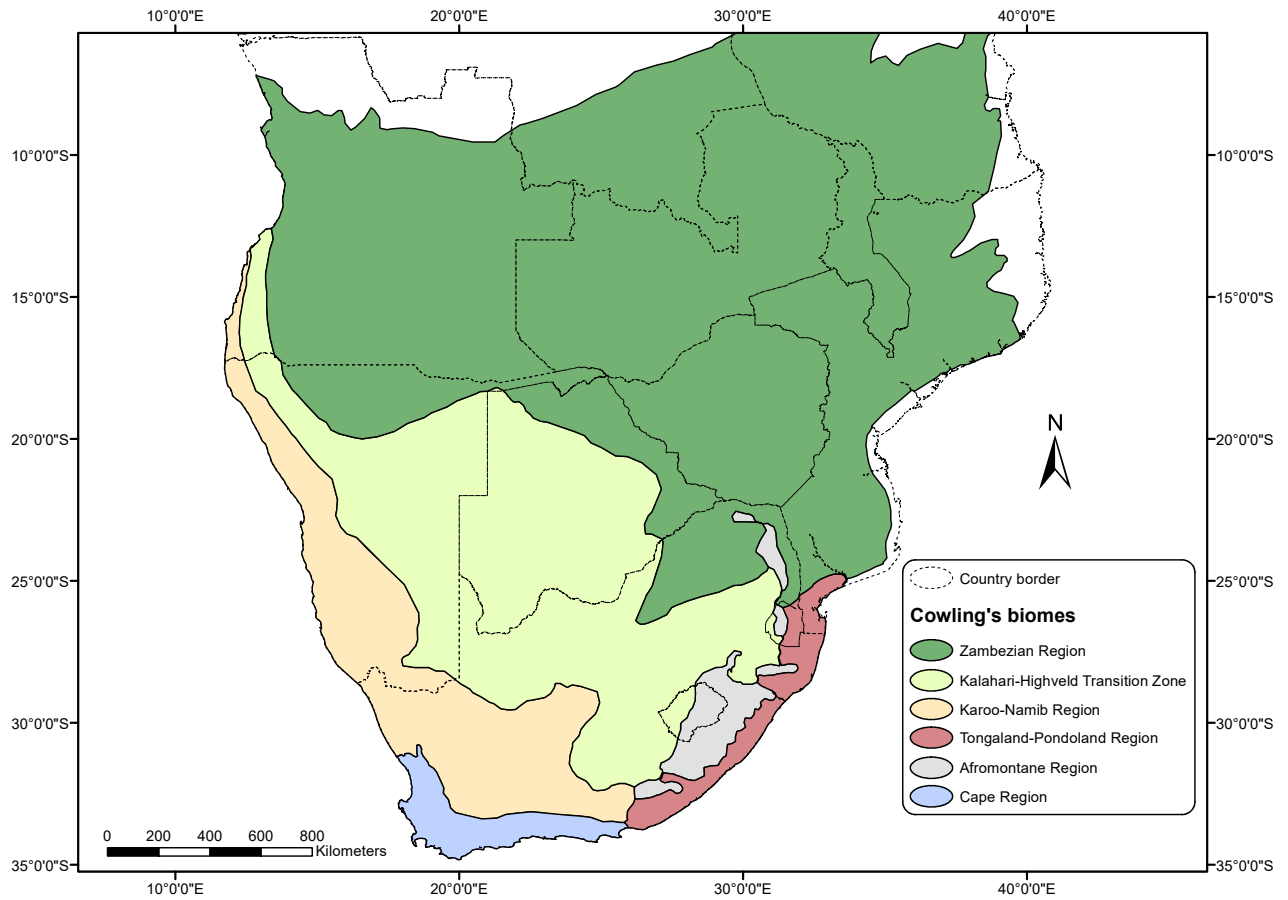


Figure 15: To illustrate the spatial distribution of the phytogeographical regions delineated by Cowling et al. (2004) and discussed in this study, we recreated the boundaries of these regions using a Geographic Information System (GIS).

Chapter 3

3 Assessing changes in the Functional Biomes of southern Africa

3.1 Summary

Biomes are large-scale vegetation zones characterized by similar functional and structural attributes. Biomes are useful in summarizing biogeochemical rates of similar ecosystems, thus improving our understanding of ecosystem function, resilience and how such ecosystems respond to environmental forcing. While global and continental analyses of biome change have been undertaken, less is known about changes in biomes at the regional scale of southern Africa. Here, we classify and assess changes in vegetation units with similar phenology and productivity, defined as Functional Biomes (FB). Our findings indicate that the FB map is homogeneous and that 3% to 15% of pixels shifted in FB state from 2000 to 2021. The FB shifts were qualitatively different. For instance, FB with medium productivity and plant growth limited by both moisture and temperature shifted to higher productive and less seasonal states, while highly productive biomes shifted to less seasonal versions of the same biome or to solely moisture-limited states. Our regional approach provides compelling evidence that suggests that anticipated FB trajectories are already ongoing in southern Africa, with diverging potential consequences for biodiversity and carbon sequestration. This study highlights the importance of understanding biome trajectories for evidence-based decision-making in conservation and management initiatives in response to future changes.

3.2 Introduction

Biomes are large-scale vegetation zones characterized by similar functional and structural attributes (Higgins et al., 2016; Moncrieff et al., 2016). Biomes serve as important constructs that synthesize our knowledge of how vegetation respond to drivers such as climate change and land use change (Conradi et al., 2020). Although there is no universal definition of the biome concept, Schimper’s work (Schimper, 1903) laid the foundation in developing the modern biome concept. Schimper emphasized that the physiological characteristics of vegetation should align in response to climatic and edaphic factors, resulting in recognizable vegetation zones we refer to as biomes. Other work (Walter, 1973; Whittaker, 1975) further expanded on Schimper’s view on the role of climate in shaping biome distribution. Despite the dominant role of climate in shaping terrestrial vegetation (Schimper, 1903; Walter, 1973; Whittaker, 1975), quantifying changes in terrestrial vegetation driven by climate change is a problem facing biogeographical research (Mucina, 2019; Martens et al., 2021). The difficulties in quantifying vegetation change may limit our capacity to develop targeted management responses. Therefore, deepening our knowledge of biome dynamics is important for quantifying and managing changes in ecosystem functioning, as biomes provide a foundational framework for studying vegetation responses to environmental drivers (Mucina, 2019).

Dynamic Global Vegetation Models (DGVMs) are commonly used tools to predict biome response to climatic forcing. DGVMs simulate how ecophysiological processes, such as photosynthesis, growth, competition and consumption interact over large spatio-temporal scales and thereby indicate how biomes might respond to climate change (Prentice et al., 2007). To group vegetation into biome types, DGVMs used model variables like Leaf Area Index of various Plant Functional Types (PFTs) or their fractional cover (Scheiter et al., 2013; Martens et al., 2021). Simulated changes in model variables allow the detection of biomes most vulnerable to future climatic forcing. Despite their utility, it has been recently suggested that DGVMs may misrepresent co-limitation effects of climate, atmospheric CO₂ and nutrient availability on vegetation activity (Smith et al., 2016; Wang et al., 2020b). This may potentially lead to large uncertainties in predicted biome responses to climatic forcing (Martens et al., 2021).

The phytoclimate concept is another prediction tool of biome shifts that has gained recent focus (Conradi et al., 2020; Higgins et al., 2023b; Conradi et al., 2024). Phytoclimes are climatic regions that support a particular combination of plant types. Specifically, the phytoclimes concept uses range modelling of plant species and climate data to reveal spatial attractors for different growth-form combinations that are closely related to biomes (Conradi et al., 2020). This suggests that phytoclimes can be used as an alternative for assessing biome shifts. The

advantage of the phytoclimate concept is that it is a data-driven approach for defining environmental preferences of the growth forms and for delimiting land surface units that have internally similar basins of attraction. This approach overcomes the limitations of expert-based biome concepts by providing a flexible, transparent and repeatable method for constructing fit-for-purpose biome maps (Conradi et al., 2020). However, phytoclimates do not represent actual biomes observed in a region. This is because ecological processes such as species competition, recruitment, dispersal, disturbance (e.g., fire and herbivory) interact over time to ensure that phytoclimates are rarely realized as biome formations (Higgins et al., 2023b).

Earth observation satellites provide opportunities to develop monitoring tools that can be used to assess historical shifts in biomes. The Functional Biomes concept (hereafter FB) classifies biomes as units with shared productivity and phenology (see Higgins et al., 2016). FB is by definition pragmatic, selecting metrics that can be monitored by satellites. Like the phytoclimates concept, the FB emerge from the data, thereby offering an objective approach on how the dominant life forms respond to environmental drivers over time. The advantage of the FB approach is that it is based on satellite data records, thus directly provide empirical evidence of changes in actual biomes in a region. Despite their importance, assessments of FB have been limited to global scales (Higgins et al., 2016). This is despite studies documenting that the response of vegetation to environmental drivers varies regionally (Zhu et al., 2016; Venter et al., 2018; Trisos et al., 2022). Furthermore, global analyses may be contaminated by the confounding effects of climatic forcing and land use change. In some cases, land use change often override climate change effects on vegetation activity (Sirami et al., 2017; Venter et al., 2018), making difficult to infer whether the observed shifts in vegetation activity are driven by climatic forcing or land use change.

Protected areas may provide a solution in separating climate change and land use change signals on FB dynamics. Protected areas are geographic boundaries designated to conserve biodiversity while remaining free of land use effects (UNEP-WCMC and IUCN, 2021). Such boundaries include forest reserves, nature reserves, game parks and national parks. One of these protected areas is the protected areas of southern Africa, which has a rich floristic diversity and high levels of endemism (Cowling et al., 2004). Despite its importance to global biodiversity, the region of southern Africa has been identified to be a hotspot of climate change effects on vegetation activity (Engelbrecht and Engelbrecht, 2016; Davis-Reddy and Vincent, 2017; Niang et al., 2014; Trisos et al., 2022; Parmesan et al., 2022). Yet how the vegetation of southern Africa is changing in response to climate change remains poorly understood.

To assess how the vegetation of southern Africa may respond to climatic forcing, previous work have used species distribution models (SDMs) to predict fu-

ture biome shifts (Rutherford et al., 1999; Higgins et al., 2023b). For example, Rutherford et al. (1999) used a species distribution model to predict widespread distribution of the biomes of South Africa and selected key plant species driven by climatic forcing. Higgins et al. (2023b) used a physiological plant growth model fitted for over 5000 vascular plant species data to predict widespread changes in phytoclimate state. The study also finds differences in the timing of the change within the region, with the central interior forecast to change earlier than the arid west and southern parts of the region. The differences in the timing of change were primarily driven by differences in the response of responses of trees, succulents, C3 and C4 grasses to the global circulation models (GCMs) forecasts.

However, when used as predictive tools, SDMs do not provide empirical evidence on how biomes in a region are actually responding to drivers such as climate change. SDMs rather forecast potential biome shifts based on model assumptions about species-environment interactions and future climate scenarios, potentially introducing uncertainties. Therefore, they may not provide direct measurement of changes in vegetation activity, which is necessary for evidence-based management responses.

Another commonly used biome map is the Mucina and Rutherford (2006) map. Mucina and Rutherford (2006) combines a data-driven approach with expert knowledge to define biomes. Biomes are aligned precisely with floristically determined boundaries through a bottom-up approach. This map shows actual biomes that exist in the region. Although this map is useful, its static nature makes it less appropriate for tracking biome changes. Therefore, we still lack a comprehensive understanding of the distribution of the FB of southern Africa, their shifts over time, which may inform their potential shifts in the future.

The goal of this study is to map the FB of the major protected of southern Africa (Figure 3) and then track shifts in FB state over a 21-year period. To achieve this, we applied a data-driven approach, such that the biomes emerge from the data rather than being subjectively defined. We built on the monitoring tool developed by Higgins et al. (2016) and used two attributes to classify FB. The first attribute is the vegetation productivity index (VPI), and the second attribute is based on growth limitation indices. Higgins et al. (2016) additionally used vegetation height to classify FB, but we do not use height in this study since products describing vegetation height do not exist at the temporal resolution needed for this analysis. The VPI mimics how the transformation of the Fraction of Photosynthetic Active Radiation (FPAR) into carbon assimilation is further co-limited by environmental forcing factors. The growth limitation indices indicate whether vegetation growth is limited by moisture or temperature or both moisture and temperature or non-seasonal. In ecosystems such as Savanna, winter conditions are associated with dryness and coldness, yet warm enough to support vegetation

activity. Therefore, attributing limitations solely to one climatic factor could be misleading when the interactions between the climatic factors are complex. We thus cautiously use the term ‘limited’ as a hypothesis, acknowledging the potential correlation between moisture and temperature and their dual influence on plant growth. The attributes used to classify FB are derived from the time series of the Enhanced Vegetation Index (EVI) and climate reanalysis data. These regional insights complement existing global knowledge, thereby offering a nuanced understanding of biome dynamics in southern Africa.

3.3 Materials and Methods

We used the EVI MOD13A2 product from the Moderate Resolution Imaging Spectroradiometer (MODIS) program (downloaded from <https://lpdaac.usgs.gov/products/mod13a2v006/>). The compositing algorithm for the MOD13A2 product selects the most unbiased estimate of the EVI of each pixel within a 16-day window. The selection is based on criteria such as lowest cloud cover, lowest aerosol content, lowest angle view (Didan, 2015). The resulting 1 km EVI product is an atmospherically corrected dataset (Didan, 2015). Each observation is provided with a data quality score (labelled Q = 0, 1, 2, 3 where = 0 is good and 3 is poor due to cloud cover). EVI data ranging from 2000 to 2021 constituted our time series.

Despite the robustness of the MODIS compositing algorithm, time series EVI data can contain missing values caused by cloud cover, sensor malfunction and orbital drifts of satellites. To account for the missing data, we used a two-step approach. First, the missing data of each pixel was linearly interpolated (using R (R Core Team, 2022) command `stats::approx`). Second, the interpolated data was further linearly filtered (command `stats::filter`). We then fitted a cubic spline to smooth the linearly filtered data (command `stats::smooth.spline`), and the smoothed spline was used to extract phenological metrics that represent a plant's growing season (Buitenwerf et al., 2015). Defining the start of the time series for each pixel required a two-step approach. First, the trough day, defined as the mean day of the year of the annual minimum EVI value, was estimated for the time series. This 21-year average provides a rough estimate of the trough day. Second, the exact trough day for each phenological year was calculated within a 180-day window around the 21-year mean trough day. The number of days between two successive trough days represents a phenological year. The amplitude of EVI was estimated by calculating the difference between the highest EVI value (peak day EVI) and the lowest EVI value (trough day EVI) for each phenological year. These steps produced a 21-year time series of EVI, annual trough days of EVI, annual amplitude of EVI and annual peak days of EVI for 345,718 pixels.

3.3.1 Functional Biomes classification scheme

We used two attributes to define and map the Functional Biomes of southern Africa. The first attribute is the vegetation productivity index (*VPI*). The second attribute is the growth limitation index. Both were based on metrics provided by Higgins et al. (2016), although we adapt them for this study as explained in the next sections. To calculate the *VPI*, we assume that EVI can be used as a proxy for the fraction of photosynthetically active radiation (FPAR) absorbed by leaves (Running and Zhao, 2015). While Higgins et al. (2016) used the Normalised

Difference Vegetation Index (NDVI) as a proxy for FPAR, we chose EVI because of its superior sensitivity in dense vegetation and reduced sensitivity to soil and atmospheric contamination (Didan, 2015). We further consider how environmental factors soil moisture (M), temperature (T) and solar radiation (S) co-limit the conversion of FPAR into assimilated carbon. Therefore, VPI is denoted by

$$VPI = EVI f(M) g(T) S. \quad (1)$$

The function $f(M)$ is denoted by

$$f(M) = \max \left(0, \min \left(1, \frac{M - WP}{FC - WP} \right) \right), \quad (2)$$

where FC and WP are the field capacity and wilting point, respectively. Soil moisture (M) is the ERA5-Land reanalysis (European Centre for Medium-Range Weather Forecasts Reanalysis version 5; ERA5, hereafter) time series product of monthly volumetric water in soil layer 1 (0 - 7 cm) (downloaded from <https://doi.org/10.24381/cds.68d2bb30>, variable name 'swvl1', units $\text{m}^3 \text{m}^{-3}$, spatial resolution 11 km but resampled to 1 km using the command `terra::resample`, method `bilinear`). We used a smoothed cubic spline to interpolate values of M for each study pixel. For FC and WP , we use 1 km raster datasets (Dai et al., 2019) (downloaded from <http://globalchange.bnu.edu.cn/research/soil5.jsp>).

The polynomial function $g(T)$ mimics how C3 photosynthesis responds to normalized temperature changes (Yamori et al., 2014),

$$g(T) = \max(0, -2.42 + 0.0937T - 0.00177T^2). \quad (3)$$

Temperature (T) is the ERA5 monthly time series product of average air temperature at 2 m above the land surface (downloaded from <https://doi.org/10.24381/cds.68d2bb30>, variable name 't2m', units $^{\circ}\text{C}$, spatial resolution 11 km but resampled to 1 km using the command `terra::resample`, method `bilinear`). We used a smoothed cubic spline to interpolate values of T for each study pixel. Solar radiation (S) is the ERA5 time series product of monthly surface solar radiation downwards (downloaded from <https://doi.org/10.24381/cds.68d2bb30>, variable name 'ssrd', units W m^{-2} , spatial resolution 11 km but resampled to 1 km using the command `terra::resample`, method `bilinear`). We used a smoothed cubic spline to interpolate values of S for each study pixel. We calculated the total VPI for each phenological year and categorized the results into three groups (High VPI (H) = ≥ 6500 , Medium VPI (M) = > 2500 and < 6500 , Low VPI (L) = < 2500) for further analysis steps. The VPI values were calculated for each pixel.

The second FB attribute provides insights into the relative limitations imposed by soil moisture and temperature on plant growth (Higgins et al., 2016). We use the moisture index (d) to define moisture limitation effects such that

$$d = \frac{(1 - q_{td}(M)) N_a}{N_{pd}}. \quad (4)$$

where $q_{td}(M)$ is a quantile that represents the relative position of the moisture level on the trough day compared to the distribution of all moisture values in a phenological year. That is, $q_{td}(M)$ is a quantile that quantitatively informs how dry the trough day is compared to other days of the year. Figure 16 represents this relationship graphically. M is defined as in equation 2 while the components N_a and N_{pd} are the annual amplitude of EVI and annual peak day EVI, respectively. The ratio between N_a and N_{pd} is a measure of seasonality. A higher ratio suggests greater seasonality, indicating more pronounced fluctuations in vegetation greenness within a phenological year relative to the peak day EVI. The values of d range between 0 and 1. A larger value of (d) indicates greater limitation due to soil moisture availability while a smaller value indicates lesser limitation. The values of d were calculated for each pixel.

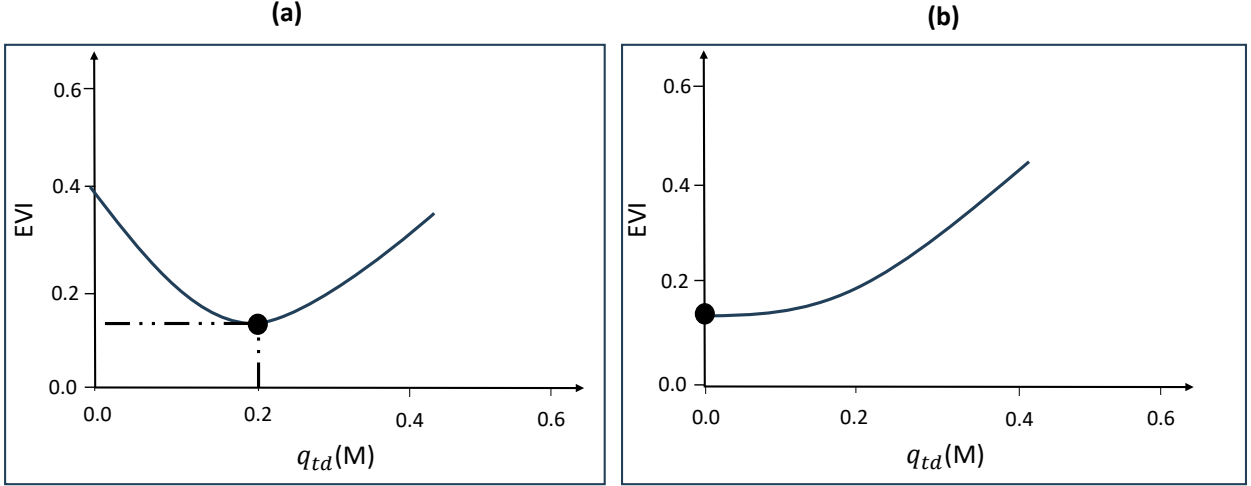


Figure 16: Graphical representation of the relationship between the trough day moisture quantile $q_{td}(M)$ and EVI, a proxy for vegetation activity. (a) Scenario 1: When the driest day does not coincide with the trough day (high $q_{td}(M)$, value of 0.2 in this example), this suggests that factors other than moisture constrained plant growth on the trough day. (b) Scenario 2: When the driest day coincides with the trough day (low $q_{td}(M)$, close to 0 in this example), this suggests that the decline in EVI was likely due to drought. The temperature index (c) uses the same logic as the moisture index (d), with $q_{td}(T)$ acting as the analogous quantile for temperature.

We use the temperature index to (c) to define temperature limitation effects such that

$$c = \frac{(1 - q_{td}(T)) N_a}{N_{pd}}. \quad (5)$$

where $q_{td}(T)$ is a quantile that represents the relative position of the temperature level on the trough day compared to the distribution of all temperature values in a phenological year. That is, $q_{td}(T)$ is a quantile that quantitatively informs how cold the trough day is compared to other days of the year. T is defined as in equation 3. Similar to d , the values of c range between 0 and 1. A larger value indicates greater limitation due to temperature conditions while a smaller value indicates lesser limitation. The values of c were calculated for each pixel.

We defined vegetation as moisture-limited (M) if $d > 0.15$ and $c \leq 0.2$, cold-limited (C) if $d \leq 0.15$ and $c > 0.2$, limited by both moisture and cold (B) if $d > 0.15$ and $c > 0.2$, and non-seasonal (N) if $d \leq 0.2$ and $c \leq 0.15$. We then used

the three *VPI* categories and the four growth limitation categories to group pixels into zones we call Functional Biomes (FB).

We tested for significant ($P < 0.05$) temporal trends to assess whether the categorized biomes are inherent to the data rather than an artefact of the subjective threshold selections. We applied simple linear regression models to the index values (*VPI*, *d* and *c*) of each pixel as a function of time (R command `stats::lm`). The regression analyses allow us to detect changes in *VPI*, *d* and *c* independent of where the cut-offs are placed, which would confirm the appropriateness of our threshold selections.

Annual maps for the 21-year time series of FB, *VPI*, *d*, and *c* are available in the Zenodo repository (Muhoko and Higgins, 2024).

3.3.2 Functional Biomes change analysis

The FB classification scheme used in this study offers the capability of monitoring biome shifts over time. Using multinomial logistic regression (R command `nnet::multinom` (Venables and Ripley, 2002)), we examined the 21-year time series of each pixel to determine if time had a statistically significant effect on FB states. We used the modal FB state of each pixel for the initial 10 years of the time series to define our reference state for the multinomial logistic regression analysis. FB transitions were only recognized when time significantly influenced the likelihood of observing a change in FB state (Z-test, $P < 0.05$). In situations where multiple significant transitions were observed for a pixel, we chose the transition with the highest Z-statistic as it provided the most robust statistical support. For example, if a pixel was detected as transitioning from MB (medium VPI, both moisture and temperature-limited) to MD (medium VPI, moisture-limited) (Z-score = 2.5) and also from MB to HN (high VPI, non-seasonal) (Z-score = 3.2), we would only report the MB to HN transition in the results since it showed stronger statistical evidence (higher Z-score) for a shift between those biome states over the time series.

3.4 Results

3.4.1 Functional Biomes of southern Africa

The biome classification was conducted annually for the entire time series, generating the plotted FB map (Figure 17). The FB map shows that the classes form contiguous zones. We use a two-letter convention to name the biomes: the first letter represents the vegetation productivity index (VPI) and can either be low (L), medium (M), or high (H), while the second letter indicates whether the trough of EVI is either dry-limited (D), cold-limited (C), both dry and cold-limited (B) or non-seasonal (N). The most common biome classes were MB (medium VPI and both dry and cold-limited), HB (high VPI and both dry and cold-limited) and LN (low VPI and non-seasonal), while HN (high VPI and non-seasonal), LB (low VPI and both dry and cold-limited) and HD (high VPI and dry-limited) were the least common.

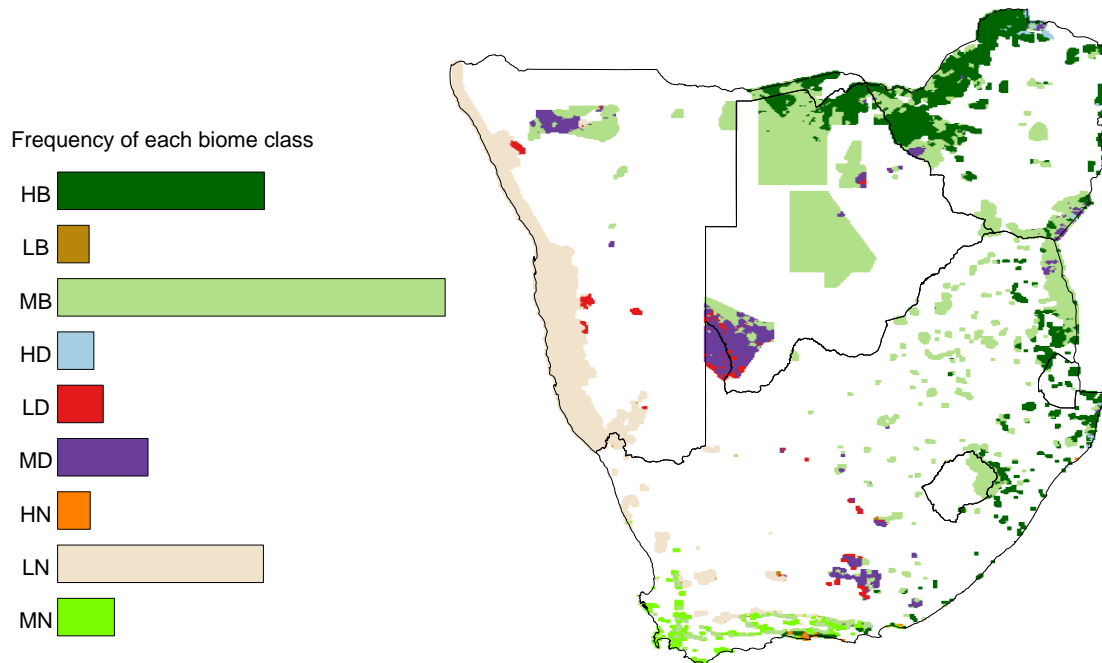


Figure 17: Functional Biomes (FB) of the major protected areas of southern Africa categorized using the vegetation productivity index (VPI), the dry limitation index and the cold limitation index. Plotted here are the most common (modal) FB assignments made for each pixel over the 21-year time series. The locations of the protected areas mentioned in the text are indicated by numbers in Figure 23 and their corresponding geographic coordinates are provided in Table VIII. The FB names are derived from two letters, the first letter is either L, M or H and indicates low, medium and high vegetation productivity index (VPI) and the second letter is either D, C, B or N and indicates whether the growth limitation index is either dry, cold, both dry and cold or non-seasonal.

Our FB spanned a wide variety of Cowling et al. (2004)'s phytogeographical regions (Figure 24). The biome type HB covered components of the Zambebian Region and Tongaland-Pondoland Region. It spread from the Caprivi in northeastern Namibia and the Chobe in northern Botswana towards the Hwange in northwestern Zimbabwe. Still in northern Zimbabwe, it further covered the Charara, the Mana Pools and Chewore Safari towards the Nyanga in the east. In South Africa,

this biome spread from the Songimvelo to the iSimangaliso in the east. This biome was characterized by high vegetation productivity with plant growth limited by both moisture and temperature. The biome LB mostly covered the Karoo-Namib Region. It spread from the Gondwana in southern Namibia to the Steenbokkie in southern South Africa. This biome was characterized by low vegetation productivity with plant growth limited by both moisture and temperature.

The MB biome type covered the Zambezi Region and the Kalahari-Highveld Transition Zone. It spread from east of Etosha in north-central Namibia through north-central Botswana in the Moremi and the Kalahari towards the Hwange and Gonarezhou in northwestern and southern parts of Zimbabwe, respectively. In South Africa, this biome covered the Kruger in the northeast to the Marakele in the north towards the Tsehlanyane in Lesotho. This biome was characterized by medium vegetation productivity with plant growth limited by both moisture and temperature.

Dry-limited biomes were more restricted. The HD biome mostly occurred in the Zambezi Region of the Mzarabani in northern Zimbabwe. It was characterized by high vegetation productivity with plant growth solely limited by moisture. Furthermore, the LD biome covered the Kalahari-Highveld Transition Zone, spreading from the Torra in northwestern Namibia, the Gemsbok in southwestern Botswana to the Camdeboo in southern South Africa. Furthermore, this biome was characterized by low vegetation productivity with plant growth solely limited by moisture. The MD biome mainly covered the Zambezi Region and Kalahari-Highveld Transition Zone, it spread from Etosha in northwestern Namibia, the Gemsbok in southwestern Botswana and to the Asanta Sana in southern South Africa. This FB was characterized by medium vegetation productivity with plant growth solely limited by moisture.

The HN biome (high VPI, non-seasonal) was restricted to the Cape Region and mostly occurred in the Garden Route. The LN (low VPI, non-seasonal) biome mostly covered the Karoo-Namib Region. This biome spread southward, from the Skeleton Coast in northwestern Namibia to the Anysberg in western South Africa. In addition, the MN (medium VPI, non-seasonal) biome occurred in the Cape Region, spreading from the Grootwinterhoek to the Garden Route of southern South Africa.

The distribution of this study's FB closely align with Mucina and Rutherford (2006)'s biomes. For example, the MB and MD align with the Savanna, the HB and HD with the miombo woodlands, biome type LN with the Namib desert and the Succulent-Karoo biomes, while the HN and MN align with the Fynbos.

The matrix-classification of the FB map (Figure 17) with White (1983)'s map showed both similarities and differences (Table VII). For instance, the MN (medium VPI, non-seasonal) corresponds to Cape shrubland (Fynbos) in the White (1983)

map, while the LN (low VPI, non-seasonal) corresponds to Deserts. The MB (medium VPI, both moisture and cold limited) biome mostly align with the Woodland, Woodland mosaics & transitions, and Bushland & thicket biome. Notable groups that did not correspond to the White (1983) map were also observed. For example, the Forest transitions & mosaics comprised two of our biomes (MB and HB), while Woodland comprised three of our biomes (MD, MB and HB).

We plot the FB's in the temperature and precipitation biplot used by Whittaker (1975). (Figure 18) shows that our FB's are reasonably segregated by climate. Unsurprisingly, most of our biomes were located in warmer parts of the Whittaker biplot associated with low precipitation in classes such as Temperate grassland/desert, Subtropical desert, Woodland/shrubland, and Tropical seasonal forest/savanna. Moreover, the biome sites limited by both moisture and temperature (ending in B) were located at a wide temperature gradient, while biomes limited by moisture or non-seasonal (ending in D or N) were located at a narrow temperature gradient. The consistency of the FB map with the region's established biome maps suggests that our functional approach offers a nuanced yet robust method for biome classification.

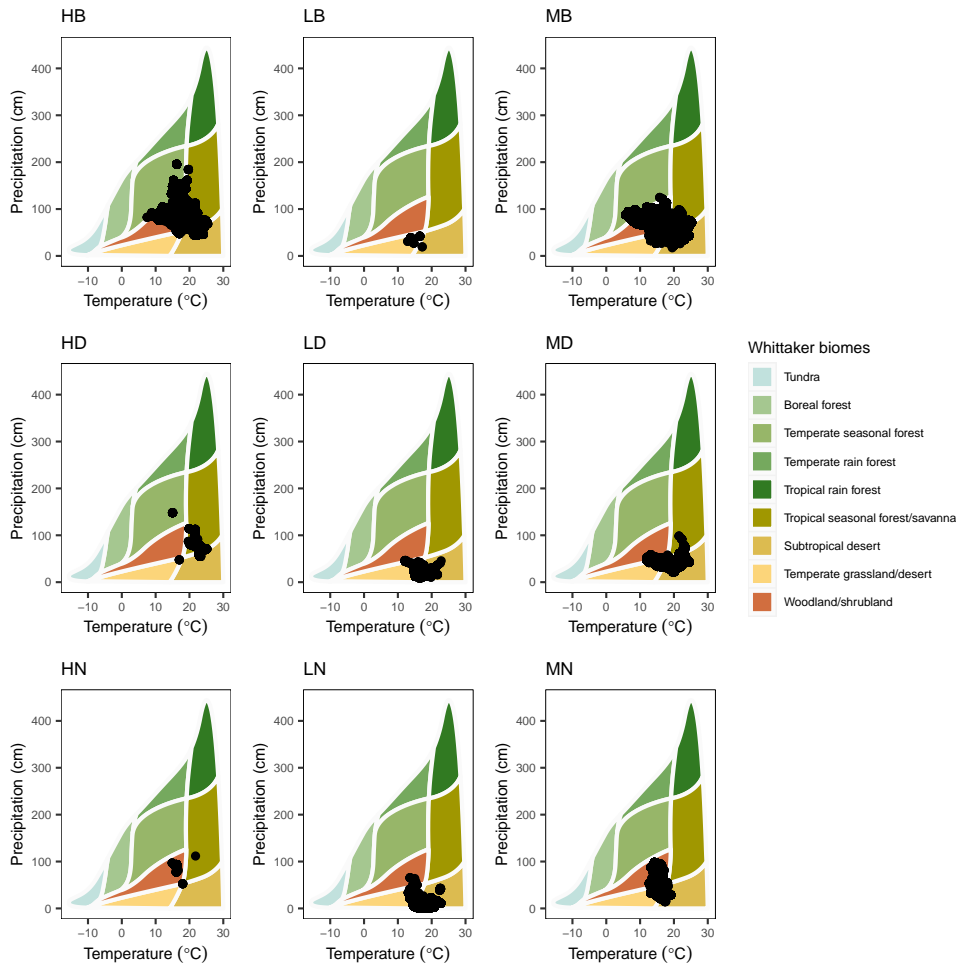


Figure 18: This study's FB's plotted in Whittaker (1975)'s bioclimatic space. Plotted here are the most common FB types over the 21-year study period. The FB names are derived from two letters, the first letter is either L, M or H and indicates low, medium and high vegetation productivity index (VPI) and the second letter is either D, C, B or N and indicates whether the growth limitation index is either dry, cold, both dry and cold or non-seasonal.

Plotting the seasonal EVI signature of each biome revealed that moisture-limited biomes (ending in D) and biomes limited by both moisture and temperature (ending in B), had larger amplitudes compared to non-seasonal biomes (ending in N) (Figure 19). Furthermore, non-seasonal biomes had longer growing seasons compared to moisture-limited biomes (ending in D) or both moisture and temperature-limited biomes (ending in B). However, a level of seasonality in the phenological characteristics of non-seasonal biomes can still be observed.

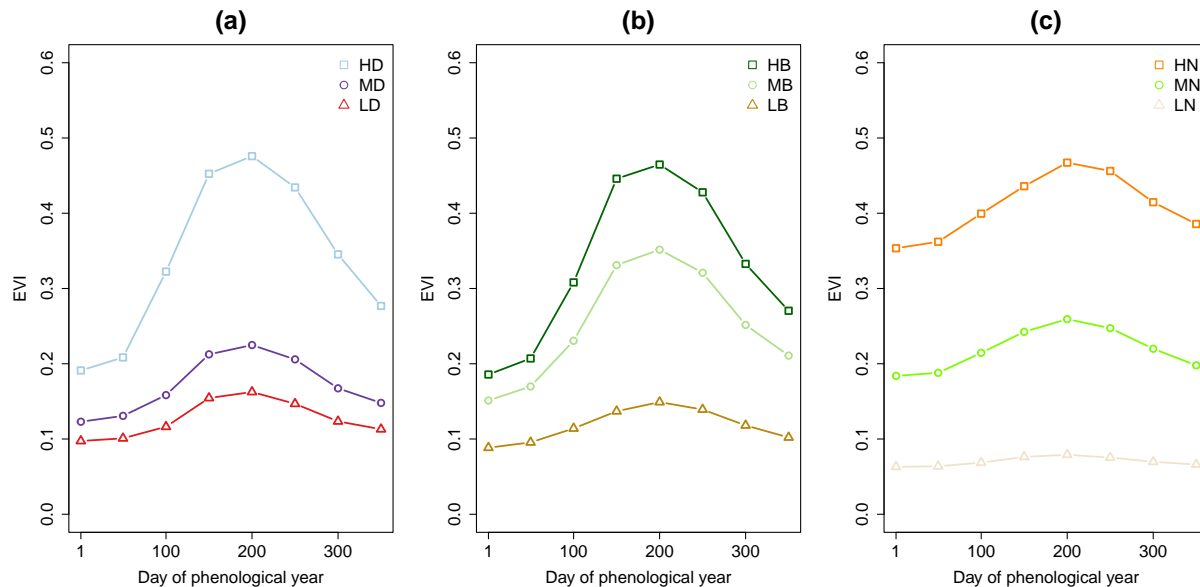


Figure 19: Average seasonal phenological signatures of the Functional Biomes (FB) shown in Figure 17. The data points illustrate mean values of phenological metrics extracted from the Enhanced Vegetation Index (EVI) specific to each FB. The points are ordered to begin from the trough of EVI (when EVI is at its lowest) to the end of a plant’s phenological cycle. The sequence of days on the x-axis are organized to represent a phenological year but does not show differences between the start of the growing season across FBs. Average phenological cycles of (a) moisture-limited FBs, (b) both moisture and temperature-limited FBs and (c) non-seasonal FBs. The FB names are derived from two letters, the first letter is either L, M or H and indicates low, medium and high vegetation productivity index (VPI) and the second letter is either D, C, B or N and indicates whether the growth limitation index is either dry, cold, both dry and cold or non-seasonal.

3.4.2 Observed trends in biome shifts

We found that 3% to 15% of pixels shifted in FB state between 2000 to 2021 when using the 2000-2010 period as the reference state (Figure 20). FBs classified as MD (medium VPI, moisture-limited) shifted mostly to MN (medium VPI, non-seasonal), suggesting no changes in productivity but decreased moisture limitation effects. Low VPI and moisture-limited biomes (LD) shifted to a higher productive and non-seasonal state (MN) and to a low productive, non-seasonal state (LN). The HD (high VPI, moisture-limited) biome shifted to a non-seasonal version of this biome type (HN). Most biomes classified as MB (medium VPI, both moisture and temperature-limited) shifted to biomes of the same productivity but with moisture

as the primary limiting factor. Furthermore, the MB biome also transitioned to biomes with higher productivity biome states (that is to HN, HD, or HB). Some of the HB biome (high VPI, both moisture and temperature-limited) transitioned to similar productive states but became non-seasonal (HN) or to moisture-limited biomes (HD).

Plotting the biome shifts in a geographic space uncovered distinct spatial patterns (Figure 21). In the Etosha of northern Namibia, biomes states such as medium VPI, moisture-limited (MD) and medium VPI, both moisture and temperature-limited (MB) shifted to medium VPI, non-seasonal states (MN) (i.e., from MD and MB to MN). This suggests that these biomes transitioned to a biome state with a longer growing season. Similarly, in the Bwabwata of north-eastern Namibia, the high VPI, both moisture and temperature-limited states (HB) shifted to a non-seasonal but high productive category (HN), indicating a transition to decreased moisture and temperature limitation in this region. However, some biomes in Namibia shifted to less productive states. For example, low VPI, moisture-limited states (LD) shifted to low VPI, non-seasonal states (LN) in the Namib-Naukluft.

In Botswana, medium VPI, both moisture and temperature-limited states (MB) shifted to medium VPI, moisture-limited states (MD) in the Moremi in the north-west and the Central Kalahari, suggesting that moisture limitation effects increased in these regions. Moreover, a cluster of medium VPI, moisture-limited states (MB) shifted to medium VPI, non-seasonal states (MN) in the Kgalagadi in southwestern Botswana, indicating that moisture limitation effects decreased in this region.

Our analysis further revealed that FB shifts in Zimbabwe were predominantly characterized by transitions from high VPI, both moisture and temperature-limited states (HB) to high VPI, non-seasonal states (HN). This pattern was ubiquitous, as it spread from the Chewore in the north through the Hwange in the north-east to the Gonarezhou in the south. Similarly, in the Kruger of northeastern South Africa, medium VPI, both moisture and temperature-limited (MB) states shifted to high VPI, non-seasonal states (HN), indicating a transition to a higher productive version and non-seasonal state. Furthermore, shifts from medium VPI, both moisture and temperature-limited states (MB) to high VPI, moisture-limited states (HD) were also detected in southern Kruger. This suggests a transition to a higher productive but moisture-limited state. Patches of high VPI, both moisture and temperature-limited sites (HB) shifted to high VPI, non-seasonal states (HN) in the Ithala of eastern South Africa. We also detected shifts from medium VPI, moisture-limited state (MD) to medium VPI, non-seasonal state (MN) in the Camdeboo of southern South Africa, suggesting that moisture limitation decreased in this region. Furthermore, we also detected shifts from medium VPI, both moisture and temperature-limited states (MB) to high VPI, non-seasonal states (HN)

in the Witdraai of southwestern South Africa, indicating that these biomes have shifted to more productive states with reduced moisture and temperature limitation effects.

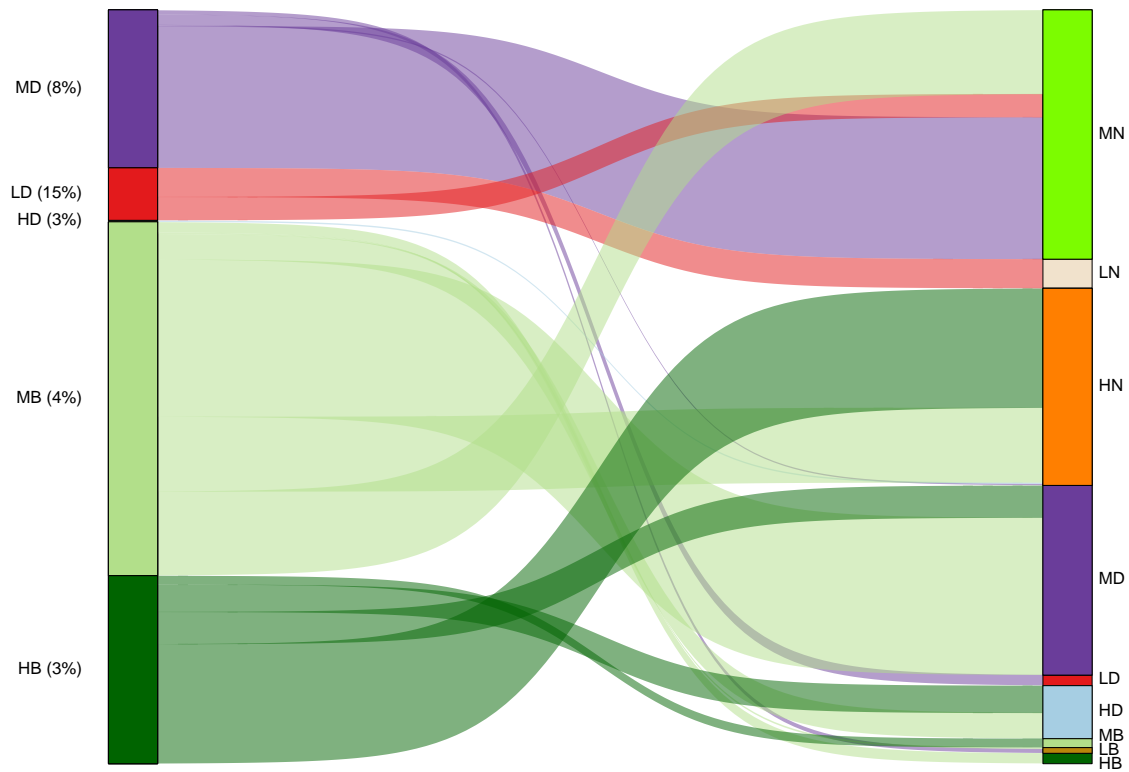


Figure 20: Shifts in Functional Biomes (FB) detected at the start and end of the 21-year period. These shifts were identified by applying multinomial regression analysis to FB state data. Shown here are FB transitions where time had a statistically significant effect (Z -test, $P < 0.05$) on FB states over the 21-year time series of each pixel. The left panel shows the initial FB state while the right panel shows the final FB state. The heights of the elements in the panels indicate the proportion of the biome states that have shifted (for example, MD (8%) indicates that 8% of pixels of the MD biome transitioned to other states). The FB names are derived from two letters, the first letter is either L, M or H and indicates low, medium and high vegetation productivity index (VPI) and the second letter is either D, C, B or N and indicates whether the growth limitation index is either dry, cold, both dry and cold or non-seasonal.

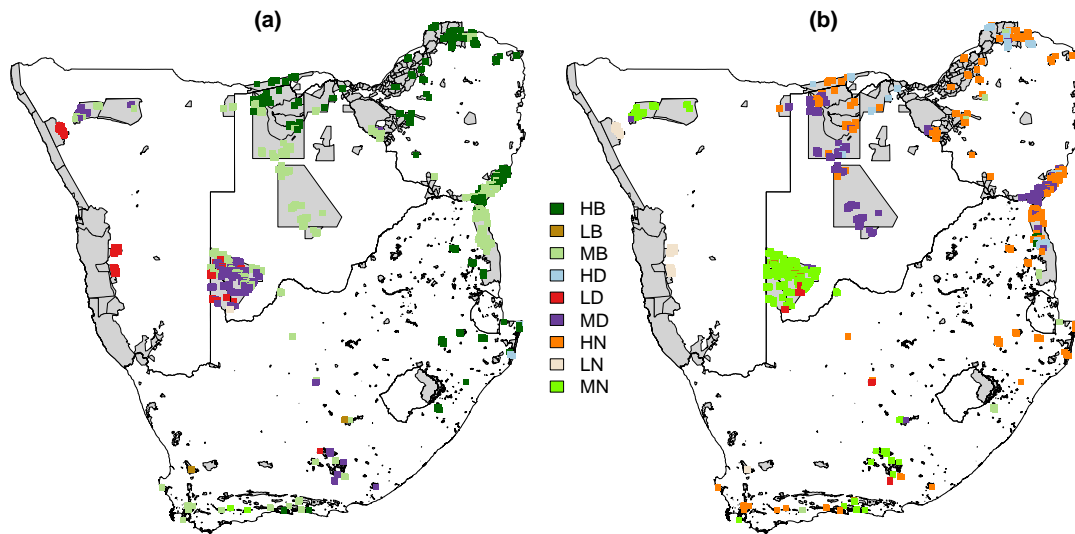


Figure 21: Biome shifts plotted geographically. These shifts were identified by applying multinomial regression analysis to FB state data. Shown here are FB transitions where time had a statistically significant effect (Z-test, $P < 0.05$) on FB states over the 21-year study period of each pixel. (a) shows the initial biome state (b) shows the final biome state. Grey colours represent the study area boundary. The FB names are derived from two letters, the first letter is either L, M or H and indicates low, medium and high vegetation productivity index (VPI) and the second letter is either D, C, B or N and indicates whether the growth limitation index is either dry, cold, both dry and cold or non-seasonal.

Plotting slopes of simple linear regression showed that time had a statistically significant effect ($P < 0.05$) on VPI, moisture and temperature limitation indices (Figure 22). This suggests temporal changes in these variables. The y-axes of the histogram in Figure 22 show that the VPI had the least changes while the temperature limitation index had the most changes. Furthermore, the VPI slopes were mostly positive, suggesting an overall increase in vegetation productivity over time. In contrast, the dominant negative slopes observed for both moisture and temperature limitation indices suggests that the trough of EVI was not clearly associated with the coldest or driest period of the year.

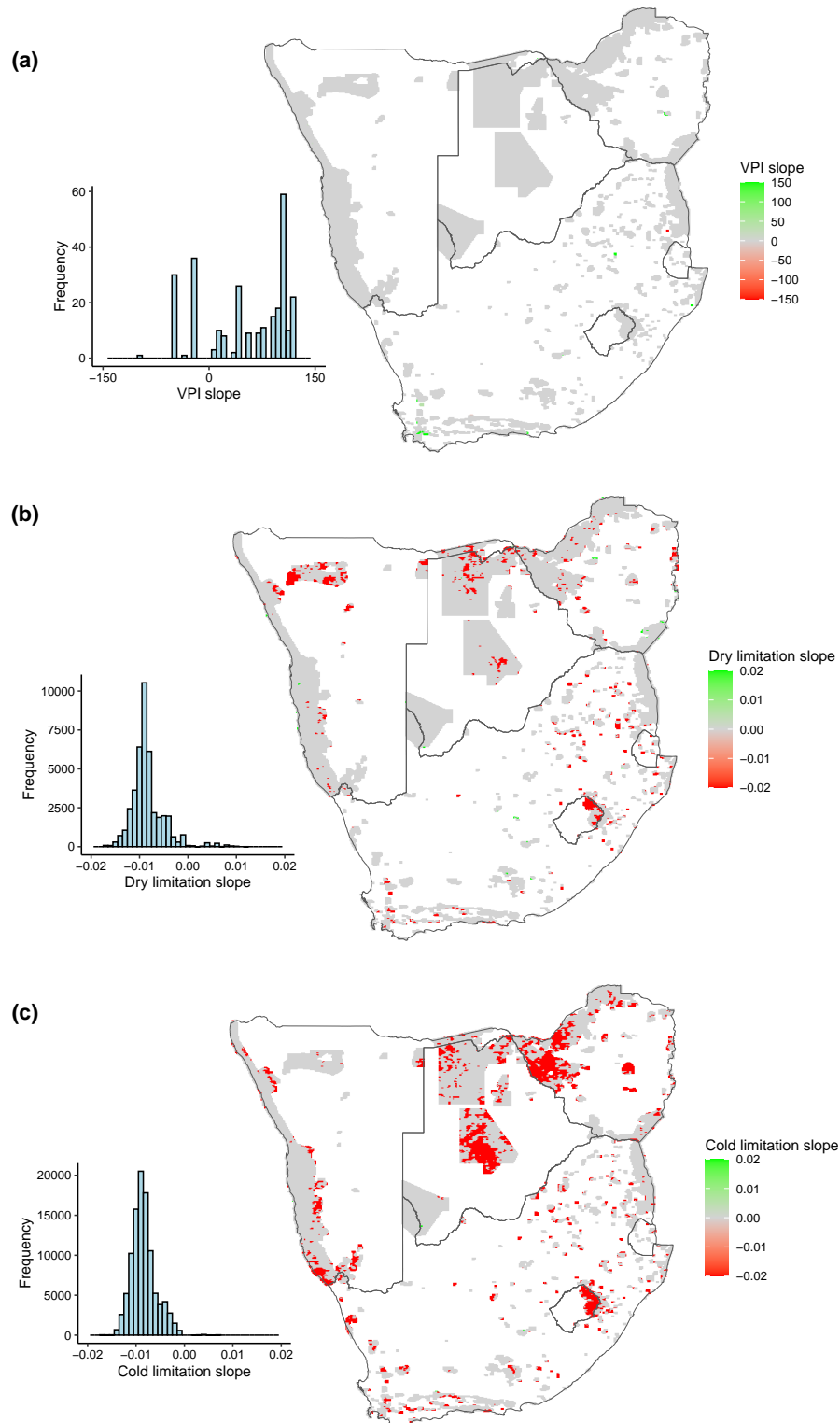


Figure 22: Slopes of a simple linear regression model fitted to the vegetation productivity index (VPI) and growth limitation indices as a function of time (a) simple linear regression slopes fitted to the VPI (b) simple linear regression slopes fitted to the moisture limitation index and (c) simple linear regression slopes fitted to the cold limitation index. Shown here are slopes where time had a statistically significant effect ($P < 0.05$) on the indices over the 21-year study period of each pixel. Only significant slopes ($P < 0.05$) are plotted on the histograms, while non-significant slopes ($P > 0.05$) on the map were set to 0.

3.5 Discussion

In this study, we examine changes in the Functional Biomes (FB) of southern Africa, a region regarded as a hotspot of climate change (Niang et al., 2014; Trisos et al., 2022). In this context, a FB refers to vegetation units that have similar functional metrics (see Higgins et al. 2016). The first metric we use is the Vegetation Productivity Index (VPI), based on the assumption that the EVI is a proxy for vegetation productivity and is further co-limited by climatic variables. The second metric is the growth limitation index, which indicates whether plant growth is limited by soil moisture or temperature. We tentatively use the term 'limited' to acknowledge the fact that in ecosystems such as savanna, dryness and coldness are correlated in winter, yet in an absolute sense it is often warm enough to support vegetation activity. By using this FB scheme, we found that 3% to 15% of pixels shifted in FB states, with notable patterns being transitions from low productive states to high productive, non-seasonal states as well as transitions from both moisture and temperature-limited states to solely moisture-limited states. Our findings demonstrate widespread changes in the functioning of ecosystems of southern Africa and may be useful in supporting conservation and management initiatives.

The shift from high VPI, both moisture and temperature-limited states (HB) to a less seasonal version of this biome (to HN) in the Hwange, Chewore, and the Gonarezhou of Zimbabwe, is consistent with regions where significant increases in aboveground carbon density have been reported (Baccini et al., 2017). In Kruger of northeastern South Africa, we found that most medium VPI, both moisture and temperature-limited states (MB) transitioned to more productive, non-seasonal states (HN) in the north, and to more productive, moisture-limited states (HD) in the south. This finding suggests increased productivity, agrees with studies reporting an increase in woody plant cover (Buitenwerf et al., 2012; Zhou et al., 2021).

We detected shifts from medium VPI, moisture-limited state (MD) to the non-seasonal version of this state (MN) in the Camdeboo of southern South Africa. This finding agrees with Masubelele et al. (2013), who used fixed-point photographs and step-point vegetation surveys to demonstrate increases in azonal vegetation. We also found that in the Fynbos of South Africa, medium VPI, non-seasonal states (MN) shifted to more productive states (HN), which supports net greening trends reported by multi-decadal studies that have used Landsat EVI time series (Venter et al., 2020) or repeat photography (Cowling and Hoffman, 2021).

The biome shifts from medium VPI, both moisture and temperature-limited states (MB), to a moisture-limited version of this biome type (MD) in the Central Kalahari of Botswana agrees with Byakatonda et al. (2020), who used the

Standardized Precipitation Evaporation Index (SPEI) to characterize this region as vulnerable to severe drought. In contrast, the shifts from states such as LD, MD, and MB to MN in the Kgalagadi of southwestern Botswana is consistent with Herrero et al. (2020), who reported increases in mean NDVI between 2000-2016. We also found that low VPI, moisture-limited (LD) states of the Skeleton Coast and Namib-Naukluft of western Namibia shifted to low VPI, non-seasonal state (LN). This finding is consistent with studies that have used high-resolution climate models to project the expansion of the Namib, driven by future warming (Engelbrecht and Engelbrecht, 2016). In addition, the shifts from MD and MB to MN in the Etosha of northern Namibia agree with studies that have correlated net gains in fractional woody cover with increases in average precipitation (Wessels et al., 2019).

The most common biome transitions observed in our study were shifts to more productive and non-seasonal states (to MN and HN biomes), which suggests that favourable conditions for plant growth and productivity are being sustained for longer periods of the growing season. This phenomenon is suggestive of CO₂ fertilization effects. Rising CO₂ directly increases light-use efficiency (LUE) and water-use efficiency (WUE) by enhancing carbon assimilation and reducing transpiration in plants, which consequently extends a plant's growing season length (Peñuelas and Filella, 2009; Higgins and Scheiter, 2012). Indeed, Higgins and Scheiter (2012) showed that rising CO₂ can shift vegetation to more productive states across Africa. Recent model projections suggest that African biomes are likely to shift to more productive and non-seasonal states (Martens et al., 2021). This may be because CO₂ effects coupled with light competition, and fire suppression may influence trends towards woody biomass by altering the competitive balance favoring trees, thereby creating positive feedback that suppresses grasses but promote tree growth (Bond and Midgley, 2012). Therefore, increased woody biomass or trees would suggest less seasonality compared to grass-dominated ecosystems.

Another mechanistic explanation for shifts to non-seasonal states may involve complex relationships between global warming and soil moisture-atmosphere feedbacks. Specifically, when soil moisture declines, evapotranspiration also decreases, leading to changes in atmospheric circulation to intensify moisture convergence, which raises surface water availability (i.e., precipitation minus evapotranspiration, P-E) in the dry season but not the wet season (Zhou et al., 2022a). Therefore, the diminishing limiting effects of temperature and moisture on plant growth (Figure 22), coupled with elevated CO₂, may lead to an extended growing season resulting in increased productivity.

Biome transitions from both moisture and temperature-limited states (from MB and HB) to solely moisture-limited states (to MD and HD) suggest increased warming. Southern Africa has experienced increased mean temperatures (Engel-

brecht and Engelbrecht, 2016; Trisos et al., 2022), which may have diminished the role of cold temperatures in limiting physiological processes such as photosynthesis and transpiration. This suggests that moisture availability has become the primary constraint on vegetation activity in these biomes. Shifts to more productive versions of these biome types (for example, from MD to HD) also suggest that plants in these ecosystems have enhanced their WUE to maintain growth and productivity into the dry season. However, the expansion of low productive moisture-limited biomes shifts to even lower productive non-seasonal states (i.e., from LD to LN which is a transition to desert environments) suggests increasing limiting effects of moisture availability. Coupled with warming temperatures, the net effect is a decrease in productivity and shifts towards arid conditions.

Our exclusive focus on protected areas allows us to eliminate the possibility that the changes we detected are due to land use change. The interactions between climate and vegetation are highly non-linear. Therefore, the detected FB trajectories could either accelerate or reach an asymptote. Continuous monitoring of these FB will reveal which of these possibilities is realized. It should be noted that the high VPI values (≥ 6500) used in this study should be considered relatively high within the context of the study region, and do not represent universally high vegetation productivity across all global biomes. Increases in vegetation productivity (for example, from MB to HN biomes) suggest increased carbon sequestration in these biomes, thus acting as carbon sinks to combat climate change. However, increased vegetation productivity can also negatively impact biodiversity. For example, increased vegetation cover can lead to increased competition between species, ultimately favouring invasive species over native species (van Wilgen et al., 2022). Such effects could alter species composition and diversity. Furthermore, it has been shown that woody encroachment decreased populations of bird and mammal species in savanna ecosystems (Péron and Altwegg, 2015; McCleery et al., 2018). Therefore, the consequences of these biome shifts to biodiversity may vary locally.

A limitation of our analyses is that although our biomes emerge from the data, we subjectively categorized the VPI and growth limitation attributes, which may have been categorized differently by different authors. To improve the objectivity of future studies, it may be necessary to develop a standardized method for categorizing these attributes. It is obvious that if one uses more classes, more transitions will be detected; that is, the fact that we report that 3% to 15% of pixels transitioned in this study is difficult to compare with the findings of a global study that used more classes (Higgins et al., 2016) and reported that 13% to 14% of pixels transitioned from their initial FB state.

The spatial resolution of the climatic forcing data was lower than that of the EVI data. This suggests that more fine-scaled variation in soil moisture and temperature may not propagate into our metrics. We anticipate that higher-resolution

reanalysis data might be available in the future, which could potentially capture such fine-scale variations in the climatic forcing data. The overall consistency of our findings with previous studies suggests that the classification scheme is robust and applicable to diverse regions.

Although the observed biome shifts are most likely to be driven by climate change and increasing CO₂, changes in local disturbance regimes such as fire and herbivores may have contributed to the detected shifts. Fire suppression and herbivore absence reduce mortality in woody plants leading to increased woody recruitment (O’connor et al., 2014; Stevens et al., 2017). To provide a comprehensive identification of the underlying drivers of functional biome shifts, future studies should consider integrating disturbance regimes in their classification schemes. In addition, studies should also consider topographical effects in biome classification, like elevation and slope. Differences in topography can cause variations in solar radiation, moisture, and temperature, which consequently affects the EVI signal. Furthermore, future studies should also incorporate ground truth data to calibrate and validate the mapping of functional biomes. Such an approach will improve the accuracy and reliability of FB assessments.

3.5.1 Management implications

Our study reveals previously undetected changes in the FB of southern Africa, thereby provide a data foundation for validating existing biophysical models used to predict future biome change. Although continental studies anticipate that Africa’s biomes will shift to more productive and non-seasonal states (Higgins and Scheiter, 2012; Martens et al., 2021), our regional approach provides compelling evidence that such anticipated biome trajectories are already ongoing. Therefore, we emphasize that it is important to understand the trajectories of change ecosystems are on, which would inform conservation management strategies.

Transitions towards higher productive and non-seasonal states may cause changes in species composition, impacting ecological processes such as competition, predation or promote the emergence of invasive species (Niang et al., 2014; Slingsby et al., 2017; Péron and Altwegg, 2015; McCleery et al., 2018). In particular, protected areas are more vulnerable to colonisation by range-shifting species than non-protected areas, suggesting that protected areas provide a more suitable habitat for colonising species (Hiley et al., 2013). Management responses in these regions may include conducting ground surveys to assess changes in species diversity and abundance, followed by applying targeted actions like removing invasive species and restoring degraded habitats. Furthermore, altering fire and herbivory regimes to maintain ecosystems in their natural state may safeguard biodiversity (Midgley and Bond, 2015).

Shifts to moisture-limited states could impact plant communities. For exam-

ple, increased drought frequency could lead to increased plant mortality (Niang et al., 2014), thus hindering natural plant succession. Furthermore, droughts could impact the availability of natural water sources obtained from fruits and flowers by wildlife. For example, it has been shown that decreased fruit production attributed to drier and warmer climate caused an 11% drop in the body condition of elephants that rely on fruit (Bush et al., 2020). Our results suggest that embracing the observed changes in dry-limited ecosystems will become increasingly necessary. Conservation responses may include promoting arid-adapted species and increasing artificial water sources to support plant succession and access to water by wildlife, respectively. Moreover, enhancing connectivity between protected areas and implementing targeted intensive management for vulnerable species may safeguard refugial areas where local populations can persist (Lee et al., 2023).

The changes in FB detected here emphasizes the need for establishing a robust biodiversity monitoring system for the region. To our knowledge, such a monitoring system does not exist. We propose a multifaceted approach that combines Earth observation data and citizen science knowledge to track the extent and magnitude of climate change impacts on the ecosystems of southern Africa. Earth observation provides advantages of obtaining increasingly available spatio-temporal data at no cost, while citizen science can be used to identify indicator species that serve as flagship warnings of ecosystem change (Siddig et al., 2016). This early detection system would enable the timely implementation of adaptation and mitigation measures. Furthermore, incorporating long-term permanent monitoring sites into the system would provide insights on the magnitude, severity and rates of ecosystem change, thus aiding the assessment of future biodiversity shifts.

In conclusion, this study set out to assess changes in the functioning of the vegetation of southern Africa. This aim along with the data availability defined our usage and interpretation of the Functional Biome (FB) concept. Here, we detected that most FB in southern Africa are on a trajectory from low productive states to high productive, non-seasonal states as well as from both moisture and temperature-limited states to solely moisture-limited states. Taken together, these findings suggest that ecosystems in southern Africa may become more productive and more vulnerable to moisture availability than previously. The empirical assessments measured here may serve as a foundation in developing monitoring systems of ecosystem change as well as guiding management responses.

3.6 Supplementary Information

TABLE VII: Cross-classification of our FB vs the Beck et al. (2018) biomes. The Beck et al. (2018) biome class names are adapted from Peel et al. (2007). The FB names are derived from two letters, the first letter is either L, M or H and indicates low, medium and high vegetation productivity index (VPI) and the second letter is either D, C, B or N and indicates whether the growth limitation index is either dry, cold, both dry and cold or non-seasonal

	HB	LB	MB	HD	LD	MD	HN	LN	MN
Aw	20	0	101	0	9	30	0	60	0
BWh	7	0	50	0	0	15	3	21	34
BSh	407	12	739	22	79	190	20	646	447
Cwa	313	0	656	4	28	90	0	168	0
Cwb	29	0	20	0	7	0	7	11	12

TABLE VIII: Locations of protected areas discussed in the text. The protected area code corresponds to the numbered points in Figure 23.

Protected area name	IUCN classification	Country	Lat	Long	Code
Chobe	National Park	Botswana	-18.421015	24.421832	2
Moremi	Game Reserve	Botswana	-19.310700	23.159593	13
Central Kalahari	Game Reserve	Botswana	-22.409874	23.894009	14
Kgalagadi	National Park	Botswana	-25.313036	21.095487	21
Tsehlanyane	National Park	Lesotho	-29.323878	28.116879	18
Caprivi	State Forest	Namibia	-17.591556	23.934189	1
Gondwana	Nature Park	Namibia	-27.580981	17.925474	10
Etosha	National Park	Namibia	-18.881923	16.043102	12
Torra	Nature Reserve	Namibia	-20.485909	13.964450	20
Skeleton Coast	National Park	Namibia	-19.987356	13.269609	24
Bwabwata	National Park	Namibia	-18.011045	21.865686	27
Namib-Naukluft	National Park	Namibia	-23.140611	15.159970	28
Songimvelo	Nature Reserve	South Africa	-25.939326	30.996112	8
iSimangaliso	Wetland Park	South Africa	-27.636241	32.582187	9
Steenbokkie	Nature Reserve	South Africa	-32.340342	22.657873	11
Kruger	National Park	South Africa	-24.249213	31.622663	16
Marakele	National Park	South Africa	-24.421302	27.603774	17
Asanta Sana	Game Reserve	South Africa	-32.293119	24.985733	22
Garden Route	National Park	South Africa	-33.837206	23.450093	23
Anysberg	Nature Reserve	South Africa	-33.463485	20.589365	25
Grootwinterhoek	Nature Reserve	South Africa	-33.199008	19.068176	26
Ithala	Game Reserve	South Africa	-27.545586	31.313910	29
Camdeboo	National Park	South Africa	-32.224315	24.504368	30
Hwange	National Park	Zimbabwe	-19.013810	26.734951	3
Charara	Safari	Zimbabwe	-16.520278	29.161508	4
Mana Pools	National Park	Zimbabwe	-15.941704	29.483376	5
Chewore	Safari	Zimbabwe	-15.829794	30.102935	6
Nyanga	National Park	Zimbabwe	-18.295038	32.725018	7
Gonarezhou	National Park	Zimbabwe	-21.731903	31.814015	15
Mzarabani	Wilderness Area	Zimbabwe	-16.477231	30.877782	19

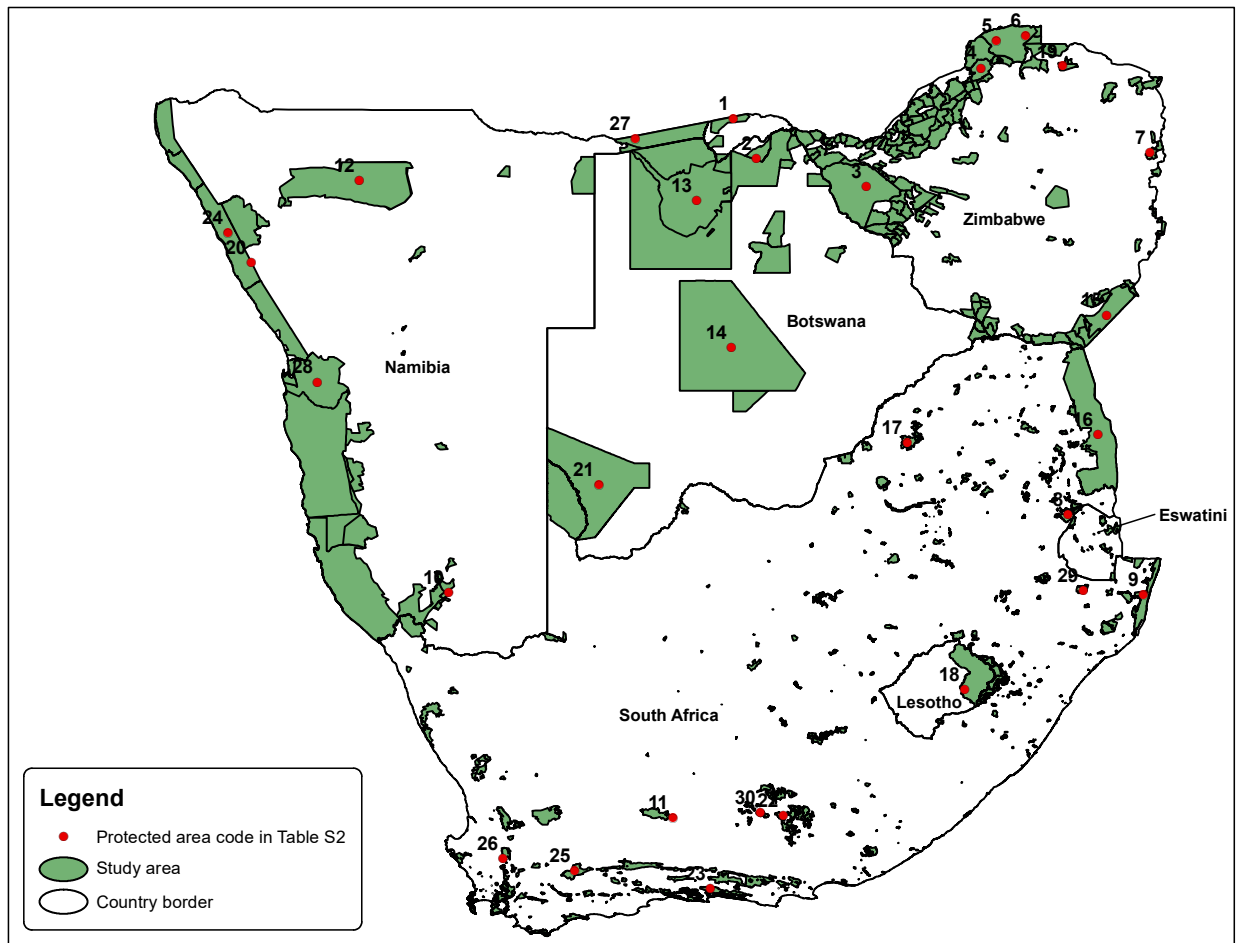


Figure 23: Locations of protected areas discussed in the text, numbered according to the codes in Table VIII.

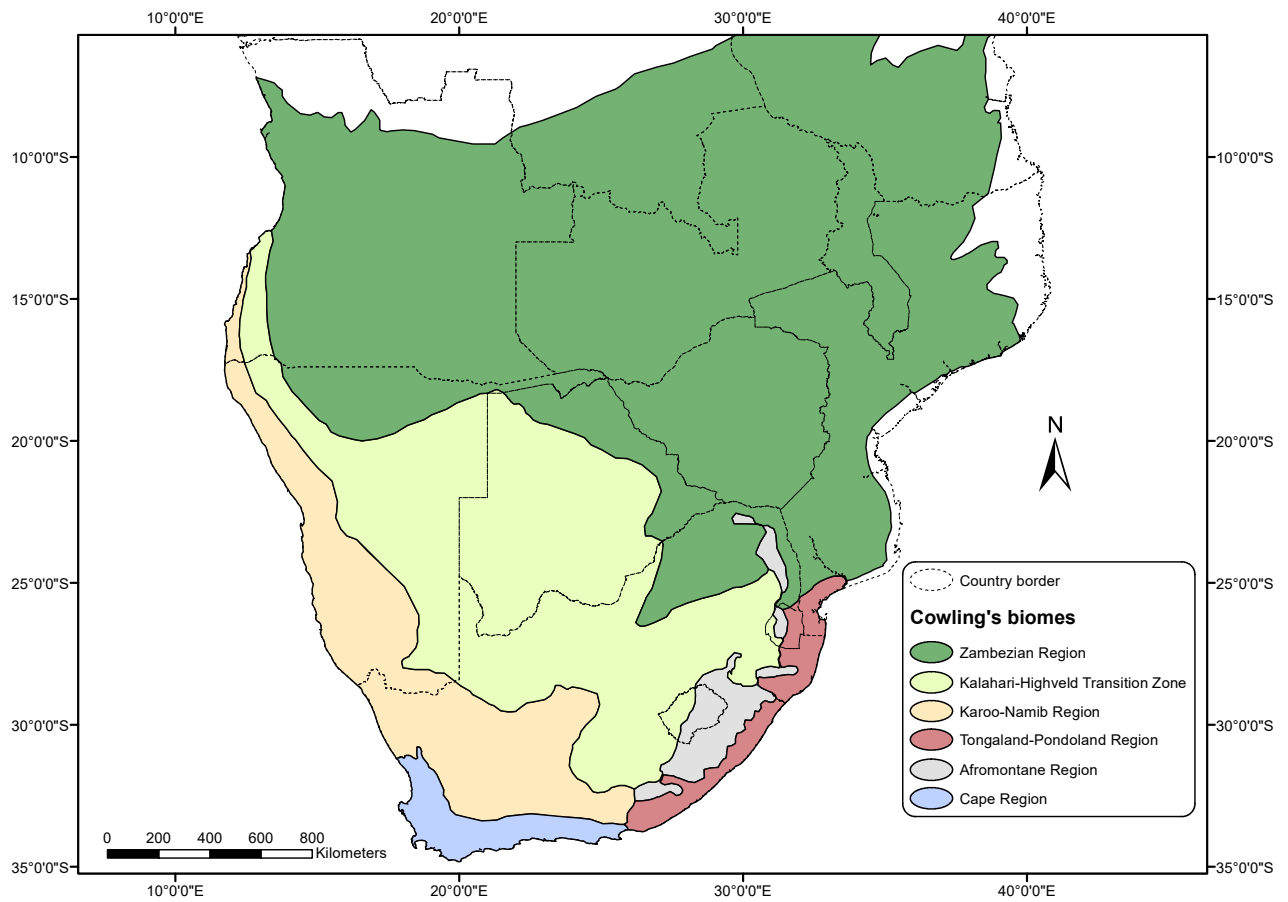


Figure 24: Geographic distribution of the phytogeographical regions defined by Cowling et al. (2004) and referred to in the text. These phytogeographical regions were recreated in a Geographic Information System.

Chapter 4

4 Detecting and attributing changes in vegetation activity to climatic forcing

4.1 Summary

Climate change and elevated CO₂ are altering dynamics of vegetation activity globally, with consequences for Earth system functioning and ecosystem service provision. Yet how terrestrial vegetation is responding to these changes and the underlying drivers of such change has emerged as a major research challenge. Here, we use solar-induced chlorophyll fluorescence (SIF) and enhanced vegetation index (EVI) data, and an ecophysiological plant growth model to detect and attribute changes in vegetation activity to trends in climatic data at 100 study sites. We found distinct response types in the anomaly of trends in SIF and EVI datasets. SIF dominantly show cup-shaped trends indicating switches from decreased photosynthetic activity to increased photosynthetic activity, while EVI dominantly show hat-shaped trends suggesting switches from greening to browning patterns. In both datasets, attribution analyses show that vegetation in cooler and moister regions are primarily sensitive to changes in temperature while ecosystems in warmer and drier regions are sensitive to changes in moisture. Our analysis further show weak CO₂ fertilization effects on the detected change, thereby highlighting the dominant role of moisture and temperature constraints on changes in vegetation activity. Our study opens new avenues for detecting and attributing change in ecosystems, allowing for informed planning on adaptation and mitigation responses to changes in terrestrial vegetation.

4.2 Introduction

Climate change and elevated CO₂ are altering the dynamics of vegetation activity globally (Zhu et al., 2016; Bonan and Doney, 2018; Nolan et al., 2018; Parmesan et al., 2022; Higgins et al., 2023a), thereby impacting ecosystem functioning and services (Settele et al., 2014; IPBES, 2019; IPCC, 2019; Parmesan et al., 2022). For example, climate change has abruptly pushed ecosystems beyond irreversible tipping points (Harris et al., 2018; Berdugo et al., 2020; Bergstrom et al., 2021), while global analyses of tree rings have shown that rising CO₂ accelerates tree growth but decreases overall lifespan (Brienen et al., 2020). Climate change and elevated CO₂ are further anticipated to remain the major drivers of ecosystem change in the near future (Settele et al., 2014; IPBES, 2019; IPCC, 2019). The prominent effects of these drivers on Earth system functioning have led to a growing interest in detecting and attributing ecosystem response to climatic drivers. Despite this growing interest, studies have questioned whether the detection and attribution process itself is possible, given the associated challenges (Parmesan et al., 2013; Stone et al., 2013).

The detection process should demonstrate that a system has statistically undergone change without offering a specific reason of the observed change (Parmesan et al., 2013; Settele et al., 2014), while the attribution process involves quantifying and determining the relative contribution of climatic drivers to the observed system change (Parmesan et al., 2013; Settele et al., 2014). Most studies do not meet these criteria, they either speculate that the observed system change is related to climatic drivers or do not attempt to attribute the detected change to climatic drivers (Van de Pol et al., 2017; Hansen et al., 2016). This suggests that robust detection and attribution approaches remain limited. Robust detection and attribution approaches are necessary to reliably link observed ecosystem changes to changes in climatic drivers, which underpins adaptation and mitigation interventions (Parmesan et al., 2022).

High-confidence detection and attribution studies use experimental analyses, correlational approaches, statistical inferences and meta-analyses (Parmesan et al., 2013, 2022). Such approaches are supported by multiple lines of converging evidence that identify climate change, for example, as the leading cause of ecosystem change. Despite this, robust attribution studies are mostly regional and have focused on northern latitudes (Feeley et al., 2017; Higgins et al., 2023a). In these regions, compelling evidence has shown that changes in plant structure and functioning are driven by rising temperatures (Settele et al., 2014; Bjorkman et al., 2018). However, such regional analyses have been criticised for their geographic bias towards northern latitudes (Feeley et al., 2017), as this may overlook the diversity of global species response to changes in the climate system. For example, climate change is expected to trigger species migrations but tropical species will

be less likely to keep pace with climate change compared to temperate species (Feeley et al., 2015; Perez et al., 2016). Therefore, global attribution analyses of regional ecosystem responses to climatic forcing are necessary to draw informed conclusions about the overall impacts of climatic drivers on terrestrial ecosystems.

Recent advances in satellite remote sensing allow constant monitoring of changes in vegetation activity at varying spatial and temporal scales. For example, global studies have applied remote sensing techniques to assess shifts in terrestrial vegetation and implicated climate change and elevated CO₂ as the primary drivers (Zhu et al., 2016; Seddon et al., 2016; Smith et al., 2016; Song et al., 2018; Wang et al., 2020b). However, such studies contain land use change effects that can mask climate change impacts on vegetation activity or may act in synergy (Sirami et al., 2017), making it challenging to accurately attribute each driver to the detected change. For example, the pronounced greening trends observed over USA, India and China are due to afforestation initiatives and intensive agricultural activity (Zhu et al., 2016; Piao et al., 2020) and not driven by ecosystems' natural responses to climatic forcing. Therefore, understanding the effects of climatic forcing on natural systems is important for predicting the consequent changes in ecosystem functioning (Feeley et al., 2017).

A new approach for detecting and attributing changes in vegetation activity has recently been proposed (Higgins et al., 2023a). This new method uses an ecophysiological plant growth model to attribute shifts in vegetation activity to trends in climatic forcing. The Higgins et al. (2023a) approach addresses challenges such as the confounding effects of land-use change and climate change on vegetation activity, biases related to short time series and small spatial scales and constraints inherent in correlative modelling approaches. This study found a dominant fingerprint of climate change across biome types. This study also surprisingly found weak CO₂ fertilization effects on changes in vegetation activity. However, the normalized difference vegetation index (NDVI) and the enhanced vegetation index (EVI) used by Higgins et al. (2023a) are not sensitive to how efficiently the fraction of photosynthetically active radiation (FAPAR) is used for carbon assimilation (light use efficiency (LUE)) (Grace et al., 2007; Smith et al., 2020). Although these 'greenness-based' vegetation indices (VIs) are useful indicators of chlorophyll content and plant biomass, VIs may miss changes in LUE which increases with elevated CO₂ (Ainsworth and Long, 2005). This implicit picture of carbon dynamics by VIs indicates that they are not direct proxies of photosynthesis or GPP (Zhang et al., 2016). This also suggests that alternative data sources should be considered when studying the effects of climatic factors on carbon assimilation dynamics, which could potentially unmask CO₂ fertilisation effects on carbon uptake.

Satellite-based observations of solar-induced chlorophyll fluorescence (SIF) pro-

vide new avenues for assessing photosynthetic activity (Joiner et al., 2011; Frankenberg et al., 2011; Guanter et al., 2012). Plants emit the SIF signal that is sensitive to LUE during photosynthesis light reactions (Porcar-Castell et al., 2014). This light signal is emitted by excited chlorophyll molecules at longer wavelengths covering two peaks in the red and far-red range between 650-850 nm of the electromagnetic spectrum. The SIF signal stems from the cores of a plant's photosynthetic machinery and quickly responds to disturbances in environmental factors like light and moisture constraints (Guanter et al., 2015). Field and theoretical modelling studies have shown a positive correlation of CO₂ assimilation and stomatal conductance with SIF, this is because increases in heat dissipation driven by high light conditions can cause a concurrent reduction in both SIF and photosynthesis yield (Frankenberg et al., 2011). Satellite remote sensing studies have also shown that the seasonal cycles of SIF and GPP estimates agree well across biomes. (Joiner et al., 2014; Damm et al., 2015; Yang et al., 2017; Li et al., 2018). Therefore, this suggests that SIF is a reliable indicator of photosynthetic activity (Frankenberg et al., 2011; Porcar-Castell et al., 2014).

However, the short SIF record has limited its usage in long-term studies. This limitation has led researchers to use machine learning algorithms to reconstruct SIF datasets (Zhang et al., 2018; Li and Xiao, 2019; Chen et al., 2022b). To reconstruct the SIF data, the short record of the dataset is used to train a machine learning algorithm. This algorithm is then used to generate missing data retrospectively, thereby filling gaps in the historical record. This allows for continuous analyses over longer periods.

Here, we assess changes in the vegetation activity of terrestrial ecosystems and attribute these shifts to changes in climatic forcing between 2001 to 2020. To do this, we use data records of SIF and EVI, and a mechanistic plant growth model simulated using climate reanalysis datasets. We improve on the state-space model developed by Higgins et al. (2023a) by simultaneously modelling two response variables; we use the reconstructed SIF dataset (Chen et al., 2022b) to model carbon uptake, hence GPP, we further use EVI to model plant biomass. Such modifications constrains the parameters of the model and explicitly attribute changes in carbon and biomass assimilation to trends in climatic forcing. That is, we use the modelling results to quantify the contributions of the trends in moisture, temperature, CO₂, and solar radiation to the trends in carbon and biomass assimilation.

4.3 Materials and Methods

4.3.1 Data and site selection

To model carbon uptake, we use a reconstructed solar-induced chlorophyll fluorescence (SIF) dataset (Chen et al., 2022b). Chen et al. (2022b) reconstructed the TROPOMI SIF dataset using the XGBoost machine learning algorithm, which is known for handling large datasets efficiently (Tan et al., 2021). Specifically, the algorithm used several input variables such as Caltech TROPOMI SIF data (Köhler et al., 2018), land surface temperature, land cover, Photosynthetically Active Radiation and surface albedo. While the Caltech TROPOMI SIF data had a time window of 2018-2020, other input datasets ranged from 2001-2020. All the input data was then split into training (80%) and testing (20%). The hyperparameters of the model were optimized using a grid search with 10-fold cross-validation. This approach finds the best parameter combination based on the Root Mean Square Error (RMSE). Model performance was evaluated by comparing the observed Caltech TROPOMI SIF data with the reconstructed TROPOMI SIF data. The R^2 value between the observed and reconstructed SIF values was 0.92 during model training and 0.91 during testing, while the regression slope was 1.00 for both training and testing. The high R^2 and regression slope values suggest that the XGBoost model performed well in reproducing the Caltech TROPOMI SIF data. To assess the reconstructed SIF product’s ability to capture seasonal and interannual changes in SIF, the data was further validated against tower-based SIF, GOME-2 SIF, OCO-2 SIF and FLUXNET GPP, achieving high accuracy in all cases (Chen et al., 2022b). The data record spans a period of 2001-2020 under clear sky conditions with a grid size of 0.05 degrees and temporal resolution of 8 days. The data-driven approach used to reconstruct the SIF dataset, robust model performance and high accuracy against various independent validation datasets motivated our usage of this product.

To model biomass assimilation, we use the EVI MOD13A2 product from the MODIS programme’s Terra satellite. The algorithm for the MOD13A2 product uses a compositing method based on criteria such as lowest cloud cover, lowest aerosol content, lowest angle view and highest EVI value to select the best pixel value (Didan, 2015). Furthermore, the 1 km product is an atmospherically corrected dataset consisting of 16-day image composites with high-quality observations (Didan, 2015). The data we used spans 2001-2020.

The environmental forcing data we used are the ERA5-Land products (Hersbach et al., 2020; Muñoz-Sabater et al., 2021) (European Centre for Medium-Range Weather Forecasts Reanalysis v.5; ERA5 henceforth). The ERA5 products are monthly reanalysis estimates of atmospheric variables at 0.1° grid size. The variables we used were volumetric soil water (0-7 cm soil depth), soil temperature

(0-7 cm soil depth), air temperature (2 m surface air temperature) and surface solar radiation. We obtained annual historical atmospheric CO₂ data from ISIMIP (<https://esg.pik-potsdam.de/projects/isimip/>).

We used 100 study sites (Figure 25) with a grid size of 9 km as identified by Higgins et al. (2023a). Large pixels sizes average out small-scale heterogeneity within landscapes. These sites are wilderness landscapes of the world’s major terrestrial ecosystems that were stratified by biome type: savanna (SA), grassland (GR), shrubland (SH), temperate evergreen and temperate deciduous forest (TF), boreal forest (BF), tropical evergreen forest (RF), Mediterranean-type ecosystems (MT) and tundra (TU). The criteria used by Higgins et al. (2023a) for selecting these pixels were as follows: (1) Pixels should have homogenous vegetation. Small-scale heterogeneity (for instance, peatlands, drainage lines, catenas) was permitted as long as they were frequently observed on the pixel over time (2) Pixels should have no evidence of land use effects (for instance, no evidence of tree harvesting, crop farming, or paved surfaces). Small agricultural or pastoral fields were allowed as long they remained constant in size over time (3) Pixels with large water bodies were excluded, but small water bodies were permitted if they did not violate criteria (1). (4) Pixels should not be adjacent to each other (i.e. neighboring pixels were not considered). Higgins et al. (2023a) used Google Earth Pro’s Time tool, which offers high resolution time series Earth observation imagery from 1984, to verify that all the 4 criteria were met.

The EVI, SIF and ERA5 forcing data were resampled to 9 km (using R (R Core Team, 2023), command `terra::resample`, method `bilinear`). The data was then linearly interpolated to provide weekly estimates for each variable (using R command `stats::approx`). This step determined the time interval of the time series analyses.

4.3.2 The TTR model excluding environmental forcing data

The description of the Thornely transport resistance (TTR) model without environmental forcing is modified from Higgins et al. (2023a)’s description of the model. We summarise the model description and do not claim any intellectual property associated with this model or how it is described.

The TTR model without environmental forcing is based on Thornley (1998)’s original model. Table IX provides a summary of the model parameters. The shoot and root mass (MS and MR , in kg) vary based on growth and loss dynamics (equations 6 and 7), while litter (k_L) and maintenance respiration (r) loss rates (in $\text{kg}\cdot\text{kg}^{-1}\cdot\text{day}^{-1}$) remain constants. The parameter K_M (in kg) indicates how loss depends on the mass pools (MS or MR). Plant growth (G_s and G_r , in $\text{kg}\cdot\text{day}^{-1}$) vary according to carbon and nitrogen concentrations (equations 8 and 9). CS , CR , NS and NR are carbon and nitrogen concentrations (in kg) in the

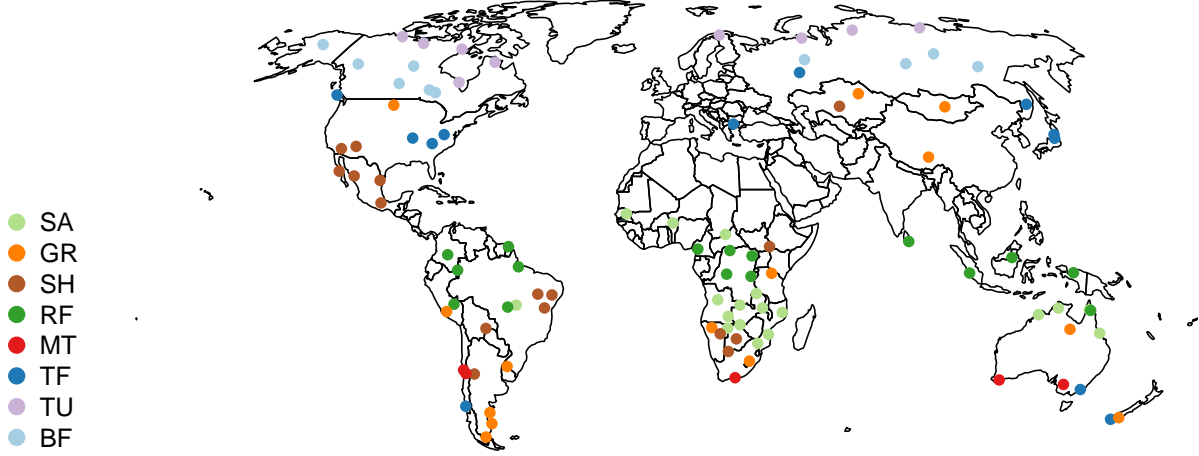


Figure 25: Geographic distribution of 100 study sites grouped by biome type. The sites represent the diversity of the major terrestrial ecosystems of the world as identified by Higgins et al. (2023a). Letters in the map legend indicate the biome type: SA= savanna, GR= grassland, SH= shrubland, RF= tropical evergreen forest, MT= Mediterranean type ecosystems, TF= temperate forest, TU= tundra, BF= boreal forest.

shoots and roots. The shoot and root dry matter are therefore represented such that,

$$MS[t + 1] = MS[t] + G_S[t] - \frac{(k_L + r)MS[t]}{1 + \frac{K_M}{MS[t]}}, \quad (6)$$

$$MR[t + 1] = MR[t] + G_R[t] - \frac{(k_L + r)MR[t]}{1 + \frac{K_M}{MR[t]}}, \quad (7)$$

where G_S and G_R are

$$G_S = g \frac{CS NS}{MS}, \quad (8)$$

$$G_R = g \frac{CR NR}{MR}, \quad (9)$$

g denote the growth coefficient (in $\text{kg.kg}^{-1}.\text{day}^{-1}$).

The shoot mass and net photosynthetic rate (a , $\text{kg.kg}^{-1}.\text{day}^{-1}$) are used to calculate carbon uptake U_C (equation 10). The root mass and the nitrogen uptake rate (b , in $\text{kg.kg}^{-1}.\text{day}^{-1}$) are used to calculate the nitrogen uptake U_N (equation 11). The parameter K_A (in kg) ensures that carbon uptake and nitrogen uptake are asymptotic relative to mass. The inhibition of carbon and nitrogen uptake are represented by parameters J_C and J_N (in kg.kg^{-1}) in equations 10 and 11, respectively. Specifically, these parameters simulate how source activity is inhibited at high substrate concentrations,

$$U_C = \frac{aMS}{\left(1 + \frac{MS}{K_A}\right)\left(1 + \frac{CS}{MS J_C}\right)}, \quad (10)$$

$$U_N = \frac{bMR}{\left(1 + \frac{MR}{K_A}\right)\left(1 + \frac{NR}{MR J_N}\right)}. \quad (11)$$

The movement of C and N substrates (τ_C and τ_N , in kg.day^{-1}) varies as a function of concentration gradients between roots and shoots and the associated resistances. Although Thornley (1998)'s model defined the resistances flexibly, we assume that resistances scale linearly with biomass,

$$\tau_C = \frac{MS MR}{MS + MR} \left(\frac{CS}{MS} - \frac{CR}{MR} \right) \quad (12)$$

$$\tau_N = \frac{MS MR}{MS + MR} \left(\frac{NR}{MR} - \frac{NS}{MS} \right) \quad (13)$$

Changes in carbon and nitrogen mass in the roots and shoots are denoted by

$$CS[t + 1] = CS[t] + U_C[t] - f_C G_s[t] - \tau_C[t] \quad (14)$$

$$CR[t + 1] = CR[t] + \tau_C[t] - f_C G_r[t] \quad (15)$$

$$NS[t + 1] = NS[t] + \tau_N[t] - f_N G_s[t] \quad (16)$$

$$NR[t + 1] = NR[t] + U_N[t] - f_N G_r[t] - \tau_N[t] \quad (17)$$

f_C and f_N (in kg.kg^{-1}) mimic the fractions of structural carbon and nitrogen.

4.3.3 The TTR model with environmental forcing data

The description of the TTR model with environmental forcing is modified from Higgins et al. (2023a)'s description of the model. We summarise the model description and do not claim any intellectual property associated with this model or how it is described.

Here, we illustrate how environmental forcing factors constrain the net photosynthetic rate (a), the nitrogen uptake (b), the growth rate (g) and the respiration rate (r). Equations (18)-(22) describe these environmental forcing effects. All remaining parameters are assumed to be constant. As in previous studies that have added environmental forcing to the TTR model (Higgins et al., 2012, 2023a), the model assumes that that environmental factors co-limit parameters a , b and g in a manner similar to the principles of Liebig's law of the minimum. In this study, the TTR model we use closely follows that of Higgins et al. (2023a), which uses the Farquhar model of photosynthesis (Farquhar et al., 1980; von Caemmerer, 2000) to mimic how air temperature, solar radiation and atmospheric CO_2 constrain photosynthesis (Conradi et al., 2020). We also assume that the parameters of the Farquhar model are considered universal and that plants use either C_3 or C_4 photosynthetic pathway. The photosynthetic rates of the Farquhar model are adjusted to $[0, a_{max}]$ to produce a_{fqr} . The influence of soil moisture (M_{soil}) on the photosynthetic rate is described by an increasing step function $S(M, \beta_1, \beta_2) = \max \left\{ \min \left(\frac{M - \beta_1}{\beta_2 - \beta_1}, 1 \right), 0 \right\}$. Therefore, a is redefined as,

$$a = a_{fqr} S(M, \beta_1, \beta_2) \quad (18)$$

Factors influencing nitrogen availability are intricate while plant nitrogen data are marked by uncertainty (Higgins et al., 2023a). Based on this, we assume that the nitrogen uptake rate (b) will vary as a function of soil temperature and soil moisture. Specifically, we assume that the nitrogen uptake rate has a maximum rate (b_{max}) constrained by both soil temperature (T_{soil}) and soil moisture (M_{soil}) such that,

$$b = b_{max} S(T_{soil}, \beta_3, \beta_4) Z(M, \beta_5, \beta_6, \beta_7, \beta_8) \quad (19)$$

We assume that the nitrogen uptake rate (b) first increases and then saturates with rising temperature (equation 19). Furthermore, we assume that the relationship between the nitrogen uptake rate and soil moisture follows a trapezoidal pattern, with low rates in dry conditions, higher rates at moderate moisture levels, and reduced rates in flooded soils. This trapezoidal function is represented by $Z(M, \beta_5, \beta_6, \beta_7, \beta_8) = \max \left\{ \min \left(\frac{M - \beta_5}{\beta_6 - \beta_5}, 1, \frac{\beta_8 - T_{max}}{\beta_8 - \beta_7} \right), 0 \right\}$.

We have described how environmental forcing factors constrain carbon and nitrogen assimilation in plants, which as a result influence plant growth as shown in equations (8) and (9). We further considered how the growth rate (g) is constrained by soil temperature (T_{soil}) and soil moisture (M_{soil}) so that,

$$g = g_{max} Z(T_{soil}, \beta_9, \beta_{10}, \beta_{11}, \beta_{12}) S(M_{soil}, \beta_{13}, \beta_{14}) \quad (20)$$

We use T_{soil} rather than air temperature (T_{air}) because vegetation activity is strongly influenced by soil temperature which also changes at slower rates compared to air temperature (Higgins et al., 2023a). In equations (6) and (7), the respiration rate (r) increases as air temperature (T_{air}) increases before reaching a peak value r_{max} such that,

$$r = r_{max} S(T_{air}, \beta_{15}, \beta_{16}). \quad (21)$$

The parameter r is the maintenance respiration. We do not explicitly consider growth respiration. We assume that the growth respiration is inherently included in the growth rate (g , equation 20) and that any temperature-related variations in growth respiration are already reflected in equation (20).

The effect of fire on the shoot mass (MS) is described as,

$$MS[t + 1] = MS[t](1 - S(F, \beta_{17}, \beta_{18})) \quad (22)$$

where F represents the fire severity indicator at time t (for instance burned area at t) and the function $S(F, \beta_{17}, \beta_{18})$ ensures that MS decreases when F is large. Previous work showed that data on fire effects was insufficient for estimating β_{17} and β_{18} (Higgins et al., 2023a); we therefore excluded fire effects in subsequent analyses. We also estimate the parameters β_a and β_b to allow each site

to have distinct maximum photosynthetic and nitrogen uptake rates, respectively. Subsequently, a is redefined as $a' = \beta_a a_{fqr}$ and b is redefined as $b' = \beta_b b$.

4.3.4 The TTR as a state-space model

We adopted a Bayesian state-space framework (Higgins et al., 2023a) to conceptually structure the analysis such that,

$$M[t] = f(M[t-1], \boldsymbol{\beta}, \boldsymbol{\theta}_{t-1}, \epsilon_{t-1}) \quad (23)$$

$$VI[t] = m M[t] + \eta. \quad (24)$$

where $M[t]$ is the predicted biomass (where biomass $M = MS + MR$) at time step t , ϵ_{t-1} is the process error of each state variable (MS , MR , CS , CR , NS and NR). The function $f(M[t-1], \boldsymbol{\beta}, \boldsymbol{\theta}_{t-1}, \epsilon_{t-1})$ mimics how the state variables MS , MR , CS , CR , NS , NR , $\boldsymbol{\beta}$ parameters and environmental forcing $\boldsymbol{\theta}_{t-1}$ influence the predicted biomass (M). Equation 24 is the observation equation that links the vegetation index (EVI) observations to the predicted M using the parameter m . Equation 24 assumes that the relationship between predicted biomass (M) and the VI is linear (Wessels et al., 2006; Zhu and Liu, 2015). We use the quality scores of the EVI product (labeled $Q = 0, 1, 2$, where 0 is good and 2 is poor; see Table X), to structure each observation error η in equation 24. These steps allow the observation error to grow larger as the quality score increases. Therefore, η is defined as $\eta = e_0 + e_1 Q$.

We formulated the model using the R package *LaplacesDemon* (Statisticat, LLC, 2021). We assigned non-informative uniform priors to all β parameters. A non-informative normal prior was given to the parameter m , constrained to be greater than 0. Gaussian distributions were used to model the process error terms while their corresponding variances were given half-Cauchy priors. We assigned non-informative normal priors to the parameters e_x , while a non-informative uniform prior was assigned to the initial biomass $M[0]$. To determine the posterior distributions of our model's parameters, we applied the twalk Markov chain Monte Carlo (MCMC) method using its default settings. We additionally used the genetic DEoptim algorithm (Storn and Price, 1997; Mullen et al., 2011) to fit the model and assess the MCMC algorithm's robustness in exploring the entire parameter space. We used DEoptim because the algorithm has been shown to be stable when handling complex multi-modal and high-dimensional challenges (Ardia et al., 2011). The log root-mean-square error of the models estimated with MCMC was significantly lower than those estimated using DEoptim (paired t-test SIF analysis: $t = -3.2946$, $d.f = 99$, $P = 1.1108 \times 10^{-5}$; paired t-test EVI analysis: $t = -4.4073$, $d.f = 99$, $P = 1.1925 \times 10^{-5}$), suggesting overall good performance of the MCMC algorithm compared to DEoptim.

4.3.5 Extracting anomalies and estimating trends

The 'seasonal and trend decomposition using Loess' (STL) (Cleveland et al., 1990) approach was applied to the data (using R command `stats::stl`). STL uses Loess smoothing to extract the seasonally-driven element s from within a time series. After extracting the seasonal element, the remainder r (or the anomaly) represents the combined effect of an existing long-term trend and random variations. This trend is estimated using two techniques. In the first approach, we fit a quadratic polynomial ($r = a + bx + cx^2$) to the remainder (r) (here x denote time while a , b and c are coefficients of the regression model). Using polynomials allowed us to determine if a trend is present, and if so, we then characterized the existing trend as either cup-shaped (i.e initial decrease in vegetation activity followed by an increase in vegetation activity) or hat-shaped (i.e an initial increase in vegetation activity followed by a decrease in vegetation activity) or linear (i.e no reversal in the trend direction). Second, we fit a bent-cable regression model to the remainder (r), to estimate the trend in the data. Bent-cable regression is a type of piece-wise linear regression that identifies the point of change where one linear phase shifts to another phase within a time series (Chiu et al., 2006; Khan and Kar, 2018). The model is of the form $r = b_0 + b_1x + b_2 q(x, \tau, \gamma)$ (Khan and Kar, 2018), where x denote time, b_0 represents the intercept, b_1 is the rate of change (or slope) in the first phase, $b_2 - b_1$ is the slope in the second phase while the function q defines the point of change such that: $q(x, \tau, \gamma) = \frac{(x-\tau+\gamma)^2}{4\gamma} I(\tau-\gamma < x < \tau+\gamma) + (x-\tau) I(x > \tau+\gamma)$; τ represents the point of change, γ determines how sharp or smooth r changes between the two linear phases at the point τ ; when A is true, the indicator function $I(A)$ returns 1; otherwise it returns 0. The bent-cable regression allowed us to determine if a trend is present, and if so, we then characterized the existing trend as either cup-shaped (i.e initial decrease in vegetation activity followed by an increase in vegetation activity) or hat-shaped (i.e an initial increase in vegetation activity followed by a decrease in vegetation activity) or linear (i.e no reversal in the trend direction), and whether the pattern is showing an overall increase or a decrease. We estimated the polynomial and bent-cable models using the Adaptive Metropolis MCMC algorithm as implemented in Laplaces Demon (Statisticat, LLC, 2021), and non-informative priors. We limited the values of τ to lie within the middle 70% range of the time series and restricted γ to a maximum of 2 years.

Extracting the seasonal components in the soil moisture, soil temperature, air temperature and solar radiation allowed us to model detrended time series (d) of the environmental forcing factors. We did not detect seasonality in the atmospheric CO₂ data. The model is of the form $d = \bar{y} + s + N(\mu, \sigma)$ where $N(\mu, \sigma)$ is a random variable with a normal distribution with mean μ and standard deviation σ estimated from the remainder r (we validated that the normal distribution provided a good description of r .), \bar{y} represents the average of the time series

while s represents the seasonal component estimated using STL. We calculated the average CO_2 over the time series to represent the CO_2 detrended time series.

Overall, the full workflow described in this section is visually summarised in Figure 26 and Figure 27.

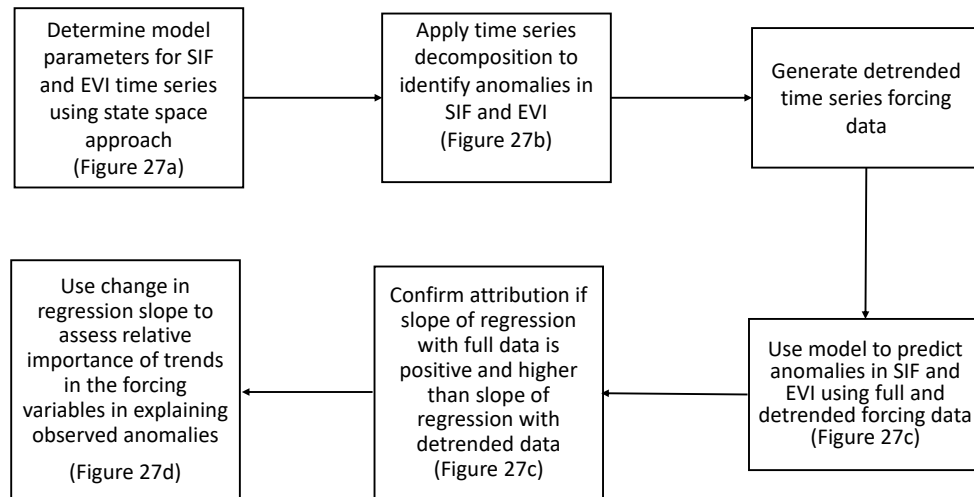


Figure 26: A schematic workflow summarising the steps in this study’s analyses. These steps were adapted from Higgins et al. (2023a).

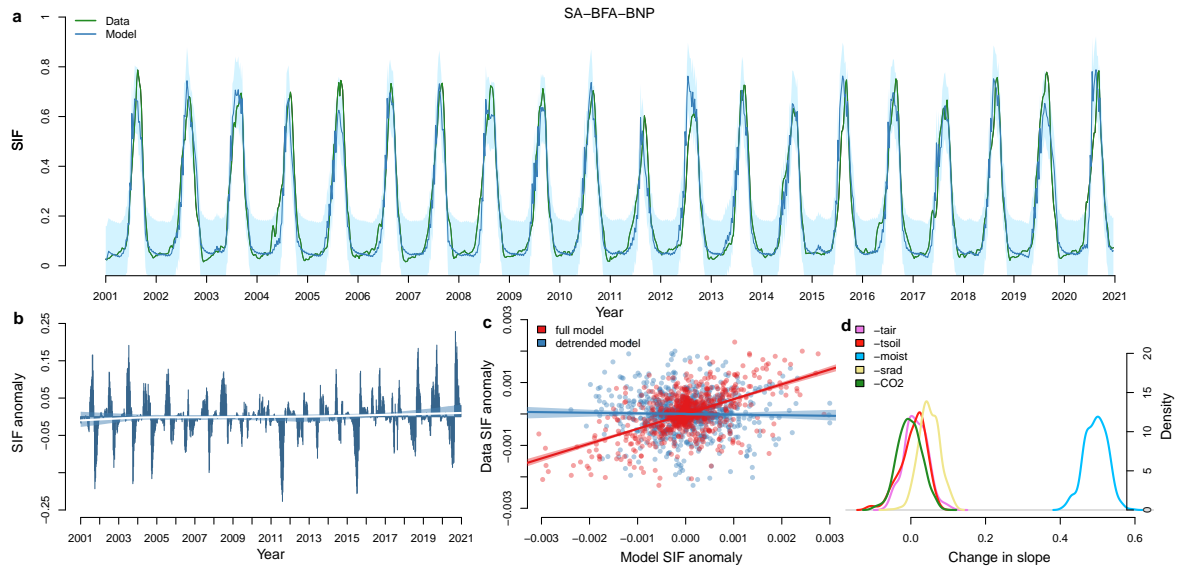


Figure 27: An analysis of SIF time series for a savanna biome in the Burkina Faso National Park, one of the 100 sites of this study. (a) The state-space model’s predictions of SIF vegetation activity data over a 2-decade period. The 95% credible intervals of the model’s predictions, shown by the light blue polygon, include uncertainties from processes in the system, observations and parameters. (b) Detected SIF data anomalies (visualised as blue bars) and a bent-cable regression model fitted to such anomalies. The shaded polygons (light blue) indicate the 95% credible intervals of the regression model’s predictions. (c) The model’s prediction of the anomalies in the SIF data using full and detrended environmental forcing factors as shown by the zero intercept regression. Prediction uncertainties are visualized as polygons (blue and red) representing 95% credible intervals. (d) The posterior density shows the sensitivity of the full model’s regression slope when removing trends in the forcing data. The example used here shows that at this study site, vegetation activity in the SIF data was dominantly sensitive to changes in moisture. Figure 32 shows a similar plot using EVI data. t_{air} = air temperature, t_{soil} = soil temperature, $moist$ = soil moisture, $srad$ = solar radiation, CO_2 = atmospheric CO_2 .

4.4 Results

4.4.1 Detected trends in vegetation activity

We found qualitatively different response types in the anomaly trends between SIF and EVI datasets using bent-cable piecewise linear regressions and quadratic polynomials. Most sites in the SIF analyses exhibited a cup-shaped trend (increased photosynthetic efficiency), while hat-shaped (decreased photosynthetic efficiency) trends were the second most common and linear trends the least (Figure 28 and 33). In contrast, most sites in the EVI analyses revealed that hat-shaped (browning) trends were the most dominant, followed by cup-shaped patterns (greening) while linear trends were the least common (Figure 34 and 35). Both datasets revealed non-linearity as the dominant pattern, with overall increasing trends being more prevalent than decreasing trends. Notably, these increasing trends were particularly pronounced in the hat-shaped patterns of both datasets.

4.4.2 Attribution of shifts in vegetation activity

We found that in 87 sites of SIF data and 79 sites of EVI data, the TTR model was able to predict observed anomalies in the datasets (SIF and EVI) and attribute them to the anomalies in the climatic forcing variables (Figure 29 and Figure 36). This suggests a detectable imprint of climatic variables on the functioning of terrestrial ecosystems. Classifying sites according to the relative importance of climatic variables in driving the detected vegetation anomalies revealed two qualitative similar groups in both the SIF and EVI datasets (Figure 30 and Figure 37). The first group was dominated by moisture as the driving factor in explaining anomalies in both datasets. This group was comprised of savanna, shrubland and grassland sites. The second group was dominated by temperature as the driving factor in explaining anomalies in both datasets. This group was comprised of temperate forest, boreal forest and tundra sites. The most striking result to emerge from both the SIF and EVI analyses is that atmospheric CO₂ and solar radiation had a weak effect on the model's prediction of the observed anomalies in the data (Figure 30 and Figure 37).

The driving factors that had a strong influence on the observed data anomalies were well-defined in a climate and geographic space. A discriminant analysis showed that the primary groups in Figure 30 and Figure 37 can be effectively distinguished using mean annual soil moisture and annual temperature (Figure 31 and Figure 38). Sites indicating anomalies in SIF and EVI primarily influenced by soil moisture anomalies were predominantly found in warm and dry environments. While sites indicating anomalies in SIF and EVI primarily influenced by temperature anomalies were located in cooler and moister regions. Sites where the state-space model could not attribute anomalies in the SIF and EVI data to

the anomalies in the forcing variables were mostly located in warmer and moister locations. These sites were primarily dominated by tropical rainforest sites, although some of the tundra sites showed similar patterns. In essence, these results adhere to fundamental ecological principles, suggesting that moisture limitation is a characteristic of warm and dry ecosystems, whereas temperature constraints are more prevalent in cooler ecosystems.

The response shapes of vegetation activity in the SIF and EVI datasets, including whether such responses exhibited increasing or decreasing trends over the study period, were not well segregated in climatic or geographic space (Figure 31 b, c, e, f and Figure 38 b, c, e, f). This suggests that changes in vegetation activity can occur at different temporal and spatial scales (Higgins and Scheiter, 2012). This further suggests that the response shapes of vegetation activity may differ even within the same time frame and geographic region (Pan et al., 2018; Sulla-Menashe et al., 2018; Hubau et al., 2020).

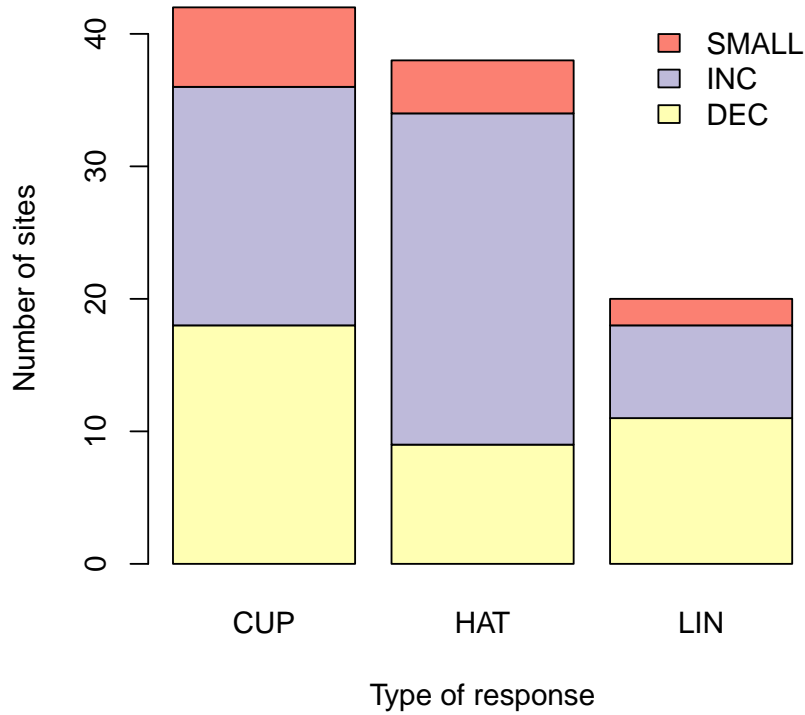


Figure 28: The frequency of SIF anomaly responses detected with bent-cable regression models over time. Shown here are the number of sites that exhibited cup-shaped trends (an initial decrease in photosynthetic activity followed by an increase), hat-shaped trends (an initial increase in photosynthetic activity followed by a decrease) and linear trends (no trend reversal in photosynthetic activity) in the SIF data anomalies. Different colours indicate the number of detected anomaly trends showing increases (INC) or decreases (DEC) over the time series. Increasing or decreasing response types of less than 5% were categorized as small. We found similar patterns when using a quadratic polynomial models (shown in Figure 33). The results for EVI data are shown in Figure 34 and Figure 35.

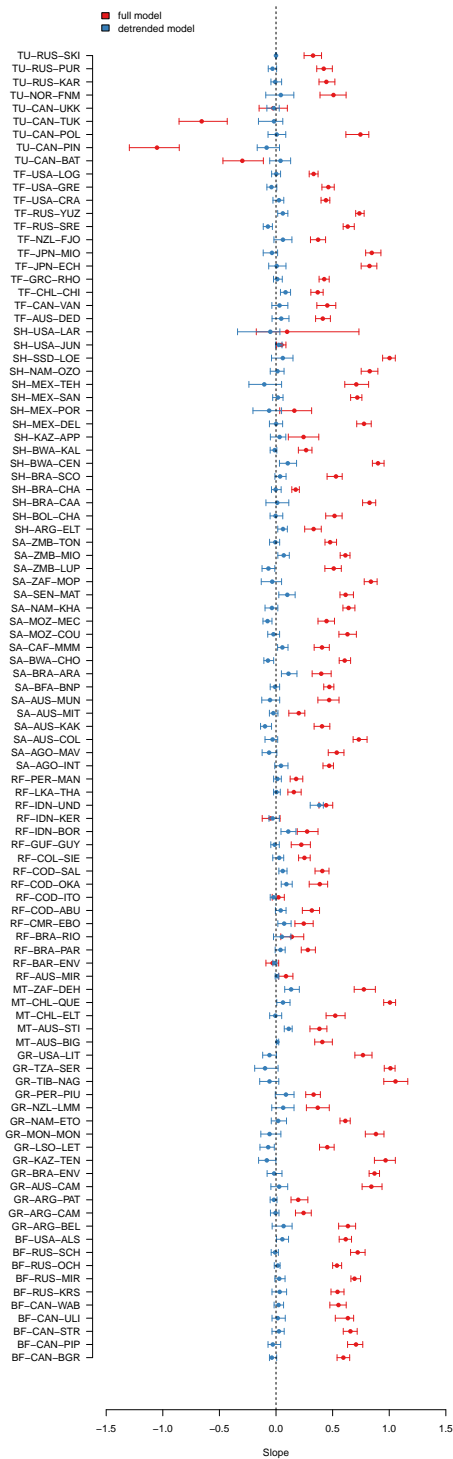


Figure 29: Predicted anomalies in SIF using full and detrended forcing data. Shown here are the slopes of the zero intercept regression of the model’s ability to predict anomalies in photosynthetic activity between the full vs detrended forcing data (as shown in Figure 27c). The points indicate the mean of the posterior estimates of the slope, with the tick marks spanning the 95 % credible intervals of the estimates. Attribution is confirmed if the slopes of the regression model with full climatic data is positive and higher (the credible intervals do not overlap) than slopes of the regression model with detrended data climatic data. Attribution was confirmed for 87 of 100 sites in the SIF data. Similar analyses are shown in Figure 36 using EVI data.

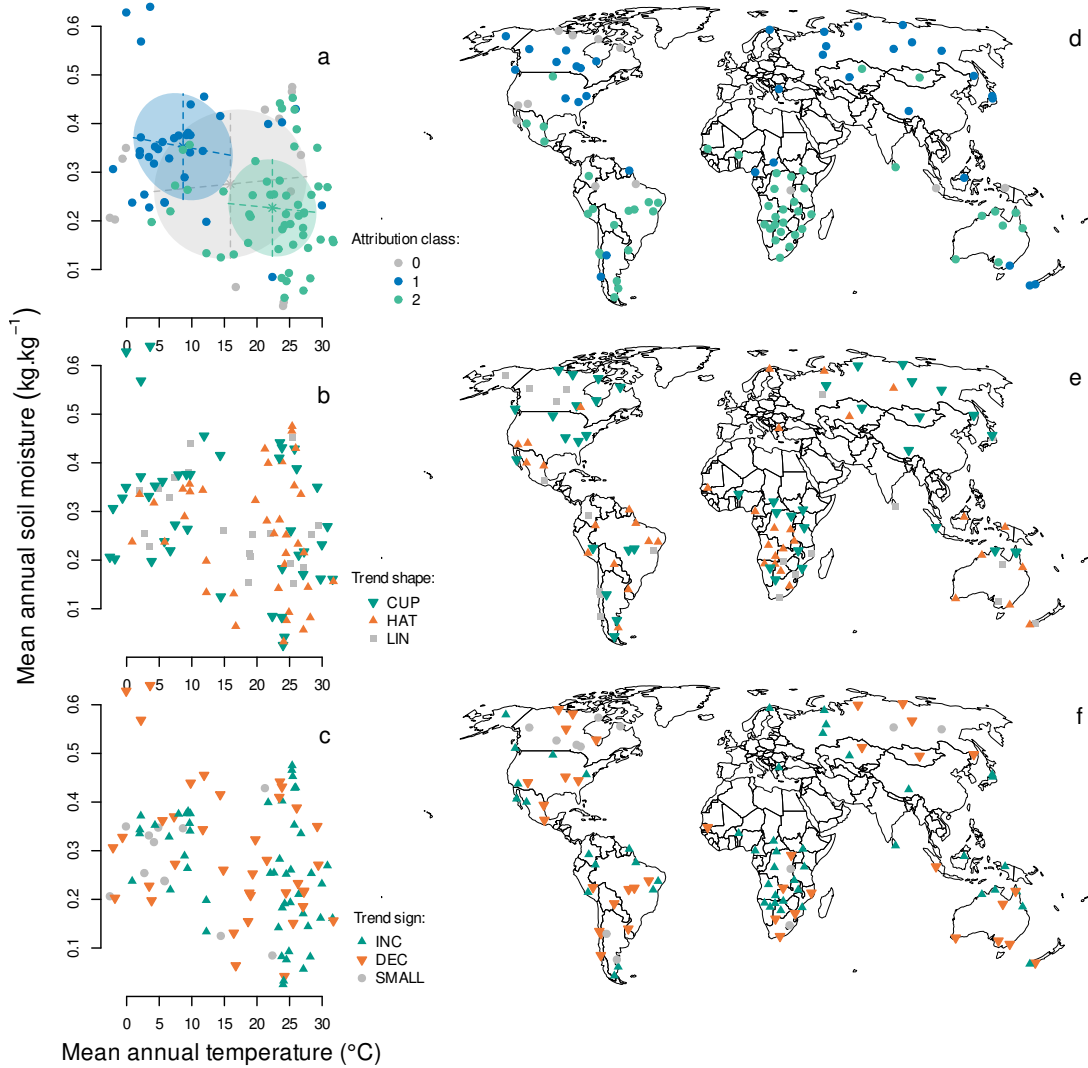


Figure 31: The sensitivity of ecosystems groups in climatic and geographic space analysed with SIF data. (a) The bicultural distribution of attribution groups shown in Figure 30. Points represent the distribution of this study's 100 study sites in a temperature and moisture space. Classes labelled 1 and 2 are the classified groups in Figure 30 while the class labelled as 0 were groups not included in Figure 30 because the model could not attribute anomalies in the SIF data. Ellipses show the class covariance estimates derived from discriminant analysis using Gaussian finite mixture models. Panels (b, c) show the shape of the trend (b) and direction of the trend (c) of the observed SIF anomaly (Figure 28) visualised in a bicultural space. The mean annual soil moisture and mean annual temperature for the time series were calculated using the ERA5 climate reanalysis data. Panels d, e and f are used to geographically plot the points in panels a, b and c. Figure 38 shows a similar analysis using EVI data.

4.5 Discussion

In this paper, we have presented an improved process-based model forced by weekly climatic variables, to detect changes in vegetation activity and attribute such changes to climatic drivers. The model uses SIF data as a novel proxy of carbon assimilation and uses EVI data as a proxy for biomass content. SIF offers the advantage of providing a signal that stems from the cores of a plant's photosynthetic machinery (Porcar-Castell et al., 2014), thereby a better proxy for carbon uptake unlike vegetation indices which provide no information on photosynthetic activity (Zhang et al., 2016), yet are commonly used in studies that assess GPP trends (Glenn et al., 2008; Zeng et al., 2022). Trend analyses showed that most study sites in the SIF data exhibited increased photosynthetic activity, while most study sites in the EVI data exhibited browning patterns. The model was able to detect anomalies in the response variables (87% for SIF and 79% for EVI) and attribute it to anomalies in the forcing data. Taken together, these findings suggest a detectable climate change signal in the functioning of terrestrial vegetation between 2001-2020.

The dominance of cup-shaped trends in SIF data suggest a switch from an initial decrease to increasing shifts in carbon uptake, which supports recent studies that have reported increasing global trends of SIF (Wang et al., 2022b; Zhou et al., 2022b) and increasing NPP and GPP trends (Smith et al., 2016; Green et al., 2019; Cai and Prentice, 2020; O'Sullivan et al., 2020; Zheng et al., 2020). The dominance of hat-shaped trends in the EVI dataset suggest shifts from an initial increase (greening) to a decrease (browning) is supported by studies that have depicted an overall decrease in EVI and NDVI trends (Zhao and Running, 2011; Higgins et al., 2023a).

The contrasting trends observed between SIF and EVI datasets may reflect different aspects of vegetation dynamics. The sensitivity of SIF to photosynthetic efficiency (LUE) may capture changes in carbon uptake driven by physiological responses to environmental drivers such as moisture availability and temperature. Since EVI is a greenness index that measures reflected light in the red, near-infrared and blue bands, which correlates with chlorophyll content, it may not always correlate with changes in photosynthetic efficiency (Huete et al., 2002). This may be because vegetation indices do not directly measure photosynthesis or related physiological processes as they constitute a mixed signal composed of chlorophyll content in leaves, canopy density and structure (Zhang et al., 2016). Therefore, this suggests that an increase in photosynthetic efficiency may not always guarantee an equivalent rise in vegetation greenness. Indeed, it has been shown that SIF and EVI exhibited contrasting responses to climatic variability, with SIF indicating stronger correlations with climatic variability (Walther et al., 2016; Wang et al., 2022a).

Another mechanism that may underlie the contrasting responses of vegetation in the SIF and EVI datasets may be related to how plants adapt to changing environmental conditions. Plants may allocate resources to stress tolerance mechanisms, such as investing in root growth instead of aboveground growth (Reich, 2014). These mechanisms cannot be captured by EVI data.

However, despite cup-shape trends being dominant in SIF and hat-shape trends in EVI, both datasets agree that increasing overall hat-shaped trends were more pronounced than decreasing trends. This suggests that a growing number of ecosystems may not sustain current productivity and greenness levels, potentially sequestering less carbon in the future (Higgins et al., 2023a). Studies have shown that future carbon sinks may slow down globally driven by nutrient constraints, increasing warming and frequent droughts (Peñuelas et al., 2017). These factors may have a negative effect on carbon sinks than the benefits gained from CO₂ and nitrogen fertilization. However, it is possible that our short time series of 2 decades may have played an important role in us detecting the increasing overall hat-shaped trends. But it is reassuring that our findings support that of Higgins et al. (2023a), who used the GIMMS NDVI dataset with a longer record of 34 years.

Both SIF and EVI analyses indicate sensitivity to climate change, with moisture primarily influencing southern latitudes and temperature affecting northern latitudes. The dominance of climate drivers support studies that have used satellite data to attribute shifts in vegetation activity to climate anomalies (Zhao and Running, 2010; Jiao et al., 2021; Higgins et al., 2023a). Surprisingly, CO₂ exhibited weak effects in both datasets, contrary to expectations of stronger CO₂ effects in SIF. The lack of CO₂ fertilization effects in driving vegetation activity contradicts studies reporting strong CO₂ effects (Zhu et al., 2016; Gonsamo et al., 2021), but our findings are supported by growing evidence that suggest that CO₂ enrichment effects on vegetation activity may be weakening globally (Smith et al., 2016; Peñuelas et al., 2017; Wang et al., 2020b; Higgins et al., 2023a; Chen et al., 2024). Studies have demonstrated that the lack of CO₂ fertilization effects on vegetation activity positively correlates with co-limiting effects of warming temperatures, moisture constraints and nutrient availability (Reich et al., 2014; Smith et al., 2016; Green et al., 2019; Xu et al., 2019; Jiao et al., 2021; Chen et al., 2024). This implies a potential saturation of CO₂ enrichment effects on terrestrial ecosystems, with a shift from CO₂ fertilization-dominated trajectory to a climate-dominated trajectory (Peñuelas et al., 2017).

We speculate that anomalies in the SIF and EVI data are driven by short-term climatic trends rather than a long-term rise in CO₂. That is, while elevated CO₂ may underlie long-term trends in vegetation activity, CO₂ effects may not explain inter-annual variations in vegetation activity. The CO₂ effects signal is

challenging because it is derived from direct and indirect factors (for example, greening, changes in canopy structure, enhanced water use efficiency (WUE), direct effect on RuBisCO, interactions with moisture and nutrient availability) (Walker et al., 2021). Separating the CO₂ signal from satellite remote sensing data is further exacerbated by the fact that all these direct and indirect factors are at play once (Wang et al., 2021). The proxies of GPP such as SIF, essentially measure these integrated factors which underlie the dynamics of CO₂ effects (Wang et al., 2021). Therefore, vegetation response to drivers such as moisture availability are more immediate and pronounced compared to the slow but cumulative effects of elevated CO₂.

Increasing warming and moisture constraints may override recent benefits gained from CO₂ fertilization effects on ecosystem carbon sequestration. This is because enhanced vegetation productivity driven by elevated CO₂ concentrations acts as a negative feedback on climate warming (Wang et al., 2020b). Specifically, by absorbing CO₂, plants dampen the rate of temperature increase caused by the greenhouse effect. Therefore, the weak CO₂ enrichment effects detected in this study suggest a declining negative feedback loop within the global climate system, potentially leading to increased overall warming trends. This also implies that weakening CO₂ enrichment effects would lead to increased dependence on policy makers and managers to create future strategies to mitigate increased warming (Peñuelas et al., 2017). This highlights the importance of global initiatives such as the Paris Agreement, which targets to limit global warming to well below 2 degrees Celsius (Parmesan et al., 2022). Understanding how climate change and nutrient constraints combine to override CO₂ enrichment in plants may be a starting point for adaptation and mitigation planning. The dominant effects of moisture constraints in southern latitudes and that of temperature in northern latitudes suggest that management efforts that adopt a one-size-fits all approach may be inappropriate. We argue that targeted responses should be tailored to regional climatic conditions of ecosystems. Scientists could focus on process-oriented model evaluation within climate models to better understand the complex relationships between climate change, elevated CO₂, and nutrient availability (Peñuelas et al., 2017). For example, conducting manipulative experiments such as FACE, warming experiments, altered rainfall experiments and nutrient fertilization experiments tailored to the environmental conditions of each region. This understanding could inform climate change policies and sustainable management responses.

Conservation responses should take into account the shifting dynamics of ecosystems. This may involve practices such as combating land degradation, preventing deforestation and reducing exploitation of natural resources, which are essential in maintaining ecosystem services such as carbon storage, carbon sequestration capacity and moisture availability of ecosystems (Dinerstein et al., 2020; Pörtner and

et al., 2021). Furthermore, to enhance the resilience of ecosystems, management efforts may prioritize reducing landscape fragmentation and providing larger habitat patches for species. This is because evidence suggests that inhabiting larger patches increases species' resilience to extreme climatic events such as droughts and warming (Oliver et al., 2015).

Although the machine learning models used to reconstruct the SIF dataset show overall good performance (Chen et al., 2022b), potential biases could be present in the SIF data. Specifically, the XGboost model used by Chen et al. (2022b) showed low accuracy in capturing the seasonal and interannual variations between predicted and observed SIF in biomes like savannas and grasslands. This bias could have propagated into our analyses. However, we do not expect this to be a long-term problem as satellite-based SIF products such as GOSAT, OCO-2 and TROPOMI SIF will expand in space and time (Köhler et al., 2018; Doughty et al., 2021).

We ignored the effects of fire on vegetation anomalies because existing global fire datasets do not provide sufficient information to estimate parameters of the TTR plant growth model (Higgins et al., 2023a). This may be because global fire datasets are highly uncertain (Chen et al., 2022a). Therefore, future studies could focus on regional attribution analyses that use localised fire datasets. Future studies could also expand on our analyses by focusing on biomes such savanna and grassland, that are historically prone to disturbance regimes (for example, herbivory and fire). This is because disturbances from fire and herbivory can override climatic forcing and may impact vegetation structure and functioning (Bond, 2005). Expanding the state-space model to include these effects would provide a comprehensive understanding of the drivers that underlie vegetation activity and their interactions over time.

In conclusion, we show that shifts in the activity of terrestrial vegetation are attributable to climatic forcing, thereby revealing a climate change signal on vegetation dynamics (Higgins et al., 2023a). We find that soil moisture is the major driver of changes of ecosystems in the southern latitudes while temperature is the main constraint in northern latitudes. We further show that weak CO₂ fertilisation effects are evident in carbon and biomass assimilation trends, suggesting that ongoing warming and moisture constraints may override previous CO₂ fertilisation benefits on vegetation activity. The contrasting forcing effects of moisture and temperature detected in different latitudes suggests that management interventions that may apply a one-size-fits-all approach may be inadequate. Therefore, regionally focused management strategies will be relevant to promote adaptation and mitigation of ongoing climate change. Future studies could consider regional attribution analyses due to differences in forcing effects between biomes.

4.6 Supplementary Information

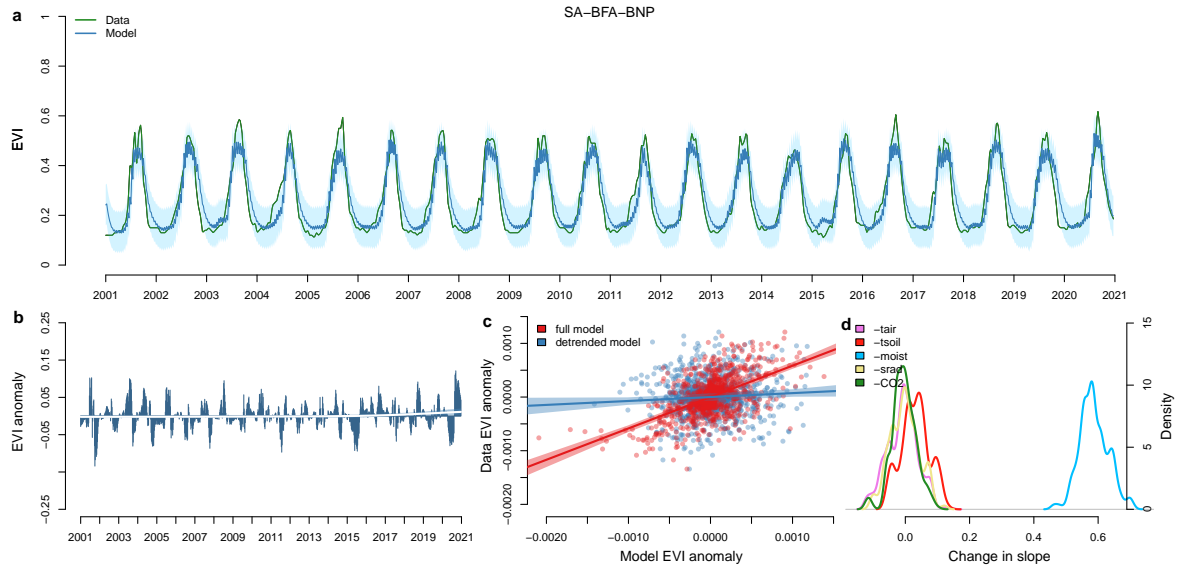


Figure 32: An analysis of EVI time series for a savanna biome in the Burkina Faso National Park, one of the 100 sites of this study. (a) The state-space model’s predictions of EVI vegetation activity data over a 2-decade period. The 95% credible intervals of the model’s predictions, shown by the light blue polygon, include uncertainties from processes in the system, observations and parameters. (b) Detected EVI data anomalies (visualised as blue bars) and a bent-cable regression model fitted to such anomalies. The shaded polygons (light blue) indicate the 95% credible intervals of the regression model’s predictions. (c) The model’s prediction of the anomalies in the EVI data using full and detrended environmental forcing factors as shown by the zero intercept regression. Prediction uncertainties are visualized as polygons (blue and red) representing 95% credible intervals. (d) The posterior density shows the sensitivity of the full model’s regression slope when removing trends in the forcing data. At this study site, vegetation activity in the EVI data was dominantly sensitive to changes in moisture. Figure 27 shows a similar plot using SIF data. t_{air} = air temperature, t_{soil} = soil temperature, $moist$ = soil moisture, $srad$ = solar radiation, CO_2 = atmospheric CO_2 .

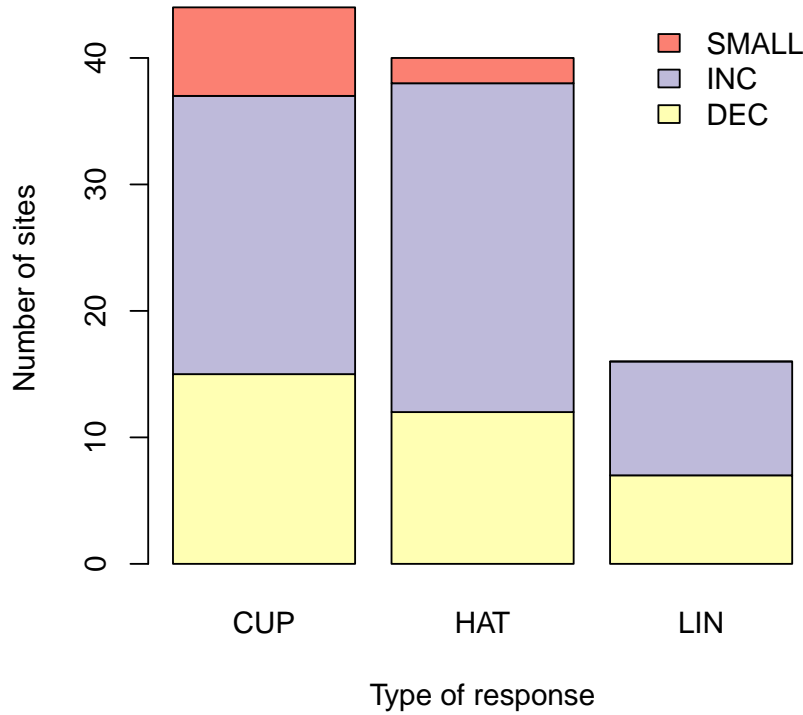


Figure 33: The frequency of SIF anomaly responses detected with quadratic polynomial regression models over time. Shown here are the number of sites that exhibited cup-shaped trends (an initial decrease in photosynthetic activity followed by an increase), hat-shaped trends (an initial increase in photosynthetic activity followed by a decrease) and linear trends (no trend reversal in photosynthetic activity) in the SIF data anomalies. Different colours indicate the number of detected anomaly trends showing increases (INC) or decreases (DEC) over the time series. Increasing or decreasing response types of less than 5% were categorized as small. We found similar patterns when using a bent-cable regression models (shown in Figure 28). The results for EVI data are shown in Figure 34 and Figure 35.

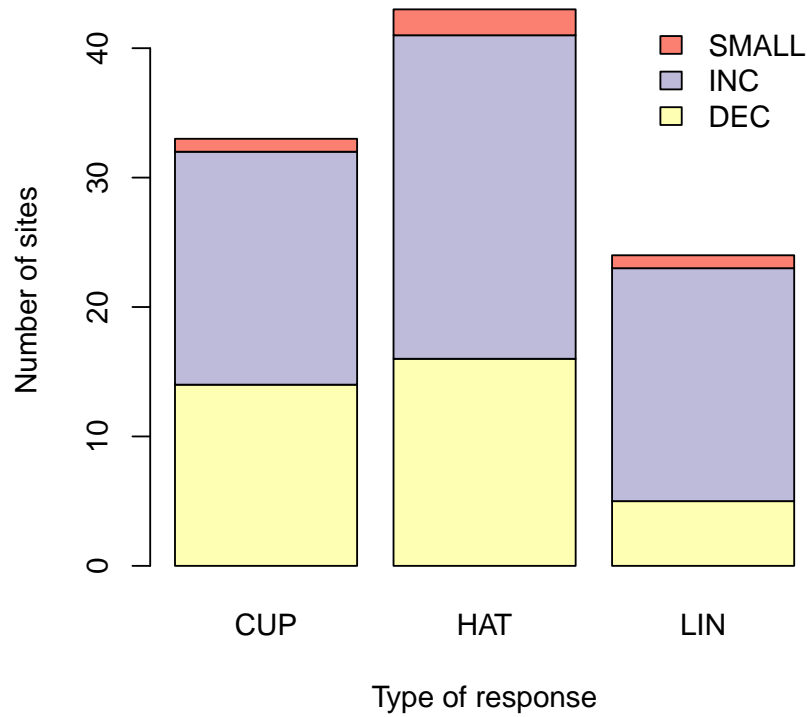


Figure 34: The frequency of EVI anomaly responses detected with bent-cable regression models over time. Shown here are the number of sites that exhibited cup-shaped trends (an initial decrease in vegetation activity followed by an increase), hat-shaped trends (an initial increase in vegetation activity followed by a decrease) and linear trends (no trend reversal in vegetation activity) in the EVI data anomalies. Different colours indicate the number of detected anomaly trends showing increases (INC) or decreases (DEC) over the time series. Increasing or decreasing response types of less than 5% were categorized as small. Results for EVI anomaly responses using polynomial regression models are shown in Figure 35. The results for SIF data are shown in Figure 28 and Figure 33.

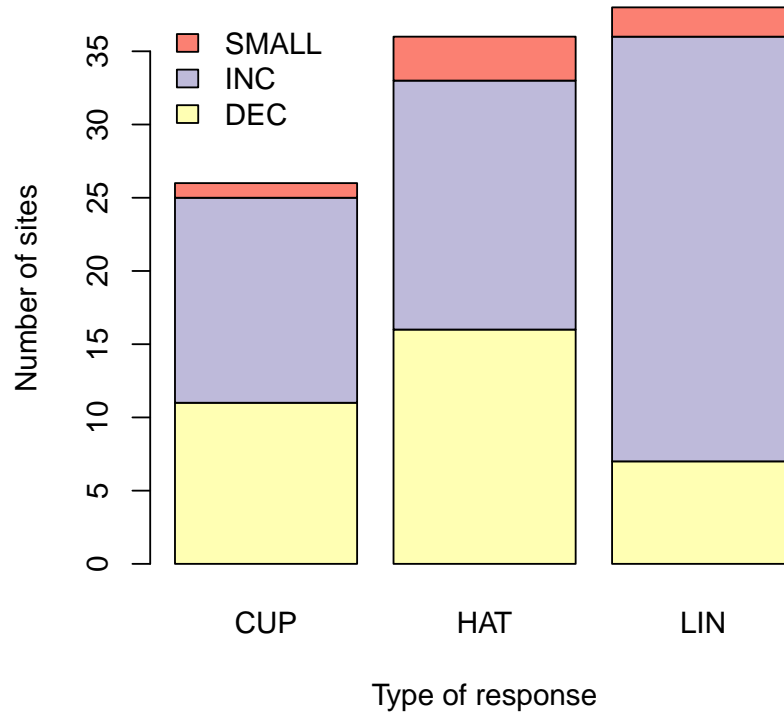


Figure 35: The frequency of EVI anomaly responses detected with quadratic polynomial regression models over time. Shown here are the number of sites that exhibited cup-shaped trends (an initial decrease in vegetation activity followed by an increase), hat-shaped trends (an initial increase in vegetation activity followed by a decrease) and linear trends (no trend reversal in vegetation activity) in the EVI data anomalies. Different colours indicate the number of detected anomaly trends showing increases (INC) or decreases (DEC) over the time series. Increasing or decreasing response types of less than 5% were categorized as small. The results for SIF data are shown in Figure 28 and Figure 33.

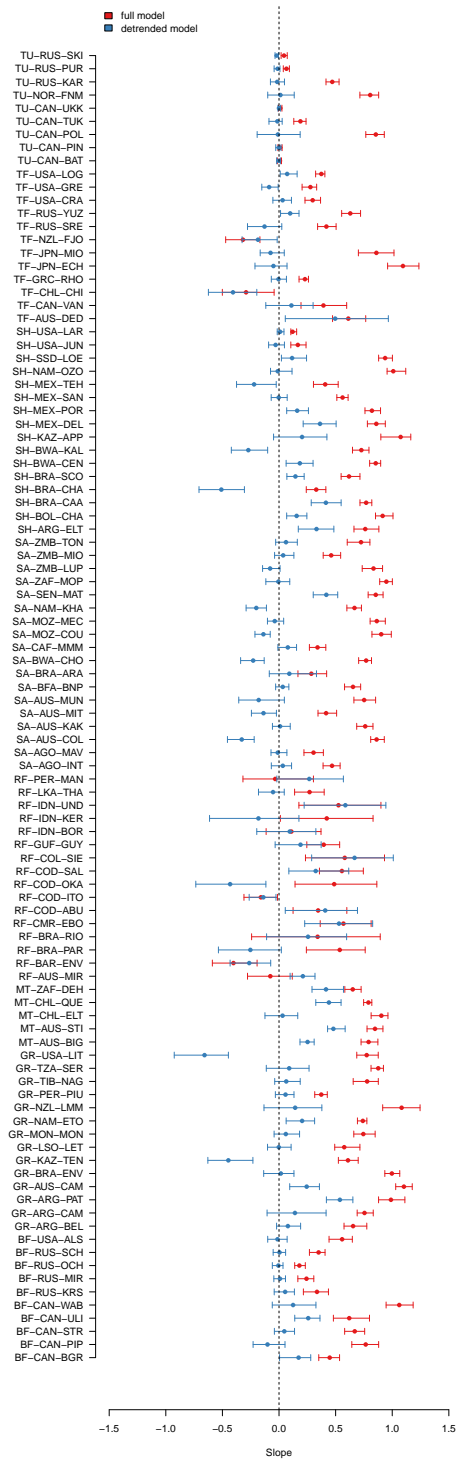


Figure 36: Predicted anomalies in EVI data using full and detrended forcing data. Shown here are the slopes of the zero intercept regression of the model’s ability to predict anomalies in biomass assimilation between the full vs detrended forcing data (as shown in Figure 32c). The points indicate the mean of the posterior estimates of the slope, with the tick marks spanning the 95 % credible intervals of the estimates. Attribution is confirmed if the slopes of the regression model with full climatic data is positive and clearly higher (the credible intervals do not overlap) than slopes of the regression model with detrended data climatic data. Attribution was confirmed for 79 of 100 sites in the EVI data.

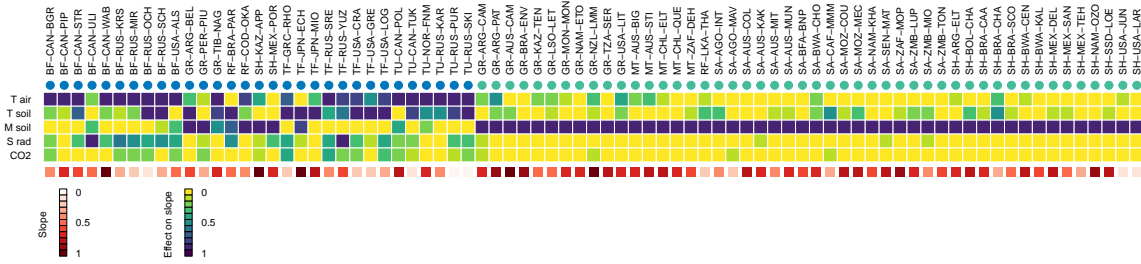


Figure 37: Sensitivity of EVI anomalies to anomalies in the forcing factors for all sites. The sensitivity quantifies the relative contribution of the forcing variables (T air = air temperature, T soil = soil temperature, M soil = soil moisture, S rad = solar radiation and CO₂ = atmospheric CO₂) on the model’s regression slope. The regression slope describes how effective the model can predict anomalies in the EVI data over time (as shown in Figure 32). The red color ramp represents the slope of the full model. The matrix shows that 79 of 100 (79%) sites where the model could attribute anomalies in the EVI data to anomalies in the forcing variables. Colored circles categorize the sites into response groups using an unsupervised classification approach. The site names are represented by codes that indicate biome type (SA=savanna, GR=grassland, SH=shrubland, TU=tundra, MT=Mediterranean type ecosystems, TF=temperate forest, RF=tropical evergreen forest, BF=boreal forest), country name based on the ISO 3166-1 alpha-3 codes and site name.

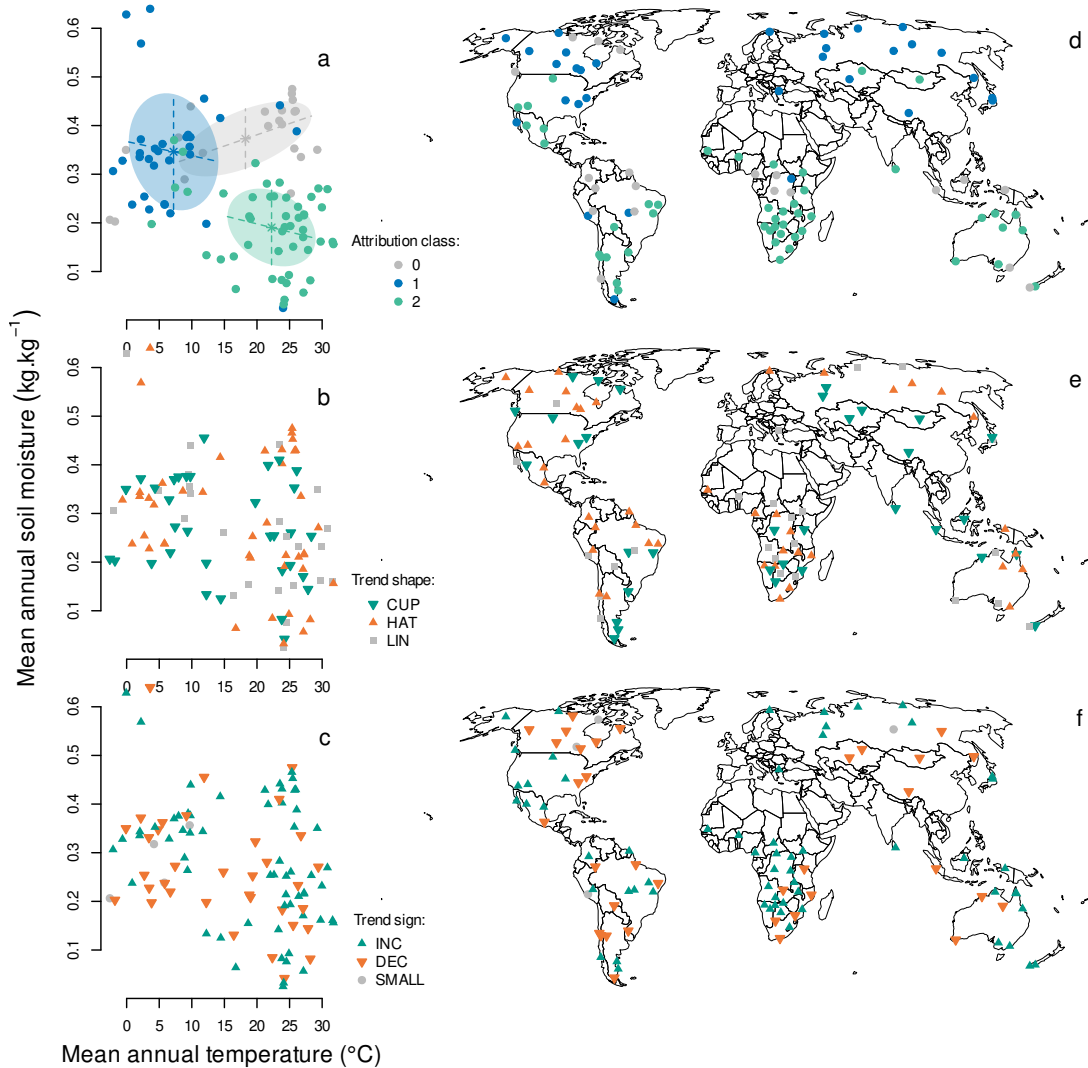


Figure 38: The sensitivity of ecosystems groups in climatic and geographic space analysed with EVI data. (a) The bicultural distribution of attribution groups shown in Figure 37. Points represent the distribution of this study’s 100 study sites in a temperature and moisture space. Classes labelled 1 and 2 are the classified groups in Figure 37 while the class labelled as 0 were groups not included in Figure 37 because the model could not attribute anomalies in the EVI data. Ellipses show the class covariance estimates derived from discriminant analysis using Gaussian finite mixture models. Panels (b, c) show the shape of the trend (b) and direction of the trend (c) of the observed EVI anomaly (Figure 34) visualised in a bicultural space. The mean annual soil moisture and mean annual temperature for the time series were calculated using the ERA5 climate reanalysis data. Panels d, e and f are used to geographically plot the points in panels a, b and c.

Summary of the TTR state space model parameters

TABLE IX: The TTR model parameters used in the state space model. The state space model uses the forcing data, constants and the β parameters to simulate the development of the state variables and link them to the SIF or EVI time series data. The β parameters described in the Methods are fitted to the time series for each site.

Symbol	Name	Value	Units
State variables			
MS	Mass shoot	-	kg biomass
MR	Mass root	-	kg biomass
CS	Carbon in shoot	-	kg C
CR	Carbon in root	-	kg C
CS	Nitrogen in shoot	-	kg N
CR	Nitrogen in root	-	kg N
Constants			
K_L	Litter loss rate	0.05	kg.kg ⁻¹ .day ⁻¹
r_{max}	Respiration loss rate	0.05	kg.kg ⁻¹ .day ⁻¹
K_M	Size dependency of loss rate	0.5	kg
g	Growth rate	200	kg.kg ⁻¹ .day ⁻¹
a	Carbon assimilation rate	0.2	kg.kg ⁻¹ .day ⁻¹
b	Nitrogen assimilation rate	0.02	kg.kg ⁻¹ .day ⁻¹
K_A	Size dependency of assimilation	1	kg
J_C	CS inhibition of C assimilation	0.5	kg.kg ⁻¹
J_N	NR inhibition of N assimilation	0.025	kg.kg ⁻¹
Forcing data			
R	Photosynthetically active radiation	-	$\mu\text{mol.m}^2.\text{s}^{-1}$
CO_2	Atmospheric CO_2 concentration	-	Pa
T_{air}	Air temperature	-	°C
T_{soil}	Soil temperature	-	°C
M	Soil moisture content	-	kg.kg ⁻¹

TABLE X: Simplified EVI and SIF quality scores used to parameterise observation uncertainty in the state space model.

Original score	Issue	Description	Simplified score
Quality			
0	Good data	Use with confidence	0
1	Marginal data	Useful, but look at other QA information	1
2	Snow/ice	Target covered with snow/ice	2
3	Cloudy	Target not visible, covered with cloud	2

The Farquhar photosynthesis model

The following model description is modified from Higgins et al. (2023a)'s description of von Caemmerer (2000)'s implementation of the Farquhar model. This description is provided as a summary of the model we used and not to claim any intellectual property associated with this model or how it is described.

The Farquhar C3 photosynthesis model is commonly used by ecophysiologicalists to simulate how temperature, solar radiation and atmospheric CO₂ concentration influence photosynthesis. We use the Farquhar model as implemented by von Caemmerer (2000) to simulate carbon assimilation in the state space model. The equations below explicitly show which of the model variants discussed by von Caemmerer (2000) we used (Table XI provides a summary of the parameters). The model assumes that the photosynthetic rate is either enzyme (biochemically) limited or electron transport limited. The Rubisco enzyme limited rate of CO₂ assimilation is,

$$A_c = \frac{(C_c - \Gamma_*)V_{cmax}}{C_c + K_c(1 + O_c/K_o)} - R_d. \quad (25)$$

C_c and O_c are the chloroplastic CO₂ and O₂ partial pressures and Γ_* is the CO₂ compensation point. V_{cmax} is the maximum rate of Rubisco activity. K_c and K_o are the Michaelis constants of Rubisco for CO₂ and O₂. R_d is the leaf mitochondrial respiration.

The electron transport rate of transpiration is defined as

$$A_j = \frac{(C_c - \Gamma_*)J_t}{4C_c + 8\Gamma_*} - R_d. \quad (26)$$

The chloroplastic CO₂ partial pressure is given as

$$C_c = C_i - A/g_m \quad (27)$$

where A is the overall assimilation rate, C_i is the internal CO₂ partial pressure.

The equations are used to derive two quadratic expressions for A_c and A_j , allowing the photosynthetic rate to be expressed as,

$$A = \min(A_c, A_j). \quad (28)$$

J_t is calculated as a function of photosynthetically active radiation (PAR), using a non-rectangular hyperbola,

$$J_t = \frac{\Theta PAR + J_{max} - \sqrt{(\Theta PAR + J_{max})^2 - 4\rho\Theta PAR J_{max}}}{2\rho}, \quad (29)$$

where J_{max} is the maximum rate of electron transport, ρ describes the curvature of the hyperbola and Θ is the initial slope of J_t versus PAR , which can be interpreted as the apparent quantum yield.

Some of the parameters in the photosynthesis models are temperature-dependent. For some parameters we use a Arrhenius function of the form

$$Y = Y_{25} \exp\left(\frac{E_Y(T_i - T_R)}{RT_i T_R}\right) \quad (30)$$

where Y_{25} is the parameter value at 25C and E_Y is the activation energy of the parameter. T_i is the leaf temperature (in Kelvin) and T_R is the reference temperature (298 K). R is the universal gas constant ($8.214 \text{ J mol}^{-1} \text{ K}^{-1}$). For the remaining parameters we used a peaked Arrhenius function,

$$Y = Y_{25} \exp\left(\frac{E_Y(T_i - T_R)}{RT_i T_R}\right) \frac{1 + \exp\left(\frac{T_R S_Y - H_Y}{RT_R}\right)}{1 + \exp\left(\frac{T_i S_Y - H_Y}{RT_i}\right)} \quad (31)$$

here E_Y is the activation energy, H_Y is the deactivation energy describing the rate of decrease for temperatures above the optimum temperature and S_Y is an entropy factor.

Applying the photosynthesis equations requires calculating the internal CO_2 concentration. We achieved this by linking a diffusion equation of photosynthesis with the biochemical equations described above using a regression model that relates stomatal conductance to photosynthesis (Ball et al., 1987). The regression equation Ball et al. (1987) is of the form $g_s = mTh/C_s + b$, where m and b are regression coefficients, T is the temperature, h is the relative humidity and C_s is the CO_2 concentration at the leaf surface. The diffusion equation is described as,

$$A_d = \frac{C_s - C_m}{1/g_s + 1/g_m} \quad (32)$$

TABLE XI: Summary of the photosynthesis model parameters used in this study, adopted from Higgins et al. (2023a).

Symbol	Name	Value	Units
V_{cmax}	Maximum Rubisco carboxylation rate	80	$\mu\text{mol.m}^2.\text{s}^{-1}$
J_{max}	Maximum rate of electron transport	$V_{cmax} * 1.8$	$\mu\text{mol.m}^2.\text{s}^{-1}$
R_d	Mitochondrial respiration in the light	$V_{cmax} * 0.01$	$\mu\text{mol.m}^2.\text{s}^{-1}$
Γ_*	CO ₂ compensation point	4.275	Pa
K_c	Michaelis constant Rubisco for CO ₂	40.49	Pa
K_o	Michaelis constant Rubisco for O ₂	27840	Pa
O_c	Chloroplast partial pressure O ₂	21000	Pa
Θ	Apparent quantum yield	0.85	$\mu\text{mol}.\mu\text{mol}^{-1}$
ρ	Curvature of light response	0.46	[-]
g_m	Mesophyll conductance for CO ₂	15	$\mu\text{mol m}^{-2}\text{s}^{-1}\text{Pa}^{-1}$
m	Ball-Berry slope	9	[-]
b	Ball-Berry intercept	0.01	[-]
E_V	Activation energy V_{cmax}	58.55	kJ mol^{-1}
S_V	Entropy factor V_{cmax}	0.62926	$\text{J mol}^{-1} \text{K}^{-1}$
H_V	Deactivation factor V_{cmax}	200	kJ mol^{-1}
E_J	Activation energy J_{max}	29.68	kJ mol^{-1}
S_J	Entropy factor J_{max}	0.63188	$\text{J mol}^{-1} \text{K}^{-1}$
H_J	Deactivation factor J_{max}	200	kJ mol^{-1}
E_{gm}	Activation energy g_m	49.6	kJ mol^{-1}
E_{Rd}	Activation energy R_d	46.4	kJ mol^{-1}
E_{Kc}	Activation energy K_c	79.43	kJ mol^{-1}
E_{Ko}	Activation energy K_o	36.38	kJ mol^{-1}
E_{Γ_*}	Activation energy Γ_*	37.83	kJ mol^{-1}

TABLE XII: Locations of the 100 sites and their names adopted from Higgins et al. (2023a). The first two letters of the site names represent the biome type: SA=savanna, GR=grassland, SH=shrubland, TU=tundra, MT=Mediterranean type ecosystems, TF=temperate forest, RF=tropical evergreen forest, BF=boreal forest. The middle three are ISO 3166-1 alpha-3 country codes and the last three letters were derived from place names near the site.

longitude	latitude	site name
-106.37	53.79	BF-CAN-BGR
-92.88	51.79	BF-CAN-PIP
-105.54	59.29	BF-CAN-STR
-129.46	59.96	BF-CAN-ULI
-89.96	50.96	BF-CAN-WAB
58.62	61.37	BF-RUS-KRS
100.46	60.04	BF-RUS-MIR
115.71	63.29	BF-RUS-OCH
129.63	59.12	BF-RUS-SCH
-153.87	66.37	BF-USA-ALS
-70.54	-51.54	GR-ARG-BEL
-66.37	-47.46	GR-ARG-CAM
-65.79	-44.13	GR-ARG-PAT
137.54	-19.38	GR-AUS-CAM
-55.79	-30.38	GR-BRA-ENV
74.38	50.62	GR-KAZ-TEN
28.79	-28.80	GR-LSO-LET
105.13	46.62	GR-MON-MON
15.38	-18.87	GR-NAM-ETO
169.79	-45.63	GR-NZL-LMM
-74.46	-14.13	GR-PER-PIU
91.96	31.62	GR-TIB-NAG
35.21	-2.79	GR-TZA-SER
-103.45	47.13	GR-USA-LIT
141.54	-35.71	MT-AUS-BIG
-70.71	-32.45	MT-CHL-ELT
-71.28	-31.45	MT-CHL-QUE
117.96	-34.38	MT-AUS-STI
24.21	-33.71	MT-ZAF-DEH
143.38	-13.79	RF-AUS-MIR
-49.71	-0.87	RF-BAR-ENV

Continued on next page

long	lat	site name
-53.71	-12.79	RF-BRA-PAR
-70.13	-1.88	RF-BRA-RIO
10.46	4.38	RF-CMR-EBO
21.21	3.96	RF-COD-ABU
28.29	-3.71	RF-COD-ITO
28.62	2.37	RF-COD-OKA
20.13	-3.04	RF-COD-SAL
-73.46	2.71	RF-COL-SIE
-53.13	5.12	RF-GUF-GUY
115.79	1.87	RF-IDN-BOR
101.62	-2.71	RF-IDN-KER
136.46	-2.62	RF-IDN-UND
81.37	6.62	RF-LKA-THA
-71.79	-11.96	RF-PER-MAN
17.21	-10.63	SA-AGO-INT
20.88	-15.54	SA-AGO-MAV
147.96	-20.54	SA-AUS-COL
132.38	-13.12	SA-AUS-KAK
125.96	-15.05	SA-AUS-MIT
142.88	-13.62	SA-AUS-MUN
2.13	12.12	SA-BFA-BNP
-50.79	-12.21	SA-BRA-ARA
24.96	-18.04	SA-BWA-CHO
19.79	8.70	SA-CAF-MMM
34.79	-20.87	SA-MOZ-COU
39.13	-14.38	SA-MOZ-MEC
20.79	-19.04	SA-NAM-KHA
-13.62	14.79	SA-SEN-MAT
31.29	-23.54	SA-ZAF-MOP
32.38	-13.04	SA-ZMB-LUP
24.71	-12.21	SA-ZMB-MIO
30.21	-8.79	SA-ZMB-TON
-67.79	-32.62	SH-ARG-ELT
-61.62	-19.13	SH-BOL-CHA
-38.62	-9.21	SH-BRA-CAA
-41.29	-13.05	SH-BRA-CHA
-43.37	-8.96	SH-BRA-SCO
23.88	-22.21	SH-BWA-CEN
21.29	-25.96	SH-BWA-KAL

Continued on next page

long	lat	site name
65.38	46.79	SH-KAZ-APP
-98.71	24.71	SH-MEX-DEL
-113.54	27.46	SH-MEX-POR
-107.96	26.04	SH-MEX-SAN
-97.21	18.04	SH-MEX-TEH
18.29	-20.71	SH-NAM-OZO
34.54	5.12	SH-SSD-LOE
-110.37	34.79	SH-USA-JUN
-115.29	34.13	SH-USA-LAR
148.54	-37.21	TF-AUS-DED
-127.54	50.21	TF-CAN-VAN
-73.96	-42.21	TF-CHL-CHI
24.46	41.42	TF-GRC-RHO
139.30	37.20	TF-JPN-ECH
139.78	38.31	TF-JPN-MIO
167.21	-46.13	TF-NZL-FJO
136.54	47.37	TF-RUS-SRE
54.37	57.21	TF-RUS-YUZ
-80.29	38.29	TF-USA-CRA
-83.62	35.62	TF-USA-GRE
-91.22	37.27	TF-USA-LOG
-90.21	64.87	TU-CAN-BAT
-72.46	60.54	TU-CAN-PIN
-82.79	54.12	TU-CAN-POL
-122.05	69.13	TU-CAN-TUK
-109.42	66.81	TU-CAN-UKK
24.54	69.71	TU-NOR-FNM
61.96	68.62	TU-RUS-KAR
88.13	71.47	TU-RUS-PUR
121.38	72.29	TU-RUS-SKI

Chapter 5

5 General Discussion

5.1 Overview

All 21 metrics we used to study vegetation phenology in southern Africa showed changes of at least 1 standard deviation for each pixel between 2000-2019. This is the first study to show multi-dimensional changes in the phenological behaviour of vegetation in the region and such changes could have consequences for ecosystem functioning. Furthermore, the Functional Biomes (FB) of southern Africa changed significantly between 2000-2021, with 3% to 15% of pixels shifting in biome state. The empirical findings in this study provide a new understanding of FB dynamics in southern Africa. Globally, we found that SIF data dominantly showed switches from decreased photosynthetic activity to increased photosynthetic activity, while EVI dominantly showed switches from greening to browning trends between 2001-2020.

Attribution analyses in both datasets agree that vegetation in northern latitudes was sensitive to changes in temperature while southern latitudes was sensitive to changes in moisture. Furthermore, both datasets revealed weak CO₂ effects on the detected change. These findings extend the work of Higgins et al. (2023a) by revealing that carbon and biomass assimilation trends are strongly influenced by climatic factors, while CO₂ fertilisation effects are less prominent than previously thought. Taken together, this thesis demonstrates a convincing climate change signal in the functioning of terrestrial ecosystems at the regional scale of southern Africa or globally.

5.2 Dynamics of vegetation phenology

5.2.1 Potential mechanisms that underlie the detected phenological patterns

Studies have shown that in regions typical of phenomes 3, 4 and 7, the start of the growing season metrics are primarily driven by precipitation and day length (Archibald and Scholes, 2007; Cho et al., 2017; Whitecross et al., 2017; Wigley et al., 2024). This suggests that early onset of the rainfall season coupled with longer summer days may trigger plant growth, leading to early initiation of the start of the growing season metrics. Our results further show that the late occurrence of the end of the growing season metrics played a more important role in shaping the observed phenological patterns in these phenomes. Delayed end of the growing season metrics suggests CO₂ effects. Elevated CO₂ enhances carbon

uptake and plant growth rates, which also improves water use efficiency. This relieves moisture constraints on plant productivity, resulting in an extended growing season and increased carbon assimilation (Peñuelas and Filella, 2009; Higgins and Scheiter, 2012; Martens et al., 2021).

However, the CO₂ fertilisation phenomena may be co-limited by moisture, temperature and nutrient constraints (Peñuelas et al., 2017), suggesting that CO₂ effects on plant growth are not ubiquitous and may vary depending on climatic and soil conditions. The late initiation of the start of the growing season metrics in phenomes 1, 2, 5 and 6 coincide with studies that have reported increased rainfall variability in these regions (Davis-Reddy and Vincent, 2017; Trisos et al., 2022). In these regions, rainfall variability is characterized by delayed onset and shortened duration of the rainfall season, with frequent dry spells. Thus, moisture constraints may hinder the triggering of green up cues of vegetation in these regions (Wigley et al., 2024). The early initiation of the end of the growing season metrics in these phenomes are also consistent with studies that suggest that senescence metrics are driven by temperature (Cho et al., 2017). Indeed, these phenomes coincide with regions where temperatures have risen by at least twice the rate of global warming (Engelbrecht et al., 2015), with such warming rates associated with frequent heatwaves (Trisos et al., 2022). Frequent heatwaves coupled with prolonged droughts may result in higher evapotranspiration rates, leading to an earlier end of the phenological cycle. This is because plants may close their stomata or reduce photosynthetic activity to conserve moisture.

5.2.2 Ecological implications of phenological changes

The qualitatively different phenological responses of vegetation in our phenome approach reflect differences in climatic forcing effects in southern Africa (Higgins et al., 2023b, 2024). Phenomes with increased vegetation activity (i.e longer growing seasons in phenomes 3, 4 and 7) suggest a greening effect. Increased biomass implies that these regions are a carbon sink, thus our dataset might be useful in regional Net Primary Productivity (NPP) estimates. However, increases in vegetation biomass can also decrease populations of species such as mammals, birds and reptiles that prefer less dense vegetation (Péron and Altwegg, 2015; McCleery et al., 2018). Increased vegetation cover also promotes invasive species which can alter plant communities and disrupt ecosystem services (Pejchar and Mooney, 2009). Therefore, there may be trade-offs between carbon sequestration and biodiversity loss because of increased vegetation biomass. Restoration efforts may include removal of invasive species, implementing heterogenous fire management regimes (Fuhlendorf et al., 2009) and increasing populations of browsers to diversify herbivore functional guilds (Hempson et al., 2015).

Long-term declines in plant and bird biodiversity driven by warming and dry-

ing climate, have been reported in regions that coincide with phenomes 1, 2, 5, 6 (Slingsby et al., 2017; McKechnie et al., 2021). This has also led to species migrations and extinctions (Foden et al., 2007). Where restoration and resilience interventions are not feasible, conservation managers could embrace and facilitate the change. For example, using inventory assessments, conservation managers could identify vulnerable species to drier and warmer climates, then facilitate their movements in refugial areas. Managers could also promote drought and heat-tolerant species (Ouédraogo et al., 2013; Abraham et al., 2019) or increase artificial water sources within protected areas to safeguard biodiversity. This study might be useful in guiding management efforts in identifying hotspots of phenological change, where risks of phenological mismatches are likely to be high (Renner and Zohner, 2018).

5.2.3 Potential future research directions on vegetation phenology

Although our study support existing literature in the region, our analyses were not validated with ground truth data. This is because there is a lack of ground phenological data in southern Africa (Adole et al., 2016). Future studies could build on our analyses by combining citizen science in phenological estimates to improve the accuracy of phenological assessments. Future studies could also use biophysical models to attribute the detected phenological changes to environmental drivers, thereby providing a relative contribution of each forcing factor on the detected change.

Emerging datasets such as Solar Induced Fluorescence (SIF), which directly measures photosynthetic activity in plants (Frankenberg et al., 2011), have been shown to provide a quicker response in tracking vegetation phenology compared to EVI in regions such as Europe, China, Australia (Walther et al., 2016; Wang et al., 2019, 2022a). However, such knowledge remains unknown in Africa. Therefore, studies could assess the influence of climatic limitations on phenological differences between SIF and EVI, NIRv (near-infrared reflectance of vegetation) in Africa. Such an approach could be applied to compare phenological responses in non-protected areas vs protected areas. These findings would deepen our knowledge of vegetation phenology from the perspectives of photosynthesis and greenness.

5.3 Changes in the Functional Biomes of southern Africa

5.3.1 Potential mechanisms that underlie the detected shifts in Functional Biomes

Biome transitions to more productive and non-seasonal states (to MN and HN states) were the most common, suggesting that favourable conditions for plant growth are being sustained for longer periods of the growing season. This may imply CO₂ fertilization effects. Elevated CO₂ increases light-use efficiency (LUE) and water-use efficiency (WUE) by enhancing carbon assimilation and reducing transpiration in plants, which consequently extends the length of the growing season (Peñuelas and Filella, 2009; Higgins and Scheiter, 2012). Indeed, Higgins and Scheiter (2012) showed that rising CO₂ can shift vegetation to more productive states across Africa. Recent model projections also show that African biomes are likely to shift to more productive and non-seasonal states (Martens et al., 2021). This may be because CO₂ fertilisation effects coupled with light competition and fire suppression may influence trends towards woody biomass by altering the competitive balance favoring trees, thereby creating positive feedback that suppresses grasses but promote tree growth (Bond and Midgley, 2012). Therefore, increased woody biomass or tree growth would suggest less seasonality compared to grass-dominated ecosystems.

FB transitions from both moisture and temperature-limited states (from MB and HB) to solely moisture-limited states (to MD and HD) suggest increased warming. Southern Africa has experienced increased mean surface temperatures (Engelbrecht and Engelbrecht, 2016; Trisos et al., 2022), which may have diminished the role of cold temperatures in limiting physiological processes such as photosynthesis and transpiration. This suggests that moisture availability has become the primary constraint on vegetation activity. However, the expansion of low productive moisture-limited biomes shifts to even lower productive non-seasonal states (i.e., from LD to LN which is a transition to desert environments) suggests increasing limiting effects of moisture availability. Coupled with warming temperatures, the net effect is a decrease in productivity and shifts towards arid conditions.

5.3.2 Ecological implications of shifts in Functional Biomes

We reveal previously undetected changes in the FB of southern Africa, thereby provide a data foundation for validating existing biophysical models commonly used to predict future biome change. Although continental studies anticipate that Africa's biomes will shift to more productive and non-seasonal states (Higgins and Scheiter, 2012; Martens et al., 2021), our empirical assessments provides compelling evidence that such anticipated biome trajectories are already ongoing. Transitions towards higher productive and non-seasonal states may lead to changes in plant

community composition, impacting ecological processes such as competition, predation or promote the emergence of invasive species (Niang et al., 2014; Slingsby et al., 2017; Péron and Altwegg, 2015; McCleery et al., 2018). This is particularly true for protected areas, as they are regarded to be vulnerable to colonisation by range-shifting species because they provide a suitable habitat for such species (Hiley et al., 2013). Conservation managers could conduct ground surveys to assess changes in species diversity and abundance, followed by applying actions like removing invasive species and restoring degraded habitats. Furthermore, altering fire and herbivory regimes to maintain ecosystems in their natural state may safeguard biodiversity (Midgley and Bond, 2015). Shifts to moisture-limited states which suggests increasing moisture constraints on plant growth, could impact plant communities. For example, increased drought frequency could lead to increased plant mortality (Niang et al., 2014), thus hindering natural plant succession. Furthermore, drier ecosystems could impact the availability of natural water sources obtained from fruits and flowers by wildlife. For example, it has been shown that decreased fruit production attributed to drier and warmer climate consequently reduced the body condition of fruit-reliant elephants by 11% (Bush et al., 2020). Our results suggest that embracing shifts to dry-limited ecosystems will become increasingly necessary. Conservation responses may include promoting arid-adapted species and increasing artificial water sources to support plant succession and access to water by wildlife, respectively. Moreover, promoting connectivity between protected areas and intensively managing vulnerable species to drought may safeguard refugial areas where local populations can persist (Lee et al., 2023).

5.3.3 Potential future research directions

Although our FB emerge from the data, we subjectively categorized the VPI and growth limitation attributes. To improve the objectivity of future studies, it may be necessary to develop a standardized method for categorizing these attributes. This is because if one uses more classes, more transitions will be detected. The spatial resolution of the climatic forcing data we used was low compared to that of the EVI data. It is therefore possible that fine-scaled variation in soil moisture and temperature may not propagate into our metrics. We anticipate that higher-resolution reanalysis data might be available in the future, which could potentially capture such fine-scale variations in the climatic forcing data.

Although the observed biome shifts are most likely to be driven by climate change and increasing CO₂, changes in local disturbance regimes such as fire and herbivores may have played an equally important role. Therefore, future studies could consider integrating disturbance regimes in their classification schemes. In addition, studies should also consider topographical effects in biome classification, such as elevation and slope. Topography can cause variations in solar radiation,

moisture, and temperature, which consequently affects the EVI signal.

Our exclusive focus on protected areas allow us to eliminate the possibility that the changes we detected are due to land use change. The interactions between climate and vegetation are highly non-linear. Therefore, the detected FB trajectories could either accelerate or reach an asymptote. Continuous monitoring of these FB will reveal which of these possibilities is realized. The changes in FB states detected here emphasizes the need for establishing a robust biodiversity monitoring system for the region. We propose a multifaceted approach that combines Earth observation data and citizen science knowledge to track the extent and magnitude of climate change impacts on biodiversity of southern Africa. Earth observation provides advantages of obtaining increasingly available spatio-temporal data at no cost, while citizen science can be used to identify indicator species that serve as flagship warnings of ecosystem change (Siddig et al., 2016). This early detection system would enable the timely implementation of adaptation and mitigation measures. Furthermore, incorporating long-term permanent monitoring sites into the system would provide insights on the magnitude, severity and rates of ecosystem change, thus aiding the assessment of future changes in ecosystem functioning. To my knowledge, such a monitoring system does not exist for southern Africa.

5.4 Beyond detection to attribution

5.4.1 Potential mechanisms that underlie the attributed shifts in vegetation activity

The contrasting trends between SIF and EVI datasets reflect different aspects of vegetation dynamics. The sensitivity of SIF to photosynthetic efficiency (LUE) captures changes in carbon uptake driven by physiological responses to environmental drivers. As a greenness index, EVI measures reflected light in the red, near infrared and blue bands. Although this reflected light correlates with chlorophyll content, it may not always correlate with changes in photosynthetic efficiency (Huete et al., 2002). This is because vegetation indices do not directly measure photosynthesis or related physiological processes, they measure a mixed signal composed of chlorophyll content in leaves, canopy density and structure (Zhang et al., 2016). This suggests that an increase in photosynthetic efficiency may not always guarantee an equivalent rise in vegetation greenness. Indeed, studies have shown that SIF and EVI exhibited contrasting responses to climatic variability, with SIF indicating stronger correlations with climatic variability (Walther et al., 2016; Wang et al., 2022a). Another mechanism that may underlie the contrasting responses of vegetation in the SIF and EVI datasets may be related to how plants adapt to changing environmental conditions. Plants may allocate resources to stress tolerance mechanisms, such as investing in root growth instead of above-ground growth (Reich, 2014). These effects may not be captured by EVI.

However, despite qualitatively different trends in SIF and EVI datasets (i.e. dominance of hat-trends in SIF and cup-trends in EVI), both datasets agree that increasing overall hat-shaped trends were more pronounced than decreasing trends. This suggests that an increasing number of ecosystems may not sustain current productivity and greenness levels, potentially sequestering less carbon in the future (Higgins et al., 2023a). Studies have shown that weak CO₂ fertilization effects positively correlates with co-limiting effects of warming temperatures, moisture constraints and nutrient availability (Reich et al., 2014; Smith et al., 2016; Green et al., 2019; Xu et al., 2019; Jiao et al., 2021). It is also possible that our time series of 2 decades may have played an important role in us detecting the increasing overall hat-shaped trends. However, our findings support that of Higgins et al. (2023a), who used the GIMMS NDVI dataset with a longer record of 34 years.

Another mechanistic explanation for the weak CO₂ effects in the SIF and EVI anomalies is that such anomalies may be driven by short-term climatic trends rather than a long-term rise in CO₂. That is, while elevated CO₂ may underlie long-term trends in vegetation activity, CO₂ effects may not explain inter-annual variations in vegetation activity. The CO₂ effects signal is challenging to measure because it is derived from direct and indirect factors (for example, greening,

changes in canopy structure, enhanced water use efficiency (WUE), its effect on the RuBisCO enzyme, interactions with moisture and nutrient availability) (Walker et al., 2021). Separating the CO₂ signal from satellite remote sensing data is further exacerbated by the fact that all these direct and indirect factors are at play once (Wang et al., 2021). The proxies of GPP such as SIF, essentially measure these integrated factors which underlie the dynamics of CO₂ effects (Wang et al., 2021). Therefore, vegetation response to drivers such as moisture availability and warming temperatures are more immediate and pronounced compared to the slow but cumulative effects of elevated CO₂.

5.4.2 Ecological implications

Warming temperatures and moisture constraints may override recent benefits gained from CO₂ fertilization effects on ecosystem carbon sequestration. Enhanced vegetation productivity driven by elevated CO₂ concentrations acts as a negative feedback on global warming (Wang et al., 2020b). By absorbing CO₂, plants dampen the rate of temperature increase driven by the greenhouse effect. Therefore, the weak CO₂ enrichment effects detected in this study suggest a diminishing ability of ecosystems to buffer against climate shifts, potentially leading to increased warming. Weak CO₂ enrichment effects would also lead to increased dependence on policy makers and managers to create future strategies to mitigate increased warming (Peñuelas et al., 2017). This highlights the importance of global initiatives such as the Paris Agreement, which targets to limit global warming to well below 2 degrees Celsius (Parmesan et al., 2022). ability of ecosystems to buffer against climate shifts. Conservation responses should consider the shifting dynamics of ecosystems. This may involve practices such as combating land degradation, preventing deforestation and reducing exploitation of natural resources, which are essential in maintaining ecosystem services such as carbon storage, carbon sequestration capacity and moisture availability of ecosystems (Dinerstein et al., 2020; Pörtner and et al., 2021). To promote ecosystem resilience, management efforts may prioritize reducing landscape fragmentation and providing larger habitat patches for species. This is because evidence suggests that inhabiting larger patches increases species' resilience to extreme climatic events such as droughts and warming (Oliver et al., 2015).

5.4.3 Potential future research directions

Understanding how climate change and nutrient constraints combine to override CO₂ enrichment in plants may be a starting point for adaptation and mitigation strategists. The dominant effects of moisture constraints in southern latitudes and that of temperature in northern latitudes imply that management efforts that

adopt a one-size-fits all approach may be inappropriate. We argue that targeted responses should be tailored to regional climatic conditions. Scientists could focus on process-oriented model evaluation within climate models to better understand the complex relationships between climate change, elevated CO₂, and nutrient availability (Peñuelas et al., 2017). For example, conducting manipulative experiments such as FACE, warming experiments, altered rainfall experiments and nutrient fertilization experiments tailored to the environmental conditions of each region. This understanding could inform climate change policies and sustainable management responses.

The XGboost model used by Chen et al. (2022b) to reconstruct the SIF dataset we used in this study showed low accuracy in capturing the seasonal and interannual variations between predicted and observed SIF in biomes like savannas and grasslands. This bias could have propagated into our analyses. However, this is likely to be a short term problem as satellite-based SIF products such as GOSAT, OCO-2 and TROPOMI SIF will expand in space and time (Köhler et al., 2018; Doughty et al., 2021). Uncertainties inherent in global fire datasets (Chen et al., 2022a) meant that fire effects on vegetation anomalies were not considered in this study. Future studies could expand on our analyses by using localised fire datasets in fire prone biomes such as savannas and grasslands. This is because disturbances such as fire and herbivory can override climatic forcing effects on vegetation activity, thus impacting vegetation structure and functioning (Bond, 2005).

5.5 Conclusions

In this thesis, I have demonstrated an integrated approach for monitoring and attributing changes in vegetation activity. This thesis showed that the phenological cycle of the vegetation of southern Africa changed by at least 1 standard deviation for each metric we used to quantify change. To further dissect this change, we grouped metrics that have similar phenological properties (phenomes). We found that the phenological activity within phenomes is qualitatively different, with some phenomes exhibiting a shortened growing season while others exhibiting an extended growing season. This suggests that studies that do not assess multi-dimensional changes in the seasonal pattern of vegetation activity may provide an incomplete picture of how terrestrial ecosystems respond to climatic variables. The magnitude and spatial extent of change revealed here provide convincing evidence that the vegetation of southern Africa is responding to climate change. The findings of this study may assist conservation managers in identifying hotspots of phenological change, thereby developing monitoring systems to strengthen the capacity for adaptation and mitigation of ongoing ecosystem changes.

We found that 3% to 15% of pixels shifted in biome state. These pixels represent vegetation units with similar phenology and productivity properties, which we defined as Functional Biomes (FB). We detected that the FB of southern Africa are on trajectory from low productive to high productive, non-seasonal states as well as from both moisture and temperature limited states to solely moisture limited states. While current knowledge suggests that the biomes of Africa are anticipated to shift to non-seasonal and moisture limited states driven by climate change and elevated CO₂, the empirical analyses of this study provide compelling evidence that suggests that such anticipated biome trajectories are already ongoing in southern Africa. Thus, this study provides a data foundation for validating existing biophysical models which can be used to predict future biome change.

At the global scale, we found that carbon assimilation trends at 100 study sites have switched from an initial decrease in photosynthetic efficiency to an increase in photosynthetic efficiency. In contrast, biomass trends have switched from an initial greening to browning. This suggests that plants may be adapting to changing environmental conditions by allocating resources to stress tolerance mechanisms, such as root growth, instead of above ground growth. We also found that changes in vegetation activity in 87% of the sites in the SIF data and 79% of sites in the EVI data can be attributed to changes in climatic factors and that CO₂ effects are weak. The attribution results challenge widely held narratives of strong CO₂ effects on the functioning of terrestrial ecosystems. Our attribution results rather show strong geographic coherence, with soil moisture the major driver of changes of ecosystems in the southern latitudes while temperature is the main constraint in northern latitudes. Overall, this study strengthens growing evidence that sug-

gests that ecosystems may be shifting from a CO₂ dominated world to a climate-dominated world. Due to differences in forcing effects between regions, we argue that management efforts need to account for the trajectories these ecosystems are on, as a one-size-fits-all approach may be inappropriate.

References

- Abraham, J. O., Hempson, G. P., and Staver, A. C. (2019). Drought-response strategies of savanna herbivores. *Ecology and evolution*, 9(12):7047–7056.
- Adole, T., Dash, J., and Atkinson, P. M. (2016). A systematic review of vegetation phenology in africa. *Ecological Informatics*, 34:117–128.
- Adole, T., Dash, J., and Atkinson, P. M. (2018a). Characterising the land surface phenology of africa using 500 m modis evi. *Applied Geography*, 90:187–199.
- Adole, T., Dash, J., and Atkinson, P. M. (2018b). Major trends in the land surface phenology (lsp) of africa, controlling for land-cover change. *International Journal of Remote Sensing*, 39(22):8060–8075.
- Adole, T., Dash, J., Rodriguez-Galiano, V., and Atkinson, P. M. (2019). Photoperiod controls vegetation phenology across africa. *Communications biology*, 2(1):1–13.
- Ainsworth, E. A. and Long, S. P. (2005). What have we learned from 15 years of free-air co2 enrichment (face)? a meta-analytic review of the responses of photosynthesis, canopy properties and plant production to rising co2. *New phytologist*, 165(2):351–372.
- Archibald, S. and Scholes, R. (2007). Leaf green-up in a semi-arid african savanna—separating tree and grass responses to environmental cues. *Journal of Vegetation Science*, 18(4):583–594.
- Ardia, D., Boudt, K., Carl, P., Mullen, K. M., and Peterson, B. G. (2011). Differential evolution with DEoptim. An application to non-convex portfolio optimization. *The R Journal*, 3(1):27–34.
- Asner, G. P., Levick, S. R., Kennedy-Bowdoin, T., Knapp, D. E., Emerson, R., Jacobson, J., Colgan, M. S., and Martin, R. E. (2009). Large-scale impacts of herbivores on the structural diversity of african savannas. *Proceedings of the National Academy of Sciences*, 106(12):4947–4952.
- Baccini, A., Walker, W., Carvalho, L., Farina, M., Sulla-Menashe, D., and Houghton, R. (2017). Tropical forests are a net carbon source based on above-ground measurements of gain and loss. *Science*, 358(6360):230–234.
- Ball, J. T., Woodrow, I. E., and Berry, J. A. (1987). *Progress in Photosynthesis Research. Volume IV.*, pages 221–224. Martinus-Nijhoff Publishers, Dordrecht, The Netherlands.

- Bar-On, Y. M., Phillips, R., and Milo, R. (2018). The biomass distribution on earth. *Proceedings of the National Academy of Sciences*, 115(25):6506–6511.
- Bascompte, J. and Jordano, P. (2007). Plant-animal mutualistic networks: the architecture of biodiversity. *Annu. Rev. Ecol. Evol. Syst.*, 38(1):567–593.
- Beck, H. E., Zimmermann, N. E., McVicar, T. R., Vergopolan, N., Berg, A., and Wood, E. F. (2018). Present and future köppen-geiger climate classification maps at 1-km resolution. *Scientific data*, 5(1):1–12.
- Berdugo, M., Delgado-Baquerizo, M., Soliveres, S., Hernández-Clemente, R., Zhao, Y., Gaitán, J. J., Gross, N., Saiz, H., Maire, V., Lehmann, A., et al. (2020). Global ecosystem thresholds driven by aridity. *Science*, 367(6479):787–790.
- Bergstrom, D. M., Wienecke, B. C., van den Hoff, J., Hughes, L., Lindenmayer, D. B., Ainsworth, T. D., Baker, C. M., Bland, L., Bowman, D. M., Brooks, S. T., et al. (2021). Combating ecosystem collapse from the tropics to the antarctic. *Global Change Biology*, 27(9):1692–1703.
- Bjorkman, A. D., Myers-Smith, I. H., Elmendorf, S. C., Normand, S., Rüger, N., Beck, P. S. A., Blach-Overgaard, A., Blok, D., Cornelissen, J. H. C., Forbes, B. C., Georges, D., Goetz, S. J., Guay, K. C., Henry, G. H. R., HilleRisLambers, J., Hollister, R. D., Karger, D. N., Kattge, J., Manning, P., Prevéy, J. S., Rixen, C., Schaepman-Strub, G., Thomas, H. J. D., Vellend, M., Wilmking, M., Wipf, S., Carbognani, M., Hermanutz, L., Lévesque, E., Molau, U., Petraglia, A., Soudzilovskaia, N. A., Spasojevic, M. J., Tomaselli, M., Vowles, T., Alatalo, J. M., Alexander, H. D., Anadon-Rosell, A., Angers-Blondin, S., Beest, M. t., Berner, L., Björk, R. G., Buchwal, A., Buras, A., Christie, K., Cooper, E. J., Dullinger, S., Elberling, B., Eskelinen, A., Frei, E. R., Grau, O., Grogan, P., Hallinger, M., Harper, K. A., Heijmans, M. M. P. D., Hudson, J., Hülber, K., Iturrate-Garcia, M., Iversen, C. M., Jaroszynska, F., Johnstone, J. F., Jørgensen, R. H., Kaarlejärvi, E., Klady, R., Kuleza, S., Kulonen, A., Lamarque, L. J., Lantz, T., Little, C. J., Speed, J. D. M., Michelsen, A., Milbau, A., Nabe-Nielsen, J., Nielsen, S. S., Ninot, J. M., Oberbauer, S. F., Olofsson, J., Onipchenko, V. G., Rumpf, S. B., Semenchuk, P., Shetti, R., Collier, L. S., Street, L. E., Suding, K. N., Tape, K. D., Trant, A., Treier, U. A., Tremblay, J.-P., Tremblay, M., Venn, S., Weijers, S., Zamin, T., Boulanger-Lapointe, N., Gould, W. A., Hik, D. S., Hofgaard, A., Jónsdóttir, I. S., Jorgenson, J., Klein, J., Magnusson, B., Tweedie, C., Wookey, P. A., Bahn, M., Blonder, B., van Bodegom, P. M., Bond-Lamberty, B., Campetella, G., Cerabolini, B. E. L., Chapin, F. S., Cornwell, W. K., Craine, J., Dainese, M., de Vries, F. T., Díaz, S., Enquist, B. J., Green, W., Milla, R., Niinemets, , Onoda, Y., Ordoñez, J. C.,

- Ozinga, W. A., Penuelas, J., Poorter, H., Poschlod, P., Reich, P. B., Sandel, B., Schamp, B., Sheremetev, S., and Weiher, E. (2018). Plant functional trait change across a warming tundra biome. *Nature*, 562(7725):57–62.
- Bonan, G. B. (2008). Forests and climate change: forcings, feedbacks, and the climate benefits of forests. *science*, 320(5882):1444–1449.
- Bonan, G. B. and Doney, S. C. (2018). Climate, ecosystems, and planetary futures: The challenge to predict life in Earth system models. *Science*, 359(6375).
- Bond, W., Midgley, G., and Woodward, F. (2003). The importance of low atmospheric co₂ and fire in promoting the spread of grasslands and savannas. *Global Change Biology*, 9(7):973–982.
- Bond, W. J. (2005). Large parts of the world are brown or black: A different view on the ‘green world’ hypothesis. *Journal of Vegetation Science*, 16(3):261–266.
- Bond, W. J. and Midgley, G. F. (2012). Carbon dioxide and the uneasy interactions of trees and savannah grasses. *Philosophical Transactions of the Royal Society B: Biological Sciences*, 367(1588):601–612.
- Brienen, R. J., Caldwell, L., Duchesne, L., Voelker, S., Barichivich, J., Baliva, M., Ceccantini, G., Di Filippo, A., Helama, S., Locosselli, G. M., et al. (2020). Forest carbon sink neutralized by pervasive growth-lifespan trade-offs. *Nature communications*, 11(1):4241.
- Buitenwerf, R., Bond, W., Stevens, N., and Trollope, W. (2012). Increased tree densities in south african savannas: 50 years of data suggests co₂ as a driver. *Global Change Biology*, 18(2):675–684.
- Buitenwerf, R., Rose, L., and Higgins, S. I. (2015). Three decades of multi-dimensional change in global leaf phenology. *Nature Climate Change*, 5(4):364–368.
- Bush, E. R., Whytock, R. C., Bahaa-El-Din, L., Bourgeois, S., Bunnefeld, N., Cardoso, A. W., Dikangadissi, J. T., Dimbonda, P., Dimoto, E., Edzang Ndong, J., et al. (2020). Long-term collapse in fruit availability threatens central african forest megafauna. *Science*, 370(6521):1219–1222.
- Byakatonda, J., Parida, B., Moalafhi, D. B., Kenabatho, P. K., and Lesolle, D. (2020). Investigating relationship between drought severity in botswana and enso. *Natural Hazards*, 100:255–278.

- Cai, W. and Prentice, I. C. (2020). Recent trends in gross primary production and their drivers: analysis and modelling at flux-site and global scales. *Environmental Research Letters*, 15(12):124050.
- Chen, C., Park, T., Wang, X., Piao, S., Xu, B., Chaturvedi, R. K., Fuchs, R., Brovkin, V., Ciais, P., Fensholt, R., et al. (2019). China and india lead in greening of the world through land-use management. *Nature sustainability*, 2(2):122–129.
- Chen, I. C., Hill, J. K., Ohlemüller, R., Roy, D. B., and Thomas, C. D. (2011). Rapid range shifts of species associated with high levels of climate warming. *Science*, 333(6045):1024–1026.
- Chen, J., Yao, Q., Chen, Z., Li, M., Hao, Z., Liu, C., Zheng, W., Xu, M., Chen, X., Yang, J., et al. (2022a). The fengyun-3d (fy-3d) global active fire product: Principle, methodology and validation. *Earth System Science Data*, 14(8):3489–3508.
- Chen, X., Huang, Y., Nie, C., Zhang, S., Wang, G., Chen, S., and Chen, Z. (2022b). A long-term reconstructed tropomi solar-induced fluorescence dataset using machine learning algorithms. *Scientific Data*, 9(1):427.
- Chen, Z., Wang, W., Forzieri, G., and Cescatti, A. (2024). Transition from positive to negative indirect co2 effects on the vegetation carbon uptake. *Nature Communications*, 15(1):1500.
- Chiu, G., Lockhart, R., and Routledge, R. (2006). Bent-cable regression theory and applications. *Journal of the American Statistical Association*, 101(474):542–553.
- Cho, M. A., Ramoelo, A., and Dziba, L. (2017). Response of land surface phenology to variation in tree cover during green-up and senescence periods in the semi-arid savanna of southern africa. *Remote Sensing*, 9(7):689.
- Cleland, E. E., Chuine, I., Menzel, A., Mooney, H. A., and Schwartz, M. D. (2007). Shifting plant phenology in response to global change. *Trends in ecology & evolution*, 22(7):357–365.
- Cleveland, R. B., Cleveland, W. S., McRae, J. E., and Terpenning, I. (1990). STL: A seasonal-trend decomposition procedure based on Loess (with discussion). *Journal of Official Statistics*, 6:3–73.
- Congalton, R. G., Gu, J., Yadav, K., Thenkabail, P., and Ozdogan, M. (2014). Global land cover mapping: A review and uncertainty analysis. *Remote Sensing*, 6(12):12070–12093.

- Conradi, T., Eggli, U., Kreft, H., Schweiger, A. H., Weigelt, P., and Higgins, S. I. (2024). Reassessment of the risks of climate change for terrestrial ecosystems. *Nature Ecology & Evolution*, pages 1–13.
- Conradi, T., Slingsby, J. A., Midgley, G. F., Nottebrock, H., Schweiger, A. H., and Higgins, S. I. (2020). An operational definition of the biome for global change research. *New Phytologist*, 227:1294–1306.
- Cowling, R. and Hoffman, M. (2021). Multi-decadal vegetation change in dune vegetation of the south-eastern cape floristic region: Is thicket expansion without fire inevitable? *South African Journal of Botany*, 142:73–81.
- Cowling, R. M., Richardson, D. M., and Pierce, S. M. (2004). *Vegetation of southern Africa*. Cambridge University Press.
- Cramer, W. et al. (2014). Detection and attribution of observed impacts. In Field, C. B., Barros, V. R., Dokken, D. J., Mach, K. J., Mastrandrea, M. D., Bilir, T. E., Chatterjee, M., Ebi, K. L., Estrada, Y. O., Genova, R. C., Girma, B., Kissel, E. S., Levy, A. N., MacCracken, S., Mastrandrea, P. R., and White, L. L., editors, *Climate Change 2014: Impacts, Adaptation, and Vulnerability. Part A: Global and Sectoral Aspects*, pages 979–1037. Cambridge University Press, Cambridge, UK and New York, NY, USA.
- Dai, Y., Xin, Q., Wei, N., Zhang, Y., Shangguan, W., Yuan, H., Zhang, S., Liu, S., and Lu, X. (2019). A global high-resolution dataset of soil hydraulic and thermal properties for land surface modeling. *Journal of Advances in Modeling Earth Systems*. Accepted.
- Damm, A., Guanter, L., Paul-Limoges, E., Van der Tol, C., Hueni, A., Buchmann, N., Eugster, W., Ammann, C., and Schaepman, M. E. (2015). Far-red sun-induced chlorophyll fluorescence shows ecosystem-specific relationships to gross primary production: An assessment based on observational and modeling approaches. *Remote sensing of Environment*, 166:91–105.
- Davis-Reddy, C. L. and Vincent, K. (2017). *Climate risk and vulnerability: A handbook for Southern Africa (Second Edition)*. CSIR, Pretoria, South Africa.
- Dickinson, J. L., Shirk, J., Bonter, D., Bonney, R., Crain, R. L., Martin, J., Phillips, T., and Purcell, K. (2012). The current state of citizen science as a tool for ecological research and public engagement. *Frontiers in Ecology and the Environment*, 10(6):291–297.

- Didan, K. (2015). Mod13a2 modis/terra vegetation indices 16-day l3 global 1km sin grid v006. Technical report, NASA EOSDIS Land Processes DAAC. <https://doi.org/10.5067/MODIS/MOD13A2.006>.
- Dinerstein, E., Joshi, A., Vynne, C., Lee, A. T., Pharand-Deschênes, F., França, M., Fernando, S., Birch, T., Burkart, K., Asner, G., et al. (2020). A “global safety net” to reverse biodiversity loss and stabilize earth’s climate. *Science advances*, 6(36):eabb2824.
- Dormann, C. F., Schymanski, S. J., Cabral, J., Chuine, I., Graham, C., Hartig, F., Kearney, M., Morin, X., Römermann, C., Schröder, B., and Singer, A. (2012). Correlation and process in species distribution models: bridging a dichotomy. *Journal of Biogeography*, 39(12):2119–2131.
- Doughty, R., Kurosu, T., Parazoo, N., Köhler, P., Wang, Y., Sun, Y., and Frankenberg, C. (2021). Global gosat, oco-2 and oco-3 solar induced chlorophyll fluorescence datasets. *Earth System Science Data Discussions*, 2021:1–28.
- Dubovyk, O., Landmann, T., Erasmus, B. F., Tewes, A., and Schellberg, J. (2015). Monitoring vegetation dynamics with medium resolution modis-evi time series at sub-regional scale in southern africa. *International Journal of Applied Earth Observation and Geoinformation*, 38:175–183.
- Eckhardt, H., Van Wilgen, B., and Biggs, H. (2000). Trends in woody vegetation cover in the kruger national park, south africa, between 1940 and 1998. *African Journal of Ecology*, 38(2):108–115.
- Engelbrecht, C. J. and Engelbrecht, F. A. (2016). Shifts in köppen-geiger climate zones over southern africa in relation to key global temperature goals. *Theoretical and applied climatology*, 123:247–261.
- Engelbrecht, F., Adegoke, J., Bopape, M.-J., Naidoo, M., Garland, R., Thatcher, M., McGregor, J., Katzfey, J., Werner, M., Ichoku, C., et al. (2015). Projections of rapidly rising surface temperatures over africa under low mitigation. *Environmental Research Letters*, 10(8):085004.
- Farquhar, G. D., von Caemmerer, S., and Berry, J. A. (1980). A biochemical model of photosynthetic CO₂ assimilation in leaves of C₃ species. *Planta*, 149(1):78–90.
- Feeley, K. J., Silman, M. R., and Duque, A. (2015). Where are the tropical plants? a call for better inclusion of tropical plants in studies investigating and predicting the effects of climate change.

- Feeley, K. J., Stroud, J. T., and Perez, T. M. (2017). Most ‘global’ reviews of species’ responses to climate change are not truly global. *Diversity and Distributions*, 23(3):231–234.
- Foden, W., Midgley, G. F., Hughes, G., Bond, W. J., Thuiller, W., Hoffman, M. T., Kaleme, P., Underhill, L. G., Rebelo, A., and Hannah, L. (2007). A changing climate is eroding the geographical range of the namib desert tree aloe through population declines and dispersal lags. *Diversity and Distributions*, 13(5):645–653.
- Frankenberg, C., Fisher, J. B., Worden, J., Badgley, G., Saatchi, S. S., Lee, J.-E., Toon, G. C., Butz, A., Jung, M., Kuze, A., et al. (2011). New global observations of the terrestrial carbon cycle from gosat: Patterns of plant fluorescence with gross primary productivity. *Geophysical Research Letters*, 38(17).
- Fuhlendorf, S. D., Engle, D. M., Kerby, J., and Hamilton, R. (2009). Pyric herbivory: rewilding landscapes through the recoupling of fire and grazing. *Conservation biology*, 23(3):588–598.
- Ge, Q., Wang, H., Rutishauser, T., and Dai, J. (2015). Phenological response to climate change in china: a meta-analysis. *Global change biology*, 21(1):265–274.
- Gill, A. L., Gallinat, A. S., Sanders-DeMott, R., Rigden, A. J., Short Gianotti, D. J., Mantooth, J. A., and Templer, P. H. (2015). Changes in autumn senescence in northern hemisphere deciduous trees: a meta-analysis of autumn phenology studies. *Annals of botany*, 116(6):875–888.
- Glenn, E. P., Huete, A. R., Nagler, P. L., and Nelson, S. G. (2008). Relationship between remotely-sensed vegetation indices, canopy attributes and plant physiological processes: What vegetation indices can and cannot tell us about the landscape. *Sensors*, 8(4):2136–2160.
- Gonsamo, A., Ciais, P., Miralles, D. G., Sitch, S., Dorigo, W., Lombardozzi, D., Friedlingstein, P., Nabel, J. E., Goll, D. S., O’Sullivan, M., et al. (2021). Greening drylands despite warming consistent with carbon dioxide fertilization effect. *Global change biology*, 27(14):3336–3349.
- Grace, J., Nichol, C., Disney, M., Lewis, P., Quaife, T., and Bowyer, P. (2007). Can we measure terrestrial photosynthesis from space directly, using spectral reflectance and fluorescence? *Global Change Biology*, 13(7):1484–1497.
- Green, J. K., Seneviratne, S. I., Berg, A. M., Findell, K. L., Hagemann, S., Lawrence, D. M., and Gentine, P. (2019). Large influence of soil moisture on long-term terrestrial carbon uptake. *Nature*, 565(7740):476–479.

- Guanter, L., Aben, I., Tol, P., Krijger, J., Hollstein, A., Köhler, P., Damm, A., Joiner, J., Frankenberg, C., and Landgraf, J. (2015). Potential of the tropospheric monitoring instrument (tropomi) onboard the sentinel-5 precursor for the monitoring of terrestrial chlorophyll fluorescence. *Atmospheric Measurement Techniques*, 8(3):1337–1352.
- Guanter, L., Frankenberg, C., Dudhia, A., Lewis, P. E., Gómez-Dans, J., Kuze, A., Suto, H., and Grainger, R. G. (2012). Retrieval and global assessment of terrestrial chlorophyll fluorescence from gosat space measurements. *Remote Sensing of Environment*, 121:236–251.
- Hansen, G., Stone, D., Auffhammer, M., Huggel, C., and Cramer, W. (2016). Linking local impacts to changes in climate: a guide to attribution. *Regional Environmental Change*, 16:527–541.
- Harris, R. M., Beaumont, L. J., Vance, T. R., Tozer, C. R., Remenyi, T. A., Perkins-Kirkpatrick, S. E., Mitchell, P. J., Nicotra, A., McGregor, S., Andrew, N., et al. (2018). Biological responses to the press and pulse of climate trends and extreme events. *Nature Climate Change*, 8(7):579–587.
- Hempson, G. P., Archibald, S., and Bond, W. J. (2015). A continent-wide assessment of the form and intensity of large mammal herbivory in africa. *Science*, 350(6264):1056–1061.
- Herrero, H., Southworth, J., Muir, C., Khatami, R., Bunting, E., and Child, B. (2020). An evaluation of vegetation health in and around southern african national parks during the 21st century (2000-2016). *Applied Sciences*, 10(7):2366.
- Hersbach, H., Bell, B., Berrisford, P., Hirahara, S., Horányi, A., Muñoz-Sabater, J., Nicolas, J., Peubey, C., Radu, R., Schepers, D., Simmons, A., Soci, C., Abdalla, S., Abellan, X., Balsamo, G., Bechtold, P., Biavati, G., Bidlot, J., Bonavita, M., De Chiara, G., Dahlgren, P., Dee, D., Diamantakis, M., Dragani, R., Flemming, J., Forbes, R., Fuentes, M., Geer, A., Haimberger, L., Healy, S., Hogan, R. J., Hólm, E., Janisková, M., Keeley, S., Laloyaux, P., Lopez, P., Lupu, C., Radnoti, G., de Rosnay, P., Rozum, I., Vamborg, F., Villaume, S., and Thépaut, J.-N. (2020). The ERA5 global reanalysis. *Quarterly Journal of the Royal Meteorological Society*, 146(730):1999–2049.
- Higgins, S. I., Buitenwerf, R., and Moncrieff, G. R. (2016). Defining functional biomes and monitoring their change globally. *Global Change Biology*, 22(11):3583–3593.
- Higgins, S. I., Conradi, T., Louw, M. A., Muhoko, E., Scheiter, S., Martens, C., Hickler, T., Wilhelm, F., Midgley, G. F., Turpie, J., et al. (2024). Biome

- change in southern africa. In *Sustainability of Southern African Ecosystems under Global Change: Science for Management and Policy Interventions*, pages 369–405. Springer.
- Higgins, S. I., Conradi, T., and Muhoko, E. (2023a). Shifts in vegetation activity of terrestrial ecosystems attributable to climate trends. *Nature Geoscience*, 16(2):147–153.
- Higgins, S. I., Conradi, T., Ongole, S., Turpie, J., Weiss, J., Eggle, U., and Slingsby, J. A. (2023b). Changes in how climate forces the vegetation of southern africa. *Ecosystems*, 26(8):1716–1733.
- Higgins, S. I., O’Hara, R. B., Bykova, O., Cramer, M. D., Chuine, I., Gerstner, E.-M., Hickler, T., Morin, X., Kearney, M. R., Midgley, G. F., and Scheiter, S. (2012). A physiological analogy of the niche for projecting the potential distribution of plants. *Journal of Biogeography*, 39(12):2132–2145.
- Higgins, S. I. and Scheiter, S. (2012). Atmospheric CO₂ forces abrupt vegetation shifts locally, but not globally. *Nature*, 488:209–212.
- Hiley, J. R., Bradbury, R. B., Holling, M., and Thomas, C. D. (2013). Protected areas act as establishment centres for species colonizing the uk. *Proceedings of the Royal Society B: Biological Sciences*, 280(1760):20122310.
- Hobbs, J. E., Lindsay, J. A., and Bridgman, H. A. (1998). *Climates of the Southern Continents: Present, Past and Future*. Wiley.
- Hoegh-Guldberg, O., Jacob, D., Bindi, M., Brown, S., Camilloni, I., Diedhiou, A., Djalante, R., Ebi, K., Engelbrecht, F., Guiot, J., et al. (2018). Impacts of 1.5 c global warming on natural and human systems. *Global warming of 1.5 C. An IPCC Special Report*.
- Hubau, W., Lewis, S. L., Phillips, O. L., Affum-Baffoe, K., Beeckman, H., Cuní-Sanchez, A., Daniels, A. K., Ewango, C. E. N., Fauset, S., Mukinzi, J. M., Sheil, D., Sonké, B., Sullivan, M. J. P., Sunderland, T. C. H., Taedoumg, H., Thomas, S. C., White, L. J. T., Abernethy, K. A., Adu-Bredu, S., Amani, C. A., Baker, T. R., Banin, L. F., Baya, F., Begne, S. K., Bennett, A. C., Benedet, F., Bitariho, R., Bocko, Y. E., Boeckx, P., Boundja, P., Brienen, R. J. W., Brncic, T., Chezeaux, E., Chuyong, G. B., Clark, C. J., Collins, M., Comiskey, J. A., Coomes, D. A., Dargie, G. C., de Haulleville, T., Kamdem, M. N. D., Doucet, J.-L., Esquivel-Muelbert, A., Feldpausch, T. R., Fofanah, A., Foli, E. G., Gilpin, M., Gloor, E., Gonmadje, C., Gourlet-Fleury, S., Hall, J. S., Hamilton, A. C., Harris, D. J., Hart, T. B., Hockemba, M. B. N., Hladik,

- A., Ifo, S. A., Jeffery, K. J., Jucker, T., Yakusu, E. K., Kearsley, E., Kenfack, D., Koch, A., Leal, M. E., Levesley, A., Lindsell, J. A., Lisingo, J., Lopez-Gonzalez, G., Lovett, J. C., Makana, J.-R., Malhi, Y., Marshall, A. R., Martin, J., Martin, E. H., Mbayu, F. M., Medjibe, V. P., Mihindou, V., Mitchard, E. T. A., Moore, S., Munishi, P. K. T., Bengone, N. N., Ojo, L., Ondo, F. E., Peh, K. S.-H., Pickavance, G. C., Poulsen, A. D., Poulsen, J. R., Qie, L., Reitsma, J., Rovero, F., Swaine, M. D., Talbot, J., Taplin, J., Taylor, D. M., Thomas, D. W., Toirambe, B., Mukendi, J. T., Tuagben, D., Umunay, P. M., van der Heijden, G. M. F., Verbeeck, H., Vleminckx, J., Willcock, S., Wöll, H., Woods, J. T., and Zemagho, L. (2020). Asynchronous carbon sink saturation in African and Amazonian tropical forests. *Nature*, 579(7797):80–87.
- Huete, A., Didan, K., Miura, T., Rodriguez, E. P., Gao, X., and Ferreira, L. G. (2002). Overview of the radiometric and biophysical performance of the modis vegetation indices. *Remote sensing of environment*, 83(1-2):195–213.
- Hufkens, K., Melaas, E. K., Mann, M. L., Foster, T., Ceballos, F., Robles, M., and Kramer, B. (2019). Monitoring crop phenology using a smartphone based near-surface remote sensing approach. *Agricultural and forest meteorology*, 265:327–337.
- Hurttt, G. C., Chini, L. P., Frohling, S., Betts, R., Feddema, J., Fischer, G., Fisk, J., Hibbard, K., Houghton, R., Janetos, A., et al. (2011). Harmonization of land-use scenarios for the period 1500–2100: 600 years of global gridded annual land-use transitions, wood harvest, and resulting secondary lands. *Climatic change*, 109:117–161.
- IPBES (2019). *Global Assessment Report on Biodiversity and Ecosystem Services of the Intergovernmental Science-Policy Platform on Biodiversity and Ecosystem Services*. IPBES secretariat, Bonn, Germany.
- IPCC (2019). Climate change and land: an IPCC special report on climate change, desertification, land degradation, sustainable land management, food security, and greenhouse gas fluxes in terrestrial ecosystems. In press.
- Janecke, B. and Smit, G. (2011). Phenology of woody plants in riverine thicket and its impact on browse availability to game species. *African Journal of Range & Forage Science*, 28(3):139–148.
- Jeong, S.-J., HO, C.-H., GIM, H.-J., and Brown, M. E. (2011). Phenology shifts at start vs. end of growing season in temperate vegetation over the northern hemisphere for the period 1982–2008. *Global change biology*, 17(7):2385–2399.

- Jiao, W., Wang, L., Smith, W. K., Chang, Q., Wang, H., and D’Odorico, P. (2021). Observed increasing water constraint on vegetation growth over the last three decades. *Nature Communications*, 12(1):3777.
- Joiner, J., Yoshida, Y., Vasilkov, A., Schaefer, K., Jung, M., Guanter, L., Zhang, Y., Garrity, S., Middleton, E., Huemmrich, K., et al. (2014). The seasonal cycle of satellite chlorophyll fluorescence observations and its relationship to vegetation phenology and ecosystem atmosphere carbon exchange. *Remote Sensing of Environment*, 152:375–391.
- Joiner, J., Yoshida, Y., Vasilkov, A., Yoshida, Y., Corp, L., and Middleton, E. (2011). First observations of global and seasonal terrestrial chlorophyll fluorescence from space. *Biogeosciences*, 8(3):637–651.
- Jolly, W. M., Nemani, R., and Running, S. W. (2005). A generalized, bioclimatic index to predict foliar phenology in response to climate. *Global Change Biology*, 11(4):619–632.
- Jones, M. O., Jones, L. A., Kimball, J. S., and McDonald, K. C. (2011). Satellite passive microwave remote sensing for monitoring global land surface phenology. *Remote Sensing of Environment*, 115(4):1102–1114.
- Khan, S. A. and Kar, S. C. (2018). Generalized bent-cable methodology for change-point data: a Bayesian approach. *Journal of Applied Statistics*, 45(10):1799–1812.
- Kniveton, D. R., Layberry, R., Williams, C. J. R., and Peck, M. (2009). Trends in the start of the wet season over africa. *International Journal of Climatology: A Journal of the Royal Meteorological Society*, 29(9):1216–1225.
- Köhler, P., Frankenberg, C., Magney, T. S., Guanter, L., Joiner, J., and Landgraf, J. (2018). Global retrievals of solar-induced chlorophyll fluorescence with tropomi: First results and intersensor comparison to oco-2. *Geophysical Research Letters*, 45(19):10–456.
- Konapala, G., Mishra, A. K., Wada, Y., and Mann, M. E. (2020). Climate change will affect global water availability through compounding changes in seasonal precipitation and evaporation. *Nature communications*, 11(1):3044.
- Lee, H., Calvin, K., Dasgupta, D., Krinner, G., Mukherji, A., Thorne, P., Trisos, C., Romero, J., Aldunce, P., Barret, K., et al. (2023). Ipcc, 2023: Climate change 2023: Synthesis report, summary for policymakers. contribution of working groups i, ii and iii to the sixth assessment report of the intergovernmental

- panel on climate change [core writing team, h. lee and j. romero (eds.)]. ipcc, geneva, switzerland.
- Li, X. and Xiao, J. (2019). A global, 0.05-degree product of solar-induced chlorophyll fluorescence derived from oco-2, modis, and reanalysis data. *Remote Sensing*, 11(5):517.
- Li, X., Xiao, J., He, B., Altaf Arain, M., Beringer, J., Desai, A. R., Emmel, C., Hollinger, D. Y., Krasnova, A., Mammarella, I., et al. (2018). Solar-induced chlorophyll fluorescence is strongly correlated with terrestrial photosynthesis for a wide variety of biomes: First global analysis based on oco-2 and flux tower observations. *Global change biology*, 24(9):3990–4008.
- Lieth, H. (1974). Purposes of a phenology book. In *Phenology and Seasonality Modeling*, pages 3–19. Springer, Berlin Heidelberg.
- Liu, Q., Fu, Y. H., Zhu, Z., Liu, Y., Liu, Z., Huang, M., Janssens, I. A., and Piao, S. (2016). Delayed autumn phenology in the northern hemisphere is related to change in both climate and spring phenology. *Global change biology*, 22(11):3702–3711.
- Martens, C., Hickler, T., Davis-Reddy, C., Engelbrecht, F., Higgins, S. I., von Maltitz, G. P., Midgley, G. F., Pfeiffer, M., and Scheiter, S. (2021). Large uncertainties in future biome changes in africa call for flexible climate adaptation strategies. *Global Change Biology*, 27(2):340–358.
- Masia, N. D., Stevens, N., and Archibald, S. (2018). Identifying phenological functional types in savanna trees. *African Journal of Range & Forage Science*, 35(2):81–88.
- Masubelele, M. L., Hoffman, M. T., Bond, W., and Burdett, P. (2013). Vegetation change (1988-2010) in camdeboo national park (south africa), using fixed-point photo monitoring: The role of herbivory and climate. *Koedoe: African Protected Area Conservation and Science*, 55(1):1–16.
- McCleery, R., Monadjem, A., Baiser, B., Fletcher Jr, R., Vickers, K., and Kruger, L. (2018). Animal diversity declines with broad-scale homogenization of canopy cover in african savannas. *Biological Conservation*, 226:54–62.
- McKechnie, A. E., Rushworth, I. A., Myburgh, F., and Cunningham, S. J. (2021). Mortality among birds and bats during an extreme heat event in eastern south africa. *Austral Ecology*, 46(4):687–691.

- Menzel, A., Yuan, Y., Matiu, M., Sparks, T., Scheifinger, H., Gehrig, R., and Estrella, N. (2020). Climate change fingerprints in recent european plant phenology. *Global Change Biology*, 26(4):2599–2612.
- Midgley, G. F. and Bond, W. J. (2015). Future of african terrestrial biodiversity and ecosystems under anthropogenic climate change. *Nature Climate Change*, 5(9):823–829.
- Moncrieff, G. R., Bond, W. J., and Higgins, S. I. (2016). Revising the biome concept for understanding and predicting global change impacts. *Journal of Biogeography*, 43(5):863–873.
- Mucina, L. (2019). Biome: evolution of a crucial ecological and biogeographical concept. *New Phytologist*, 222(1):97–114.
- Mucina, L. and Rutherford, M. C. (2006). *The Vegetation of South Africa, Lesotho and Swaziland. Strelitzia 19*. South African National Biodiversity Institute, Pretoria.
- Mullen, K., Ardia, D., Gil, D., Windover, D., and Cline, J. (2011). DEoptim: An R package for global optimization by differential evolution. *Journal of Statistical Software, Articles*, 40(6):1–26.
- Muñoz-Sabater, J., Dutra, E., Agustí-Panareda, A., Albergel, C., Arduini, G., Balsamo, G., Boussetta, S., Choulga, M., Harrigan, S., Hersbach, H., et al. (2021). Era5-land: A state-of-the-art global reanalysis dataset for land applications. *Earth system science data*, 13(9):4349–4383.
- NASA (2024). What is climate change? <https://science.nasa.gov/climate-change/what-is-climate-change/>. Accessed: 29 March 2024.
- Nemani, R. R., Keeling, C. D., Hashimoto, H., Jolly, W. M., Piper, S. C., Tucker, C. J., Myeni, R. B., and Running, S. W. (2003). Climate-driven increases in global terrestrial net primary production from 1982 to 1999. *Science*, 300:1560–1563.
- NG (2024). Terrestrial ecosystems. <https://education.nationalgeographic.org/resource/resource-library-terrestrial-ecosystem/>. Accessed: 29 March 2024.
- Niang, I., Ruppel, O. C., Abdrabo, M. A., Essel, A., Lennard, C., Padgham, J., and Urquhart, P. (2014). Africa climate change 2014: Impacts, adaptation, and vulnerability. part b: Regional aspects. contribution of working group ii to the fifth assessment report of the intergovernmental panel on climate change ed vr

- barros et al. *Climate Change 2014: Impacts, Adaptation and Vulnerability: Part B: Regional Aspects: Working Group II Contribution to the Fifth Assessment Report of the Intergovernmental Panel on Climate Change*, pages 1199–1266.
- Nolan, C., Overpeck, J. T., Allen, J. R. M., Anderson, P. M., Betancourt, J. L., Binney, H. A., Brewer, S., Bush, M. B., Chase, B. M., Cheddadi, R., Djamali, M., Dodson, J., Edwards, M. E., Gosling, W. D., Haberle, S., Hotchkiss, S. C., Huntley, B., Ivory, S. J., Kershaw, A. P., Kim, S.-H., Latorre, C., Leydet, M., Lézine, A.-M., Liu, K.-B., Liu, Y., Lozhkin, A. V., McGlone, M. S., Marchant, R. A., Momohara, A., Moreno, P. I., Müller, S., Otto-Bliesner, B. L., Shen, C., Stevenson, J., Takahara, H., Tarasov, P. E., Tipton, J., Vincens, A., Weng, C., Xu, Q., Zheng, Z., and Jackson, S. T. (2018). Past and future global transformation of terrestrial ecosystems under climate change. *Science*, 361(6405):920–923.
- O’connor, T. G., Puttick, J. R., and Hoffman, M. T. (2014). Bush encroachment in southern africa: changes and causes. *African Journal of Range & Forage Science*, 31(2):67–88.
- Oliver, T. H., Marshall, H. H., Morecroft, M. D., Breerton, T., Prudhomme, C., and Huntingford, C. (2015). Interacting effects of climate change and habitat fragmentation on drought-sensitive butterflies. *Nature Climate Change*, 5(10):941–945.
- O’Sullivan, M., Smith, W. K., Sitch, S., Friedlingstein, P., Arora, V. K., Haverd, V., Jain, A. K., Kato, E., Kautz, M., Lombardozzi, D., et al. (2020). Climate-driven variability and trends in plant productivity over recent decades based on three global products. *Global Biogeochemical Cycles*, 34(12):e2020GB006613.
- Ouédraogo, D.-Y., Mortier, F., Gourlet-Fleury, S., Freycon, V., and Picard, N. (2013). Slow-growing species cope best with drought: evidence from long-term measurements in a tropical semi-deciduous moist forest of central africa. *Journal of Ecology*, 101(6):1459–1470.
- Palmer, W. C. (1965). *Meteorological drought*, volume 30. US Department of Commerce, Weather Bureau.
- Pan, N., Feng, X., Fu, B., Wang, S., Ji, F., and Pan, S. (2018). Increasing global vegetation browning hidden in overall vegetation greening: Insights from time-varying trends. *Remote Sensing of Environment*, 214:59 – 72.
- Parmesan, C., Burrows, M. T., Duarte, C. M., Poloczanska, E. S., Richardson, A. J., Schoeman, D. S., and Singer, M. C. (2013). Beyond climate change attribution in conservation and ecological research. *Ecology letters*, 16:58–71.

- Parmesan, C., Morecroft, M., Trisurat, Y., Adrian, R., Anshari, G., Arneth, A., Gao, Q., Gonzalez, P., Harris, R., Price, J., Stevens, N., and Talukdarr, G. (2022). Terrestrial and freshwater ecosystems and their services. In Pörtner, H.-O., Roberts, D., Tignor, M., Poloczanska, E., Mintenbeck, K., Alegría, A., Craig, M., Langsdorf, S., Löschke, S., Möller, V., Okem, A., and Rama, B., editors, *Climate Change 2022: Impacts, Adaptation and Vulnerability. Contribution of Working Group II to the Sixth Assessment Report of the Intergovernmental Panel on Climate Change*, pages 197–377. Cambridge University Press, Cambridge, UK and New York, NY, USA.
- Parmesan, C. and Yohe, G. (2003). A globally coherent fingerprint of climate change impacts across natural systems. *nature*, 421(6918):37–42.
- Peel, M. C., Finlayson, B. L., and McMahon, T. A. (2007). Updated world map of the köppen-geiger climate classification. *Hydrology and earth system sciences*, 11(5):1633–1644.
- Pejchar, L. and Mooney, H. A. (2009). Invasive species, ecosystem services and human well-being. *Trends in ecology & evolution*, 24(9):497–504.
- Peñuelas, J., Ciais, P., Canadell, J. G., Janssens, I. A., Fernández-Martínez, M., Carnicer, J., Obersteiner, M., Piao, S., Vautard, R., and Sardans, J. (2017). Shifting from a fertilization-dominated to a warming-dominated period. *Nature ecology & evolution*, 1(10):1438–1445.
- Peñuelas, J. and Filella, I. (2009). Phenology feedbacks on climate change. *Science*, 324(5929):887–888.
- Perez, T. M., Stroud, J. T., and Feeley, K. J. (2016). Thermal trouble in the tropics. *Science*, 351(6280):1392–1393.
- Péron, G. and Altwegg, R. (2015). Twenty-five years of change in southern african passerine diversity: nonclimatic factors of change. *Global change biology*, 21(9):3347–3355.
- Pettorelli, N., Laurance, W. F., O’Brien, T. G., Wegmann, M., Nagendra, H., and Turner, W. (2014). Satellite remote sensing for applied ecologists: opportunities and challenges. *Journal of Applied Ecology*, 51(4):839–848.
- Peñuelas, J., Ciais, P., Canadell, J. G., Janssens, I. A., Fernández-Martínez, M., Carnicer, J., Obersteiner, M., Piao, S., Vautard, R., and Sardans, J. (2017). Shifting from a fertilization-dominated to a warming-dominated period. *Nature Ecology & Evolution*, 1(10):1438–1445.

- Piao, S., Liu, Q., Chen, A., Janssens, I. A., Fu, Y., Dai, J., Liu, L., Lian, X., Shen, M., and Zhu, X. (2019). Plant phenology and global climate change: Current progresses and challenges. *Global change biology*, 25(6):1922–1940.
- Piao, S., Tan, J., Chen, A., Fu, Y. H., Ciais, P., Liu, Q., Janssens, I. A., Vicca, S., Zeng, Z., Jeong, S.-J., et al. (2015). Leaf onset in the northern hemisphere triggered by daytime temperature. *Nature communications*, 6(1):1–8.
- Piao, S., Wang, X., Park, T., Chen, C., Lian, X., He, Y., Bjerke, J. W., Chen, A., Ciais, P., Tømmervik, H., et al. (2020). Characteristics, drivers and feedbacks of global greening. *Nature Reviews Earth & Environment*, 1(1):14–27.
- Porcar-Castell, A., Tyystjärvi, E., Atherton, J., Van der Tol, C., Flexas, J., Pfündel, E. E., Moreno, J., Frankenberg, C., and Berry, J. A. (2014). Linking chlorophyll a fluorescence to photosynthesis for remote sensing applications: mechanisms and challenges. *Journal of experimental botany*, 65(15):4065–4095.
- Prentice, I. C., Bondeau, A., Cramer, W., Harrison, S. P., Hickler, T., Lucht, W., Sitch, S., Smith, B., and Sykes, M. T. (2007). *Dynamic Global Vegetation Modelling: Quantifying Terrestrial Ecosystem Responses to Large-Scale Environmental Change*, pages 175–192. Springer Berlin Heidelberg, Berlin, Heidelberg.
- Pörtner, H.-O. and et al. (2021). Scientific outcome of the ipbes-ipcc co-sponsored workshop on biodiversity and climate change. Bonn, Germany, IPBES and IPCC.
- R Core Team (2021). *R: A Language and Environment for Statistical Computing*. R Foundation for Statistical Computing, Vienna, Austria.
- R Core Team (2022). *R: A Language and Environment for Statistical Computing*. R Foundation for Statistical Computing, Vienna, Austria.
- R Core Team (2023). *R: A Language and Environment for Statistical Computing*. R Foundation for Statistical Computing, Vienna, Austria.
- Reich, P. B. (2014). The world-wide ‘fast–slow’ plant economics spectrum: a traits manifesto. *Journal of ecology*, 102(2):275–301.
- Reich, P. B., Hobbie, S. E., and Lee, T. D. (2014). Plant growth enhancement by elevated co2 eliminated by joint water and nitrogen limitation. *Nature Geoscience*, 7(12):920–924.
- Renner, S. S. and Zohner, C. M. (2018). Climate change and phenological mismatch in trophic interactions among plants, insects, and vertebrates. *Annual review of ecology, evolution, and systematics*, 49:165–182.

- Running, S. W. and Zhao, M. (2015). Daily gpp and annual npp (mod17a2/a3) products nasa earth observing system modis land algorithm. *MOD17 User's Guide*, 2015:1–28.
- Running, S. W. and Zhao, M. (2019). User's guide daily gpp and annual npp (mod17a2h/a3h) and year-end gap-filled (mod17a2hgf/a3hgf) products nasa earth observing system modis land algorithm (for collection 6). *University of Montana, Missoula, MT*.
- Rutherford, M. C., Midgley, G. F., Bond, W. J., Powrie, L. W., Roberts, R., and Allsopp, J. (1999). *Plant biodiversity: vulnerability and adaptation assessment. South African Country Study on Climate Change*. National Botanical Institute, Claremont, South Africa.
- Ryan, C. M., Williams, M., Grace, J., Woollen, E., and Lehmann, C. E. (2017). Pre-rain green-up is ubiquitous across southern tropical africa: Implications for temporal niche separation and model representation. *New Phytologist*, 213(2):625–633.
- Scheiter, S. and Higgins, S. I. (2009). Impacts of climate change on the vegetation of africa: an adaptive dynamic vegetation modelling approach. *Global Change Biology*, 15(9):2224–2246.
- Scheiter, S., Kumar, D., Corlett, R. T., Gaillard, C., Langan, L., Lapuz, R. S., Martens, C., Pfeiffer, M., and Tomlinson, K. W. (2020). Climate change promotes transitions to tall evergreen vegetation in tropical asia. *Global Change Biology*, 26(9):5106–5124.
- Scheiter, S., Langan, L., and Higgins, S. I. (2013). Next-generation dynamic global vegetation models: learning from community ecology. *New Phytologist*, 198(3):957–969.
- Scherber, C., Eisenhauer, N., Weisser, W. W., Schmid, B., Voigt, W., Fischer, M., Schulze, E.-D., Roscher, C., Weigelt, A., Allan, E., et al. (2010). Bottom-up effects of plant diversity on multitrophic interactions in a biodiversity experiment. *Nature*, 468(7323):553–556.
- Schimper, A. F. W. (1903). *Plant-geography upon a physiological basis*. Oxford University Press.
- Scrucca, L., Fop, M., Murphy, T. B., and Raftery, A. E. (2016). mclust 5: clustering, classification and density estimation using Gaussian finite mixture models. *The R Journal*, 8(1):289–317.

- Seddon, A. W. R., Macias-Fauria, M., Long, P. R., Benz, D., and Willis, K. J. (2016). Sensitivity of global terrestrial ecosystems to climate variability. *Nature*, 531(7593):229–232.
- Settele, J., Scholes, R., Betts, R., Bunn, S., Leadley, P., Nepstad, D., Overpeck, J. T., and Taboada, M. A. (2014). *Climate Change 2014: Impacts, Adaptation, and Vulnerability, Part A: Global and Sectoral Aspects*, chapter Chapter 4: Terrestrial and Inland Water Systems, page 271–359. Contribution of Working Group II to the PCC Fifth Assessment Report, Fifth Assessment Report of the Intergovernmental Panel on Climate Change. Cambridge University Press, Cambridge, United Kingdom and New York, NY, USA.
- Siddig, A. A., Ellison, A. M., Ochs, A., Villar-Leeman, C., and Lau, M. K. (2016). How do ecologists select and use indicator species to monitor ecological change? insights from 14 years of publication in ecological indicators. *Ecological Indicators*, 60:223–230.
- Sirami, C., Caplat, P., Popy, S., Clamens, A., Arlettaz, R., Jiguet, F., Brotons, L., and Martin, J.-L. (2017). Impacts of global change on species distributions: obstacles and solutions to integrate climate and land use. *Global Ecology and Biogeography*, 26(4):385–394.
- Skowno, A. L., Thompson, M. W., Hiestermann, J., Ripley, B., West, A. G., and Bond, W. J. (2017). Woodland expansion in south african grassy biomes based on satellite observations (1990–2013): general patterns and potential drivers. *Global change biology*, 23(6):2358–2369.
- Slingsby, J. A., Merow, C., Aiello-Lammens, M., Allsopp, N., Hall, S., Kilroy Mollmann, H., Turner, R., Wilson, A. M., and Silander Jr, J. A. (2017). Intensifying postfire weather and biological invasion drive species loss in a mediterranean-type biodiversity hotspot. *Proceedings of the National Academy of Sciences*, 114(18):4697–4702.
- Smith, W. K., Fox, A. M., MacBean, N., Moore, D. J., and Parazoo, N. C. (2020). Constraining estimates of terrestrial carbon uptake: New opportunities using long-term satellite observations and data assimilation. *New Phytologist*, 225(1):105–112.
- Smith, W. K., Reed, S. C., Cleveland, C. C., Ballantyne, A. P., Anderegg, W. R. L., Wieder, W. R., Liu, Y. Y., and Running, S. W. (2016). Large divergence of satellite and earth system model estimates of global terrestrial CO₂ fertilization. *Nature Climate Change*, 6(3):306–310.

- Song, X.-P., Hansen, M. C., Stehman, S. V., Potapov, P. V., Tyukavina, A., Vermote, E. F., and Townshend, J. R. (2018). Global land change from 1982 to 2016. *Nature*, 560(7720):639–643.
- Statisticat, LLC (2021). *LaplacesDemon: Complete Environment for Bayesian Inference*. Bayesian-Inference.com. R package version 16.1.6.
- Stevens, N., Lehmann, C. E., Murphy, B. P., and Durigan, G. (2017). Savanna woody encroachment is widespread across three continents. *Global change biology*, 23(1):235–244.
- Stone, D., Auffhammer, M., Carey, M., Hansen, G., Huggel, C., Cramer, W., Lobell, D., Molau, U., Solow, A., Tibig, L., et al. (2013). The challenge to detect and attribute effects of climate change on human and natural systems. *Climatic Change*, 121:381–395.
- Storn, R. and Price, K. (1997). Differential evolution - a simple and efficient heuristic for global optimization over continuous spaces. *Journal of Global Optimization*, 11(4):341–359.
- Sulla-Menashe, D., Woodcock, C. E., and Friedl, M. A. (2018). Canadian boreal forest greening and browning trends: an analysis of biogeographic patterns and the relative roles of disturbance versus climate drivers. *Environmental Research Letters*, 13(1):014007.
- Tan, W., Wei, C., Lu, Y., and Xue, D. (2021). Reconstruction of all-weather daytime and nighttime modis aqua-terra land surface temperature products using an xgboost approach. *Remote Sensing*, 13(22):4723.
- Terrer, C., Phillips, R. P., Hungate, B. A., Rosende, J., Pett-Ridge, J., Craig, M. E., van Groenigen, K. J., Keenan, T. F., Sulman, B. N., Stocker, B. D., et al. (2021). A trade-off between plant and soil carbon storage under elevated co₂. *Nature*, 591(7851):599–603.
- Thackeray, S. J., Henrys, P. A., Hemming, D., Bell, J. R., Botham, M. S., Burthe, S., Helaouet, P., Johns, D. G., Jones, I. D., Leech, D. I., et al. (2016). Phenological sensitivity to climate across taxa and trophic levels. *Nature*, 535(7611):241–245.
- Thornley, J. H. (1998). Modelling shoot : Root relations: the only way forward? *Annals of Botany*, 81(2):165–171.
- Trisos, C. H., Adelekan, I. O., Totin, E., Ayanlade, A., Efitre, J., Gameda, A., Kalaba, F. K., Lennard, C., Masao, C., Mgaya, Y., Ngaruiya, G., Olago, D.,

- Simpson, N. P., and Zakieldean, S. (2022). Africa. In Pörtner, H.-O., Roberts, D. C., Tignor, M., Poloczanska, E. S., Mintenbeck, K., Alegría, A., Craig, M., Langsdorf, S., Löschke, J., Möller, V., Okem, A., and Rama, B., editors, *Climate Change 2022: Impacts, Adaptation and Vulnerability*, pages 1285–1455. Cambridge University Press, Cambridge, UK and New York, NY, USA.
- Tylianakis, J. M., Didham, R. K., Bascompte, J., and Wardle, D. A. (2008). Global change and species interactions in terrestrial ecosystems. *Ecology letters*, 11(12):1351–1363.
- UNEP-WCMC and IUCN (2021). Protected Planet: The World Database on Protected Areas (WDPA) [Online], [July 2021], Cambridge, UK: UNEP-WCMC and IUCN. Available at: www.protectedplanet.net.
- UNFCCC (2024). Introduction to mitigation. <https://unfccc.int/topics/introduction-to-mitigation/>. Accessed: 29 March 2024.
- USGS (2024). What is remote sensing. <https://www.usgs.gov/faqs/what-remote-sensing-and-what-it-used/>. Accessed: 29 March 2024.
- Van de Pol, M., Jenouvrier, S., Cornelissen, J. H., and Visser, M. E. (2017). Behavioural, ecological and evolutionary responses to extreme climatic events: challenges and directions. *Philosophical Transactions of the Royal Society B: Biological Sciences*, 372(1723):20160134.
- van Wilgen, B. W., Zengeya, T. A., and Richardson, D. M. (2022). A review of the impacts of biological invasions in south africa. *Biological Invasions*, 24(1):27–50.
- Venables, W. N. and Ripley, B. D. (2002). *Modern Applied Statistics with S*. Springer, fourth edition.
- Venter, Z., Cramer, M., and Hawkins, H.-J. (2018). Drivers of woody plant encroachment over africa. *Nature communications*, 9(1):1–7.
- Venter, Z. S., Scott, S. L., Desmet, P. G., and Hoffman, M. T. (2020). Application of landsat-derived vegetation trends over south africa: Potential for monitoring land degradation and restoration. *Ecological Indicators*, 113:106206.
- Verger, A., Filella, I., Baret, F., and Peñuelas, J. (2016). Vegetation baseline phenology from kilometeric global lai satellite products. *Remote sensing of environment*, 178:1–14.
- von Caemmerer, S. (2000). *Biochemical Models of Leaf Photosynthesis*. Techniques in plant sciences. CSIRO Publishing.

- Walker, A. P., De Kauwe, M. G., Bastos, A., Belmecheri, S., Georgiou, K., Keeling, R. F., McMahon, S. M., Medlyn, B. E., Moore, D. J., Norby, R. J., et al. (2021). Integrating the evidence for a terrestrial carbon sink caused by increasing atmospheric CO_2 . *New phytologist*, 229(5):2413–2445.
- Walter, H. (1973). *Vegetation of the Earth in relation to climate and the eco-physiological conditions*. Springer, New York.
- Walther, S., Voigt, M., Thum, T., Gonsamo, A., Zhang, Y., Köhler, P., Jung, M., Varlagin, A., and Guanter, L. (2016). Satellite chlorophyll fluorescence measurements reveal large-scale decoupling of photosynthesis and greenness dynamics in boreal evergreen forests. *Global change biology*, 22(9):2979–2996.
- Wang, C., Beringer, J., Hutley, L. B., Cleverly, J., Li, J., Liu, Q., and Sun, Y. (2019). Phenology dynamics of dryland ecosystems along the north australian tropical transect revealed by satellite solar-induced chlorophyll fluorescence. *Geophysical Research Letters*, 46(10):5294–5302.
- Wang, C., Wu, Y., Hu, Q., Hu, J., Chen, Y., Lin, S., and Xie, Q. (2022a). Comparison of vegetation phenology derived from solar-induced chlorophyll fluorescence and enhanced vegetation index, and their relationship with climatic limitations. *Remote Sensing*, 14(13):3018.
- Wang, H., Wang, H., Ge, Q., and Dai, J. (2020a). The interactive effects of chilling, photoperiod, and forcing temperature on flowering phenology of temperate woody plants. *Frontiers in plant science*, 11:443.
- Wang, S., Yang, B., Yang, Q., Lu, L., Wang, X., and Peng, Y. (2016). Temporal trends and spatial variability of vegetation phenology over the northern hemisphere during 1982-2012. *PLoS One*, 11(6):e0157134.
- Wang, S., Zhang, Y., Ju, W., Chen, J. M., Cescatti, A., Sardans, J., Janssens, I. A., Wu, M., Berry, J. A., Campbell, J. E., et al. (2021). Response to comments on “recent global decline of CO_2 fertilization effects on vegetation photosynthesis”. *Science*, 373(6562):eabg7484.
- Wang, S., Zhang, Y., Ju, W., Chen, J. M., Ciais, P., Cescatti, A., Sardans, J., Janssens, I. A., Wu, M., Berry, J. A., et al. (2020b). Recent global decline of CO_2 fertilization effects on vegetation photosynthesis. *Science*, 370(6522):1295–1300.
- Wang, S., Zhang, Y., Ju, W., Wu, M., Liu, L., He, W., and Penuelas, J. (2022b). Temporally corrected long-term satellite solar-induced fluorescence leads to improved estimation of global trends in vegetation photosynthesis during 1995–2018. *ISPRS Journal of Photogrammetry and Remote Sensing*, 194:222–234.

- Wessels, K., Mathieu, R., Knox, N., Main, R., Naidoo, L., and Steenkamp, K. (2019). Mapping and monitoring fractional woody vegetation cover in the arid savannas of namibia using lidar training data, machine learning, and alos palsar data. *Remote Sensing*, 11(22):2633.
- Wessels, K. J., Prince, S. D., Zambatis, N., MacFadyen, S., Frost, P. E., and Zyl, D. V. (2006). Relationship between herbaceous biomass and 1-km² advanced very high resolution radiometer (AVHRR) NDVI in Kruger National Park, South Africa. *International Journal of Remote Sensing*, 27(5):951–973.
- White, F. (1983). *The vegetation of Africa: a descriptive memoir to accompany the Unesco/AETFAT/UNSO vegetation map of Africa*. United Nations Educational, Scientific and Cultural Organization, Paris.
- Whitecross, M. A., Witkowski, E. T., and Archibald, S. (2017). Assessing the frequency and drivers of early-greening in broad-leaved woodlands along a latitudinal gradient in southern africa. *Austral ecology*, 42(3):341–353.
- Whittaker, R. H. (1975). *Communities and Ecosystems*. Macmillan Publishing, New York.
- Wigley, B. J., Coetsee, C., February, E. C., Dobelmann, S., and Higgins, S. I. (2024). Will trees or grasses profit from changing rainfall regimes in savannas? *New Phytologist*, 241(6):2379–2394.
- Winkler, A. J., Myneni, R. B., Hannart, A., Sitch, S., Haverd, V., Lombardozzi, D., Arora, V. K., Pongratz, J., Nabel, J. E., Goll, D. S., et al. (2021). Slowdown of the greening trend in natural vegetation with further rise in atmospheric co₂. *Biogeosciences*, 18(17):4985–5010.
- Wolfe, D. W., Schwartz, M. D., Lakso, A. N., Otsuki, Y., Pool, R. M., and Shaulis, N. J. (2005). Climate change and shifts in spring phenology of three horticultural woody perennials in northeastern usa. *International Journal of Biometeorology*, 49:303–309.
- Xu, C., McDowell, N. G., Fisher, R. A., Wei, L., Sevanto, S., Christoffersen, B. O., Weng, E., and Middleton, R. S. (2019). Increasing impacts of extreme droughts on vegetation productivity under climate change. *Nature Climate Change*, 9(12):948–953.
- Yamori, W., Hikosaka, K., and Way, D. A. (2014). Temperature response of photosynthesis in c₃, c₄, and cam plants: temperature acclimation and temperature adaptation. *Photosynthesis research*, 119:101–117.

- Yang, H., Yang, X., Zhang, Y., Heskell, M. A., Lu, X., Munger, J. W., Sun, S., and Tang, J. (2017). Chlorophyll fluorescence tracks seasonal variations of photosynthesis from leaf to canopy in a temperate forest. *Global change biology*, 23(7):2874–2886.
- Zeng, Y., Hao, D., Huete, A., Dechant, B., Berry, J., Chen, J. M., Joiner, J., Frankenberg, C., Bond-Lamberty, B., Ryu, Y., et al. (2022). Optical vegetation indices for monitoring terrestrial ecosystems globally. *Nature Reviews Earth & Environment*, 3(7):477–493.
- Zhang, X., Friedl, M. A., and Schaaf, C. B. (2006). Global vegetation phenology from moderate resolution imaging spectroradiometer (modis): Evaluation of global patterns and comparison with in situ measurements. *Journal of Geophysical Research: Biogeosciences*, 111(G4).
- Zhang, X., Friedl, M. A., Schaaf, C. B., Strahler, A. H., Hodges, J. C., Gao, F., Reed, B. C., and Huete, A. (2003). Monitoring vegetation phenology using modis. *Remote sensing of environment*, 84(3):471–475.
- Zhang, Y., Guanter, L., Berry, J. A., van der Tol, C., Yang, X., Tang, J., and Zhang, F. (2016). Model-based analysis of the relationship between sun-induced chlorophyll fluorescence and gross primary production for remote sensing applications. *Remote Sensing of Environment*, 187:145–155.
- Zhang, Y., Joiner, J., Alemohammad, S. H., Zhou, S., and Gentine, P. (2018). A global spatially contiguous solar-induced fluorescence (csif) dataset using neural networks. *Biogeosciences*, 15(19):5779–5800.
- Zhao, M., Running, S., Heinsch, F. A., and Nemani, R. (2011). Modis-derived terrestrial primary production. *Land remote sensing and global environmental change: NASA’s Earth observing system and the science of ASTER and MODIS*, pages 635–660.
- Zhao, M. and Running, S. W. (2010). Drought-induced reduction in global terrestrial net primary production from 2000 through 2009. *science*, 329(5994):940–943.
- Zhao, M. and Running, S. W. (2011). Response to comments on “drought-induced reduction in global terrestrial net primary production from 2000 through 2009”. *Science*, 333(6046):1093–1093.
- Zheng, Y., Shen, R., Wang, Y., Li, X., Liu, S., Liang, S., Chen, J. M., Ju, W., Zhang, L., and Yuan, W. (2020). Improved estimate of global gross primary

- production for reproducing its long-term variation, 1982–2017. *Earth System Science Data*, 12(4):2725–2746.
- Zhou, S., Williams, A. P., Lintner, B. R., Findell, K. L., Keenan, T. F., Zhang, Y., and Gentile, P. (2022a). Diminishing seasonality of subtropical water availability in a warmer world dominated by soil moisture–atmosphere feedbacks. *Nature communications*, 13(1):5756.
- Zhou, Y., Tingley, M. W., Case, M. F., Coetsee, C., Kiker, G. A., Scholtz, R., Venter, F. J., and Staver, A. C. (2021). Woody encroachment happens via intensification, not extensification, of species ranges in an african savanna. *Ecological Applications*, 31(8):e02437.
- Zhou, Z., Liu, S., Ding, Y., Fu, Q., Wang, Y., Cai, H., and Shi, H. (2022b). Assessing the responses of vegetation to meteorological drought and its influencing factors with partial wavelet coherence analysis. *Journal of Environmental Management*, 311:114879.
- Zhu, W., Tian, H., Xu, X., Pan, Y., Chen, G., and Lin, W. (2012). Extension of the growing season due to delayed autumn over mid and high latitudes in north america during 1982–2006. *Global Ecology and Biogeography*, 21(2):260–271.
- Zhu, X. and Liu, D. (2015). Improving forest aboveground biomass estimation using seasonal Landsat NDVI time-series. *ISPRS Journal of Photogrammetry and Remote Sensing*, 102:222 – 231.
- Zhu, Z., Piao, S., Myneni, R. B., Huang, M., Zeng, Z., Canadell, J. G., Ciais, P., Sitch, S., Friedlingstein, P., Arneeth, A., et al. (2016). Greening of the earth and its drivers. *Nature climate change*, 6(8):791–795.

Contribution Statement

Chapter 2: Patterns of phenological change in the ecosystems of southern Africa

The idea and concept were jointly developed by Edward Muhoko and Prof. Dr. Steven Higgins. Edward Muhoko acquired and analysed the data. The findings of the study were further discussed among the two authors. Edward Muhoko **led the writing with support from Prof. Dr. Steven Higgins.**

Chapter 3: Assessing functional changes in the biomes of southern Africa

The idea and concept were jointly developed by Edward Muhoko and Prof. Dr. Steven Higgins. Edward Muhoko acquired and analysed the data. The findings of the study were further discussed among the two authors. Edward Muhoko **led the writing with support from Prof. Dr. Steven Higgins.**

Chapter 4: Attributing shifts in vegetation activity to climatic forcing

The idea and concept were jointly conceived by Edward Muhoko and Prof. Dr. Steven Higgins. Prof. Dr. Steven Higgins developed the process model. Edward Muhoko acquired and processed the data, applied sensitivity analyses using the model, and created figures. Both Edward Muhoko and Prof. Dr. Steven Higgins interpreted the findings. Edward Muhoko **led the writing with contributions from Prof. Dr. Steven Higgins and Prof. Dr. Cyrus Samimi.**

Overall, I performed all the analyses and wrote the text of each chapter. The assistance provided by Prof. Dr. Steven Higgins and Prof. Dr. Cyrus Samimi was at a supervisory level. Such assistance included tips on how to perform the analyses and suggestions for improving the writing.

Publication list

Below is a complete list of my publication record.

Publication 1

- Higgins, Steven I., Timo Conradi, Michelle A. Louw, **Muhoko Edward**, Simon Scheiter, Carola Martens, Thomas Hickler et al. "Biome Change in Southern Africa." In Sustainability of Southern African Ecosystems under Global Change: Science for Management and Policy Interventions, pp. 369-405. Cham: Springer International Publishing, 2024.

Publication 2

- Higgins, Steven I., Timo Conradi, and **Muhoko Edward**. "Shifts in vegetation activity of terrestrial ecosystems attributable to climate trends." Nature Geoscience 16, no. 2 (2023): 147-153.

Publication 3

- **Muhoko, Edward**, Carlos De Wasseige, and Vera De Cauwer. "Assessing land cover change in Namibia's Kavango East region: a multi-date object approach." BOIS & FORETS DES TROPIQUES 344 (2020): 17-32.

Relation of publications to this thesis

Publication 1 is a review of biome change in southern Africa that uses preliminary findings originally conducted in **Chapter 2** of this thesis. That is, **Chapter 2** is the original work while **Publication 1** reviews this work along with several other studies on biome change in southern Africa. **Publication 2** developed the methods I applied in **Chapter 4** of this thesis. **Chapter 4** builds and expands on this original study by using the same methodological approach applied to Solar Induced Fluorescence (SIF) time series data. The rationale is that the SIF data may provide more robust estimates of ecosystem-level photosynthesis compared to the Normalised Difference Vegetation Index (NDVI) and Enhanced Vegetation Index (EVI) datasets used in **Publication 2**. **Publication 3** is unrelated to this thesis, although it uses remote sensing methods to assess vegetation change in southern Africa. As highlighted previously, each chapter represents original work I conducted.

Acknowledgements

I give glory and honour to God for his love, grace and protection over the last four years of my time in Bayreuth, Germany.

I am eternally grateful towards Prof. Dr. Steven Higgins for offering an opportunity to an African 'child' like me to collaborate closely with him. His kindness, support and belief in my abilities have made this dissertation possible. The knowledge and skills gained from our interactions will undoubtedly shape the trajectory of my future career.

I am also deeply appreciative of the financial support provided by the DAAD during my time in Germany.

I thank the entire staff members, past and present, at the Chair of Plant Ecology, University of Bayreuth. Special thanks to Dr Timo Conradi, Dr. Henning Nottebrock, Arne Burkhardt, Fabian Nützel, Linda Winkhart, Theresa Schödel, Dagmar Hanke, Michaela Neff, Joseph Benjamin, Fatih Fazlioglu and Burkhard Stumpf. They all directly or indirectly contributed to my scientific growth and also made me feel part of the Plant Ecology group.

I thank Prof. Dr. Cyrus Samimi for the long but insightful discussions we used to have. I also thank Richard Careaga and Sam Bowers for their invaluable support.

I am also grateful to Amy Schroeder, Shashank Ongole, Lakshmipriya Cannanbilla, Marius Dufner and Marius Klotz. The bonds we formed transcended academia and I will always cherish the moments we shared. I wish each of them all the best in their future endeavors and I am confident that our paths will cross again.

I also extend my gratitude to the friends I made in Bayreuth, including Bathuel Obwanah, Benjamin, Oliver, Ridwan Shittu, Bachir Ibrahim, Odessi Erick, Baraka Mbise, Aziz 'Zweistein' and everyone else I may have forgotten. Your companionship enriched my experience in Bayreuth.

Lastly, I would like to thank my family and friends in Namibia for your unwavering mental, emotional and psychological support. I appreciate your understanding that I had to leave Namibia for Germany to fulfil a childhood dream. To my girlfriend Dorcas Manuel, your patience and understanding mean the world to me. To my son David Muhoko, your resilience in my absence fills me with pride. It was hard to leave you all behind and go to Germany. I hope you both understand the significance of this journey in fulfilling our aspirations.

Thank you all from the bottom of my heart.

Truly yours,

Edward Mukoya Muhoko

(Eidesstattliche) Versicherungen und Erklärungen

(§ 9 Satz 2 Nr. 3 PromO BayNAT)

Hiermit versichere ich eidesstattlich, dass ich die Arbeit selbstständig verfasst und keine anderen als die von mir angegebenen Quellen und Hilfsmittel benutzt habe (vgl. Art. 64 Abs. 1 Satz 6 BayHSchG).

(§ 9 Satz 2 Nr. 3 PromO BayNAT)

Hiermit erkläre ich, dass ich die Dissertation nicht bereits zur Erlangung eines akademischen Grades eingereicht habe und dass ich nicht bereits diese oder eine gleichartige Doktorprüfung endgültig nicht bestanden habe.

(§ 9 Satz 2 Nr. 4 PromO BayNAT)

Hiermit erkläre ich, dass ich Hilfe von gewerblichen Promotionsberatern bzw. -vermittlern oder ähnlichen Dienstleistern weder bisher in Anspruch genommen habe noch künftig in Anspruch nehmen werde.

(§ 9 Satz 2 Nr. 7 PromO BayNAT)

Hiermit erkläre ich mein Einverständnis, dass die elektronische Fassung meiner Dissertation unter Wahrung meiner Urheberrechte und des Datenschutzes einer gesonderten Überprüfung unterzogen werden kann.

(§ 9 Satz 2 Nr. 8 PromO BayNAT)

Hiermit erkläre ich mein Einverständnis, dass bei Verdacht wissenschaftlichen Fehlverhaltens Ermittlungen durch universitätsinterne Organe der wissenschaftlichen Selbstkontrolle stattfinden können.

Ört, Datum, Unterschrift